

University of Alberta

**Three-dimensional Numerical Modelling of the Wagner Natural Area
Groundwater Flow System**

by

Heather Margaret von Hauff



**A thesis submitted to the Faculty of Graduate Studies and Research in partial
fulfillment of the requirements for the degree of Master of Science**

Department of Earth and Atmospheric Sciences

**Edmonton, Alberta
Fall 2004**



Library and
Archives Canada

Bibliothèque et
Archives Canada

Published Heritage
Branch

Direction du
Patrimoine de l'édition

395 Wellington Street
Ottawa ON K1A 0N4
Canada

395, rue Wellington
Ottawa ON K1A 0N4
Canada

Your file *Votre référence*

ISBN: 0-612-95874-4

Our file *Notre référence*

ISBN: 0-612-95874-4

The author has granted a non-exclusive license allowing the Library and Archives Canada to reproduce, loan, distribute or sell copies of this thesis in microform, paper or electronic formats.

L'auteur a accordé une licence non exclusive permettant à la Bibliothèque et Archives Canada de reproduire, prêter, distribuer ou vendre des copies de cette thèse sous la forme de microfiche/film, de reproduction sur papier ou sur format électronique.

The author retains ownership of the copyright in this thesis. Neither the thesis nor substantial extracts from it may be printed or otherwise reproduced without the author's permission.

L'auteur conserve la propriété du droit d'auteur qui protège cette thèse. Ni la thèse ni des extraits substantiels de celle-ci ne doivent être imprimés ou autrement reproduits sans son autorisation.

In compliance with the Canadian Privacy Act some supporting forms may have been removed from this thesis.

Conformément à la loi canadienne sur la protection de la vie privée, quelques formulaires secondaires ont été enlevés de cette thèse.

While these forms may be included in the document page count, their removal does not represent any loss of content from the thesis.

Bien que ces formulaires aient inclus dans la pagination, il n'y aura aucun contenu manquant.

Canada

"In the end, we conserve only what we love. We will love only what we understand. We will understand only what we are taught."

- Baba Dioum, Senegalese poet

Acknowledgements

Firstly, I would like to thank my supervisors, Dr. Carl Mendoza and Dr. Ben Rostron, for their support, assistance and encouragement. Thank you to Dr. Kevin Devito for your interest, time and support, and to Dr. Rob Donahue for your feedback on my thesis.

Thank you to the entire hydrogeology research group at the University of Alberta: Jennifer, Heather, Dan B., Trevor, Brian, Kristine, Dan K., Sarah, and Adrienne, Gavin, and Dan P. for your support and friendship. Special thanks to Tannis for your support, friendship, and editing my thesis.

Thank you to Joe Tóth for his mentoring and encouragement. Your interest in hydrogeology is infectious. I truly enjoyed the field trips that you led.

Thank you to Valdis and Matt. The partnership with NAIT helped to provide valuable data, and field experience.

I would like to thank my family for a lifetime of support and encouragement. Thank you to my parents for fostering an interest in the environment, through summers at Purdy. Special thanks to my father for never tiring of my incessant question, "what kind of rock is this?", all those years ago.

Finally, I would like to thank Michael for his love, encouragement, and interest in everything I do.

Table of Contents

Chapter 1 Introduction	1
Chapter 2 Theory and Background.....	8
2.1 Groundwater Flow Equations	8
2.1.1 Darcy's Law.....	8
2.1.2 The Continuity Equation	9
2.2 Groundwater Flow Systems.....	10
2.3 Characteristics of Recharge and Discharge Areas	12
2.3.1 Recharge Areas	12
2.3.2 Discharge Areas.....	13
Chapter 3 Data Collection and Processing.....	21
3.1 Data Origin and Quality	21
3.2 Preparation of Maps	22
3.2.1 Bedrock Surface Mapping	22
3.2.2 Groundwater Elevation Mapping in Surficial Sediments.....	24
3.3 Field Work.....	24
Chapter 4 Physical Setting	27
4.1 Climate	27
4.2 Surface Topography and Features	27
4.3 Geology	29
4.3.1 Bedrock.....	29
4.3.2 Surficial Deposits.....	31
4.3.3 Significant High Hydraulic Conductivity Sediments.....	39
4.4 Hydrogeology	39
4.4.1 Bedrock.....	39
4.4.2 Surficial Deposits.....	41
4.4.3 Groundwater Elevations in the Study Area	42
4.4.4 Groundwater Elevations in the WNA	42
Chapter 5 Model Design and Callibration.....	47
5.1 Model Construction	47
5.1.1 Dimensionality.....	47
5.1.2 A Case for Steady State Representation	47

5.1.3 Code	49
5.1.4 Grid Design	51
5.1.5 Hydrostratigraphic Units	57
5.1.6 MODFLOW Layer Types	61
5.1.7 Boundary Conditions	61
5.2 Model Calibration	67
5.2.1 Calibration Targets and Associated Errors	67
5.2.2 Calibration Points and Target	70
5.2.3 Calibration Process	70
Chapter 6 Model Results and Sensitivity Analysis	74
6.1 Results	74
6.1.1 Parameter Values.....	74
6.1.2 Hydraulic Head Distribution and Groundwater Flow	74
6.1.3 Groundwater Velocities	78
6.1.4 Model Water Balance	83
6.2 Evaluation of Calibration.....	83
6.2.1 Methods	83
6.2.2 Evaluation of the Calibrated Model.....	85
6.3 Sensitivity Analysis.....	88
6.3.1 Effects of Varying Hydraulic Conductivity	90
6.3.2 Effects of Varying Recharge	95
6.3.3 Discussion.....	97
Chapter 7 Location of the WNA Recharge Area and Effects of Reduced Recharge on Groundwater Levels in the WNA.....	99
7.1 Location of the WNA Recharge Area.....	99
7.1.1 Particle-tracking Method.....	99
7.1.2 Location of the Recharge Area.....	100
7.1.3 Particle Travel Time.....	100
7.2 Sensitivity Analysis.....	102
7.2.1 Effects of Varying Hydraulic Conductivity	102
7.3 Reduced Recharge Scenarios.....	104
Chapter 8 Discussion, Conclusions and Recommendations.....	111
8.1 Discussion of Results	111
8.1.1 Regional Hydrogeology	111
8.1.2 Location of WNA Recharge Area.....	112
8.1.3 Effects of Reduced Recharge.....	113
8.1.4 Particle Travel Time.....	118
8.2 Conclusions and Recommendations	118
8.2.1 Conclusions.....	118

8.2.2 Recommendations	120
References	122
Appendix A: Borehole Logs	128
Appendix B: Locations of Wells Used in Cross-Sections	138

List of Tables

Table 5.1	Groundwater Levels in Representative Sections	49
Table 5.2	Wells Used as Calibration Points.....	73
Table 6.1	Water balance for Calibrated Model	84
Table 6.2	Residuals for Calibration Points	88
Table 8.1	Land Use Zoning in the WNA Recharge Area	117
Table B.1	Locations of Wells Used in Cross-Sections	138

List of Figures

Figure 1.1	Map Showing Area Considered by Study	2
Figure 1.2	Airphotograph of Wagner Natural Area	3
Figure 1.3	Map Showing Location of Proposed Recharge Area	6
Figure 3.1	Map Showing Distribution of Bedrock and Surficial Well Data	23
Figure 3.2	Airphotograph Showing Locations of Monitoring Wells in the WNA	25
Figure 4.1	Ground Surface Elevation Map	28
Figure 4.2	Stratigraphic Column of Sediments in Study Area	30
Figure 4.3	Bedrock Surface Elevation Map	32
Figure 4.4	Surficial Geology Map	34
Figure 4.5	Cross-section through West Side of Study Area	35
Figure 4.6	Cross-section through WNA	36
Figure 4.7	Cross-section through Big Lake	37
Figure 4.8	Isopach Map	40
Figure 4.9	Map of Groundwater Elevations in the Surficial Sediments.....	43
Figure 4.10	Graph Showing Correlation between Groundwater Elevations and Elevations of Bedrock and Ground Surfaces	44
Figure 4.11	Map Showing Regions where Groundwater Elevations are Above the Land Surface.....	45
Figure 4.12	Hydrographs for Monitoring Wells in the WNA.....	46
Figure 5.1	Model Domain Superimposed on Map of Groundwater Elevations in Surficial Sediments	52
Figure 5.2	Plan View of Model Domain	55
Figure 5.3	Sample Cross-section through Grid.....	56
Figure 5.4	Stratigraphic Column, Hydrostratigraphic Units, Calibrated and Reported Values of Hydraulic Conductivity.....	58
Figure 5.5	Plan View of Model Domain Showing Hydrostratigraphic Units in Model Layers 1 to 3.....	59
Figure 5.6	Plan View of Model Domain Showing Hydrostratigraphic Units in Model Layers 4 and 5.....	60
Figure 5.7	Boundary Conditions Implemented in the Model	63
Figure 5.8	Representation of Evapotranspiration Function.....	66
Figure 5.9	Locations of Calibration Points	71

Figure 6.1	Calibrated Hydraulic Head in Layer 1	75
Figure 6.2	Calibrated Hydraulic Head in Layer 3	76
Figure 6.3	Calibrated Hydraulic Head in Layer 5	77
Figure 6.4	Locations of Discharge Areas Predicted by the Model.....	79
Figure 6.5	Horizontal Groundwater Velocities in Layer 1	80
Figure 6.6	Horizontal Groundwater Velocities in Layer 3	81
Figure 6.7	Horizontal Groundwater Velocities in Layer 5	82
Figure 6.8	Graph of Simulated Heads versus Observed Heads	87
Figure 6.9	Change in RMS from Increasing and Decreasing Hydraulic Conductivity	91
Figure 6.10	Change in Evapotranspiration in the Central Discharge Area Resulting from Increasing and Decreasing Hydraulic Conductivity	93
Figure 6.11	Change in Evapotranspiration in the WNA Resulting from Increasing and Decreasing Hydraulic Conductivity	94
Figure 6.12	Change in RMS Error and Evapotranspiration Resulting From Increasing and Decreasing Recharge	96
Figure 7.1	Location of Recharge Area Predicted by Prosser and by Model.....	101
Figure 7.2	Sensitivity of the Location of the Recharge Area to Changes in Hydraulic Conductivity	103
Figure 7.3	Change in Time Required to Travel from the Recharge Area to the WNA Resulting from Increasing and Decreasing Hydraulic Conductivity	105
Figure 7.4	Map Showing Area where Recharge was Reduced.....	106
Figure 7.5	Map Showing Declines in Hydraulic Head in the WNA Resulting from Decreasing Recharge by 25 Percent.....	108
Figure 7.6	Map Showing Declines in Hydraulic Head in the WNA Resulting from Decreasing Recharge by 50 Percent.....	109
Figure 7.6	Map Showing declines in Hydraulic Head in the WNA Resulting from Decreasing Recharge by 100 Percent	110
Figure 8.1	Map Showing WNA Recharge Area in Relation to the Pitted Delta (east).....	114
Figure 8.2	Map Showing Land Use Zoning in the WNA Recharge Area	116

Chapter 1 Introduction

The Wagner Natural Area (WNA) is a conservation area protected under the Alberta *Wilderness Areas, Ecological Reserves and Natural Areas Act* (Mowat, 1987). It occupies more than 230 hectares, approximately 7 km west of the City of Edmonton, in Parkland County (Figure 1.1), and is renowned for its mineral-rich fen made up of wet meadows, marl ponds, black spruce and tamarack forest (Figure 1.2; Spencer, 1990). William Wagner originally owned the property; he recognized the uniqueness of the site and preserved it (Mowat, 1987). While neither bogs nor fens are rare in Alberta, the WNA is the only mineral-rich fen within 160 km of Edmonton, and is one of only a couple of such sites east of the Rocky Mountains and south of Fort McMurray (Vitt, 1982).

The WNA may be the most extensively studied natural laboratory in Alberta and is used for scientific research, educational and interpretive purposes (Spencer, 1990). Three factors significantly enhance the educational and research value of the WNA (Spencer, 1990). First, it exhibits unusually high biodiversity of flora and fauna species for its size. Second, Wagner is close to several population centres (Edmonton, Spruce Grove, St. Albert, and Stony Plain). Third, a significant portion of the natural area remains relatively undisturbed.

The overall biodiversity in the WNA is unusual for such a small area (Mowat, 1987); it hosts some 310 species of vascular plants, representing about 1/6 of the species in Alberta, and 16 of the 26 species of orchids found in the province (Vitt, 1982). Additionally, Wagner is home to over 2000 species of insects, three species of fish, six species of herptiles, 41 species of mammals and 138 species of birds; of these birds, 97 species are known to nest in the WNA (Spencer, 1990).

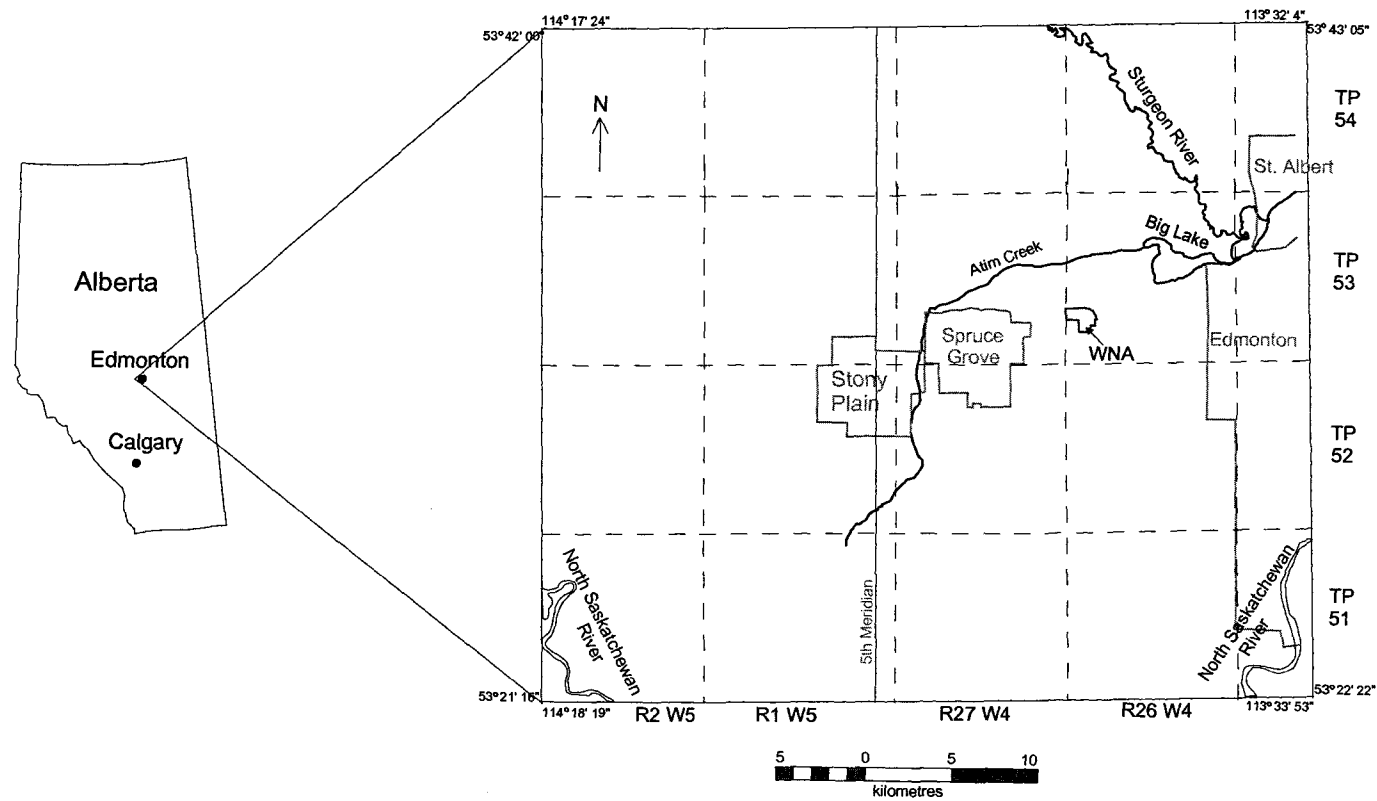


Figure 1.1 Map showing population centers, significant water features and the Wagner Natural Area (WNA) in the area considered by this study

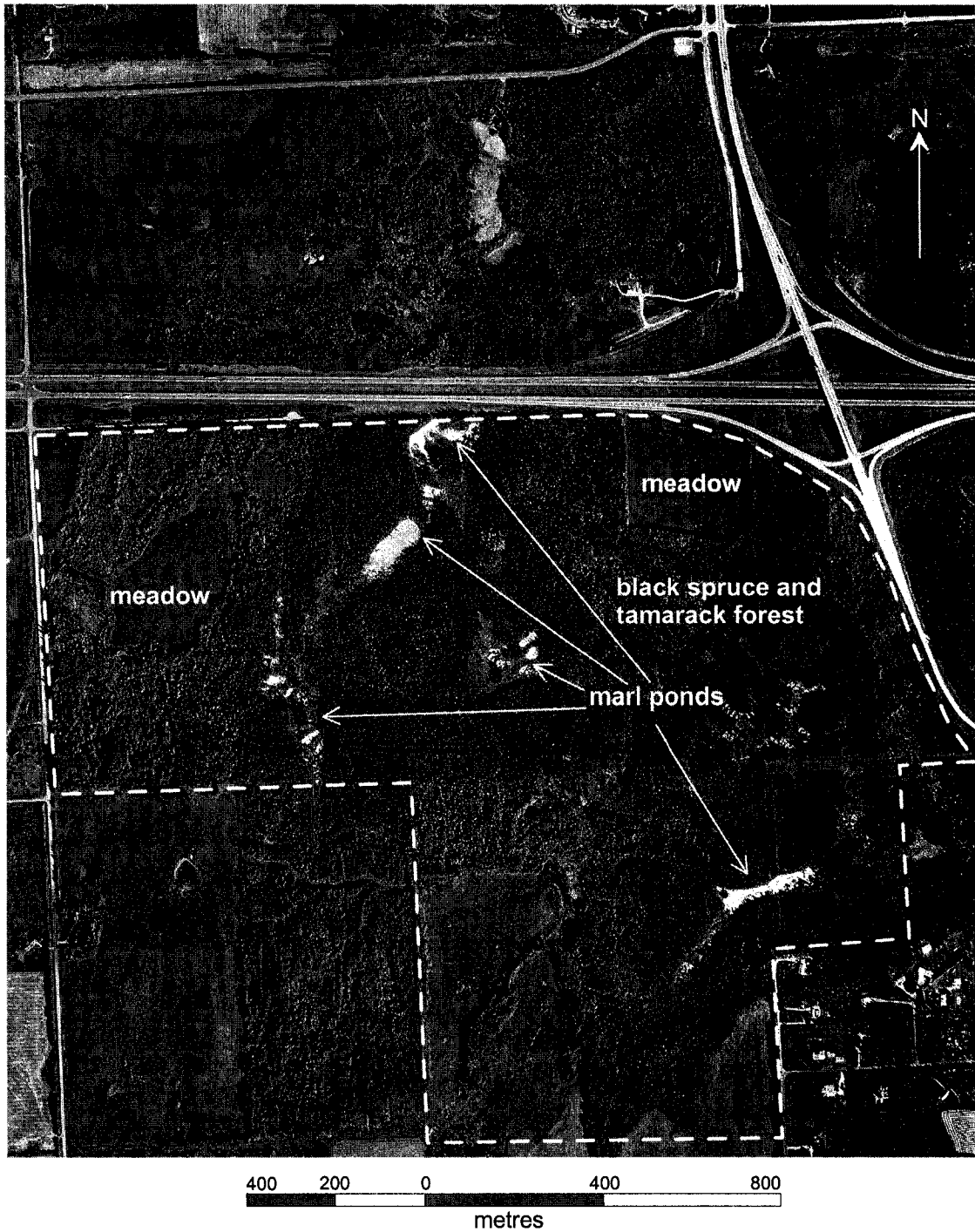


Figure 1.2 Wagner Natural Area (07-053-26-W4), dashed white line indicates boundaries of natural area, and white non-treed areas are marl ponds (airphotograph modified from UMA, 2000)

It is primarily due to its incredible biodiversity that this fen has been recognized as both a Provincial Natural Area and a Natural Ecological Monitoring Assessment Network (EMAN) site (Mowat, 1987). The Wagner Natural Area Society has applied to have the WNA considered as a UNESCO Index site (Miller, 2003).

The WNA is located within a groundwater discharge area and owes its diverse array of flora and fauna to the calcareous springs that flow year-round and precipitate marl (Prosser, 1982). These mineral-rich springs flow into a complex, diffuse drainage system that supports the natural area's diverse ecosystem in four ways (Mowat, 1987; Spencer, 1990):

1. It provides a constant supply of moisture and nutrients to the vegetation;
2. It mixes alkaline spring water with acidic boreal forest soil, a combination that fosters diverse habitats;
3. It has a stable temperature of 4°C, minimizing winter freezing and hastening spring thawing;
4. It reduces the risk of forest fire.

The long-term stability of the natural flow regime in the vicinity of the WNA is crucial for the protection of the rare and significant plants (Mowat, 1987). Increased urban development in the recharge area could threaten the WNA's biodiversity by adversely affecting the springs that flow within the natural area. First, development may reduce the quantity of water infiltrating into the groundwater flow system. Lower groundwater recharge rates would eventually manifest themselves as lower discharge rates. Lower discharge rates would subsequently result in decreased surface water levels. This could harm many species of the WNA that are adapted to specific moisture regimes.

Second, urban development carries the risk of groundwater contamination. Pollutants often linked to development include those associated with human sewage, leaking underground storage tanks, animal and feedlot waste, agricultural chemicals (e.g., insecticides, herbicides, and fertilizers) and urban runoff (e.g., hydrocarbons, pesticides, fertilizers, detergents, and solvents). Introduction of these pollutants into the groundwater system and their subsequent transport to the WNA discharge area may have a deleterious effect on the WNA ecosystem.

Spencer (1990) advocates effective land zoning regulations to restrict further residential, commercial and industrial development in the vicinity of the WNA and its recharge area. Such restrictions would protect the long-term integrity of the ecosystem (Spencer 1990).

Prosser (1982) hypothesized that the recharge area is 4 to 8 km south of the WNA (Figure 1.3), a region under increasing pressure from development (Spencer, 1990; Banack, 1992; UMA 2000). However, the recharge area has never been delineated.

Thus, the primary objectives of this study were to:

1. Characterize the regional groundwater flow system surrounding the WNA
2. Delineate the WNA recharge area
3. Quantitatively assess the effect changes in recharge would have on groundwater levels and discharge rates in the WNA.

To achieve these objectives, a three-dimensional numerical groundwater model of the WNA was constructed using MODFLOW (McDonald and Harbaugh, 1988). Calibration of the model was achieved using existing field data, provincial well data, and field data

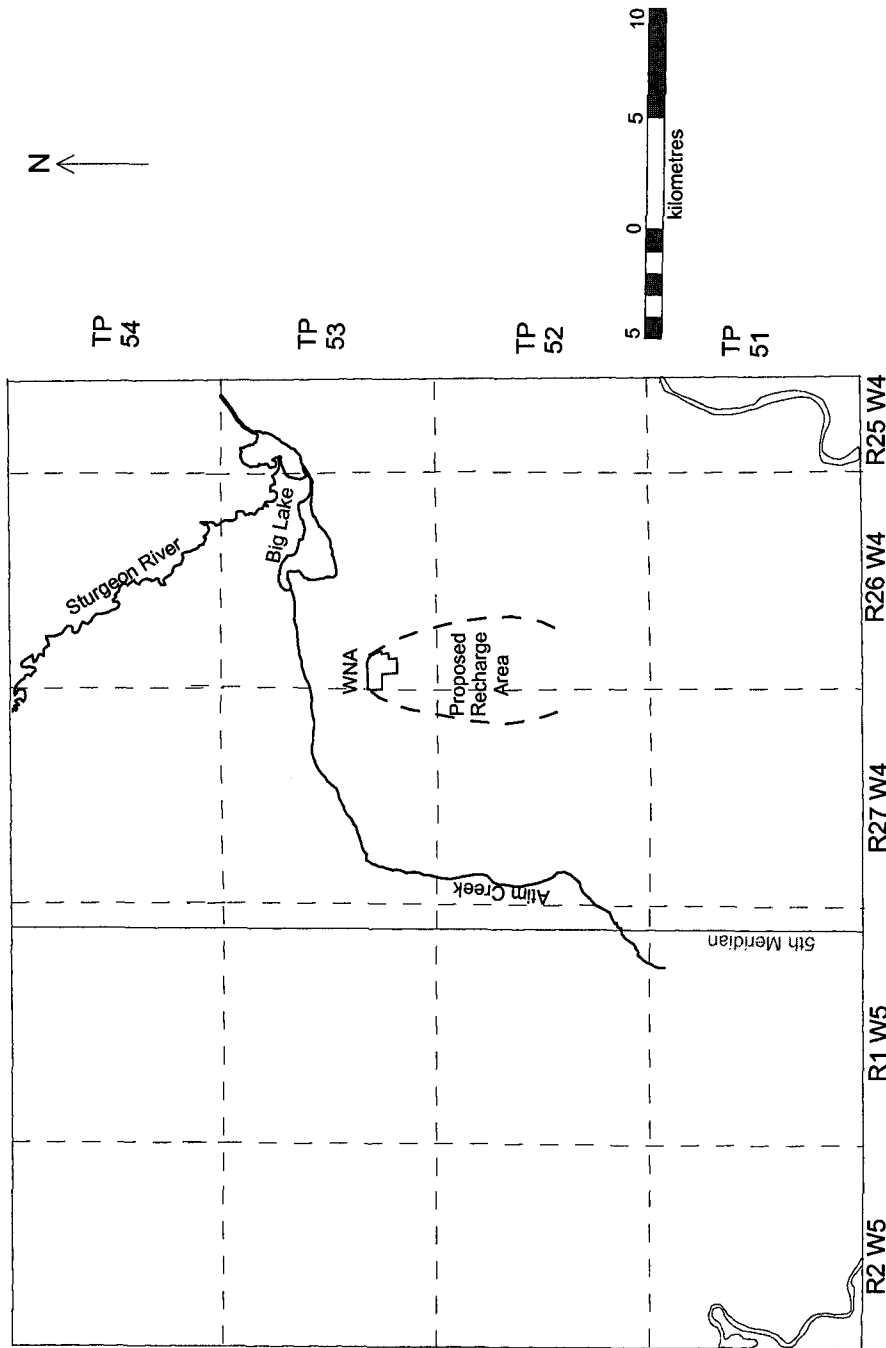


Figure 1.3 Location of WNA recharge area proposed by Prosser (1982) shown by dashed lines

collected during the course of this study. The calibrated model was then used to assess the potential effect of changes in recharge on groundwater levels and discharge rates within the Wagner Natural Area. In addition, MODPATH (Pollock, 1989), a particle-tracking program, was used to delineate the recharge area, map the flow paths, and determine the amount of time required for water molecules or solute particles to travel from the recharge area to the WNA.

Chapter 2 Theory and Background

The purpose of this chapter is to discuss briefly the important underlying concepts that provide the foundation for this study. Topics discussed in this chapter include: groundwater flow equations, groundwater flow systems, and the distinguishing characteristics of groundwater recharge and discharge areas.

2.1 Groundwater Flow Equations

Darcy's Law and the Continuity Equation are the fundamental equations that describe quantitatively how groundwater flows. Darcy's Law describes how fluid flows through a porous medium. The Continuity Equation describes net fluid motion into and out of a volume of porous medium.

2.1.1 Darcy's Law

Darcy's Law is the fundamental equation of hydrogeology. In one dimension

$$q = -K \frac{\partial h}{\partial l} \quad (2.1)$$

where: q is flux, K is hydraulic conductivity, and $\frac{\partial h}{\partial l}$ is the hydraulic head gradient in direction l .

Hydraulic conductivity, K , is a coefficient of proportionality that relates the rate at which water can move through a porous medium due to a hydraulic gradient; it is a function of the properties of the medium and the fluid passing through it.

Hydraulic head, h , is a measure of fluid potential, and describes the elevation of the water level in a well or piezometer. The following equation describes hydraulic head:

$$h = z + \psi \quad (2.2)$$

where: z is elevation head (measured from an arbitrary datum) and ψ is pressure head. Pressure head is the height to which water will rise in a well, and is measured from the screened interval.

2.1.2 The Continuity Equation (Steady State)

Steady state represents long-term average behaviour, without a trend. For this reason, it is a useful approximation for many groundwater systems. However, the steady-state approximation is appropriate only under the following two conditions: first, if the fluctuations in the water table are small relative to the total vertical thickness of the system; second, if the general configuration of the water table does not change during these minor fluctuations (Schwartz and Zhang, 2003).

In steady state systems, there can be no net change in mass of a fluid contained in a small volume of porous media. Flow into the volume is equal to flow out of the volume. Steady state groundwater flow through this volume can be defined by the following equation:

$$\frac{\partial}{\partial x} \left(K_x \frac{\partial h}{\partial x} \right) + \frac{\partial}{\partial y} \left(K_y \frac{\partial h}{\partial y} \right) + \frac{\partial}{\partial z} \left(K_z \frac{\partial h}{\partial z} \right) = 0 \quad (2.4)$$

Where: x , y , and z are the coordinate axes, and K_x , K_y , and K_z are the principal components of hydraulic conductivity along the axes.

2.2 Groundwater Flow Systems

Groundwater flow systems contain recharge and discharge areas. Tóth (1962, 1963) defined the relations between recharge areas and discharge areas in his extensive examination of groundwater flow systems in small drainage basins. A drainage basin as defined by Tóth (1963) is “an area bounded by topographic highs, its lowest parts being occupied by an impounded body of surface water or by a relatively low order stream and having similar physiographic conditions over the whole of its surface.” A groundwater flow system is “a set of flow lines in which any two flow lines adjacent at one point of the flow region remain adjacent through the whole region; they can be intersected anywhere by an uninterrupted surface across which flow takes place in one direction only” (Tóth, 1963).

Tóth (1962) demonstrated that simple groundwater flow systems are symmetrical, and can be subdivided into two limbs. The first limb is located between the recharge area and the midline, and the second limb is located between the midline and the basin bottom. Between the water divide and the midline net saturated flow is directed away from the water table (groundwater recharge). Between the midline and basin bottom, net saturated flow is directed toward the water table (groundwater discharge). At the midline net saturated flow is approximately parallel to the water table.

Tóth’s analytical approach led him to conclude that there is a hierarchical pattern of flow systems in a groundwater basin. He termed these systems: local, intermediate and regional (Tóth, 1963).

Local flow systems have a recharge area in a topographic high, and a discharge area in the adjacent topographic low. In intermediate systems there are one or more topographic highs between the recharge and discharge areas; however, the recharge and discharge areas do not necessarily occupy the highest and lowest points in the basin. Finally, in regional systems, the recharge area is located at the highest part in the basin and the discharge area occupies the lowest part of the basin (Tóth, 1963).

Tóth (1963) lists a general set of conclusions with respect to regional flow systems:

1. In flat lying areas of considerable extent, neither regional nor local systems will develop. Discharge occurs primarily by evapotranspiration. Groundwater flow is very slow and, as a result, groundwater in these flow systems typically has a high concentration of dissolved minerals.
2. In areas where local relief is negligible, a regional system will develop due to the slope of the topography.
3. In areas of well-defined relief, local flow systems will develop; the greater the relief, the deeper the flow system.
4. Local flow systems often exhibit a much higher flow velocity than regional flow systems.
5. Major streams in a basin are fed principally by local systems.
6. Groundwater at shallow depths is influenced by seasonal variations in recharge, while groundwater at greater depths is not influenced by such changes.

Groundwater flow system length influences groundwater chemistry. Tóth (1984) outlines the general relations between groundwater chemistry and flow system types:

1. Local flow systems are typically characterized by low total dissolved solids (TDS) concentrations, and water dominated by bicarbonate, calcium and magnesium. Groundwater chemistry may also change in response to meteorological events.
2. Intermediate flow systems are characterized by increased concentrations in TDS, and a greater variety of chemical species when compared to local flow systems. Intermediate flow systems also show greater concentrations in sodium, sulphate and chloride than local flow systems.
3. Regional flow systems typically have high concentrations of TDS, sodium and chloride when compared to local and intermediate flow systems.

2.3 Characteristics of Recharge and Discharge Areas

Groundwater recharge and discharge areas can be distinguished based on their characteristics. The following discussion is about recharge areas, discharge areas and some characteristic features that may be associated with them.

2.3.1 Recharge Areas

Recharge areas generally have deeper water tables than discharge areas and show more seasonal variation (Tóth, 1962). The water table in recharge areas responds dramatically to changes in recharge; they tend to be high in the late spring and early summer, and low in the fall and winter. Conversely, water tables in discharge areas are fairly stable throughout the year (Tóth, 1962).

Fetter (1994) lists several factors that control the amount of recharge to unconfined aquifers:

1. Net precipitation, which is the amount of precipitation not lost by interception, evapotranspiration or surface runoff;
2. The vertical hydraulic conductivity of the sediments in the recharge area, which determines the amount of water capable of infiltrating into the ground;
3. The transmissivity and potentiometric gradient of the porous media, which determine how much water can move away from the recharge area toward the discharge area; and,
4. The presence of standing water, and the depth of the water table.

Also, timing is an important factor controlling the amount of recharge. In the study area, recharge usually occurs in the late spring, when snowmelt provides moisture and low temperatures impede plant growth and transpiration (Bibby, 1974). During the growing season, recharge is inhibited because potential evaporation often exceeds precipitation (Alberta Environment, 1978). Potential evaporation is equal to “the water loss, which will occur if at no time there is a deficiency of water in the soil for the use of vegetation” (Thornthwaite, 1944). The variability of all of these factors leads to varying recharge rates in basins.

2.3.2 Discharge Areas

Discharge areas are usually located in topographic lowlands, and are characterized by shallow water tables that may be at, near or above the land surface.

It is often possible to map discharge areas by direct field observations of surface water and vegetation (Tóth, 1999). The presence of springs, seepage areas, streams, lakes,

wetlands, certain kinds of vegetation, and mineral deposits often indicate groundwater discharge.

Evapotranspiration

Evapotranspiration is a mechanism of groundwater discharge, and an important component of the hydrologic water balance. Evapotranspiration is the combined process of evaporation and transpiration. Evaporation is the net transfer of water in the soil from the liquid phase to the vapour phase in the atmosphere. Transpiration occurs during photosynthesis and is the process by which plants remove water from the soil and release it to the atmosphere as vapour through their leaves (Hillel, 1982). While evapotranspiration can occur anywhere, higher rates frequently occur in discharge areas because the water supply is not limited.

The rate of evapotranspiration is controlled by vegetation type, external evaporativity (i.e., wind speed, relative humidity, incoming solar radiation, and temperature) and the water transmitting properties of the soil (i.e., soil texture and moisture content) (Hillel, 1982). As a result, evapotranspiration rates vary spatially, and on a daily and seasonal basis (Shjeflo, 1968).

Typically the actual rate of evapotranspiration is compared to the potential rate of evapotranspiration. Actual evapotranspiration is equal to the field-measured rate of evapotranspiration. Potential evapotranspiration is “the amount of water transpired per unit time by a short green crop, completely shading the ground, of uniform height and never short of water” (Penman, 1956). Within the study area the actual rate of

evapotranspiration is less than potential evapotranspiration, because soil moisture is a limiting factor (Dr. Yongsheng Feng, 2000).

Springs and Seeps

Springs are small areas where groundwater discharges at the surface or within a water body. Springs can be ephemeral or permanent features, and the volume of water discharged from a spring can range from a small trickle to a large stream (Tóth, 1971). In contrast, seeps are areas where groundwater discharges at the surface at a rate less than or equal to that of local evapotranspiration (Tóth, 1971). As a result, there often is no direct evidence of a seepage area. However, both seeps and springs are commonly associated with various kinds of grass, phreatophytes and aquatic plants (Tóth, 1966). Springs and seeps commonly occur where the down-gradient part of an aquifer outcrops at the surface, such as on mountain slopes or canyon walls; they also occur along the base or break in slope of a hill where shallow water tables reach the surface (Tóth, 1966).

Phreatophytes

Phreatophytes, a group of water-loving and often salt tolerant plants, obtain their water from the zone of saturation (Meinzer, 1923). As a result, the presence of phreatophytes often indicates shallow water tables, and therefore groundwater discharge (Batelaan *et al.*, 2003).

Phreatophytes commonly occur in discharge areas because the water table is close to the surface and able to recover quickly from daily drawdown caused by the plants.

During the day, phreatophytes use significant amounts of water through the process of

photosynthesis and transpiration, which can lead to a lowering of the water table.

Phreatophytes depend on the nightly recovery of the water table; if the water table did not recover, the plants' water consumption would eventually lower the water table to a depth below the root zone and the phreatophytes would die, and be replaced by other plant types (Meyboom, 1967b).

Common phreatophytes on the Canadian Prairies include: Manitoba maple, salt grass, Baltic rush, sedges, alfalfa, alder, birch, oak, poplar, tamarack, willow and buffalo berry (Tóth 1966, 1999). Marsh marigold is another reliable indicator of groundwater discharge (Klijn and Witte, 1998; Rosenberry *et al.*, 2000). Phreatophytes are also found in areas where discharging groundwater is saline and evaporation rates are high. In this type of environment, salts may precipitate at the surface. Halophytes, salt-loving plants, are commonly found in these areas (Tóth, 1999).

Mineral Deposits

Precipitates and mineral deposits can be indicators of groundwater discharge.

Conditions that favour the precipitation of minerals are: evapotranspiration rates greater than groundwater discharge rates, groundwater with high concentrations of dissolved salts, a groundwater flow system with a residence time long enough to allow the dissolution of minerals, and low levels of precipitation (Tóth, 1971). Salts containing sodium, calcium, magnesium, and chloride and sulphate are most common (Tóth, 1971).

Marl is another common groundwater precipitate found in discharge areas. Marl is a soft, friable, fine-grained freshwater limestone, and is usually found in ponded discharge sites (MacDonald, 1984). Marl forms when calcium carbonate is leached from the drift

or shallow bedrock in the recharge area by infiltrating, acidic groundwater. Calcium and carbonate ions are then transported from the recharge to the discharge area by groundwater flow. These ions remain in solution during transport, due to the high partial pressure of carbon dioxide in the groundwater. However, once the groundwater is discharged, carbon dioxide is removed from the groundwater, resulting in a reduction of the partial pressure of carbon dioxide. This decrease in partial pressure of carbon dioxide reduces the solubility of the calcium and carbonate ions, and causes the precipitation of calcium carbonate, or marl (MacDonald, 1982).

Conditions that favour the formation of marl are those that maximize the leaching of calcium carbonate from sediments in the recharge area by infiltrating groundwater. Leaching is maximized in humid areas with highly permeable recharge areas, because these conditions generally result in enhanced recharge. Spruce forest cover also contributes to the formation of marl. Spruce trees tend to acidify the soil, and calcium carbonate is more soluble under acidic conditions. Thus, spruce cover increases the dissolution of calcium carbonate, and may contribute to the formation of marl. In addition, locally strong topographic relief, which enhances hydraulic gradients, and short groundwater flow systems contribute to the formation of marl (MacDonald, 1984). Such systems are characterized by groundwater dominated by calcium and bicarbonate.

Wetlands

Wetlands are areas where the water table is at, near, or above the ground surface long enough to promote the development of hydric soil, hydrophytic vegetation, and biological activities adapted to wet environments (Price and Waddington, 2000). Wetlands are classified as either mineral-soil or peatland. Mineral wetlands produce little or no peat

because of climatic or edaphic conditions, and include marshes, shallow water and some swamps (Zoltai and Vitt, 1995). Peatlands are wetlands with an accumulation of peat greater than 40 cm, and include bogs, fens and some swamps (National Wetland Working Group, 1997).

Wetlands comprise 14 percent of the land area in Canada, and Canadian wetlands account for approximately 24 percent of the world's wetlands (Price and Waddington, 2000). In Alberta, wetlands account for about 21 percent of the land area (National Wetland Working Group, 1997).

Wetland development is related to regional groundwater conditions and surface water drainage patterns (Winter, 1999). Wetlands can be located in recharge areas, and act to recharge the groundwater system; alternatively, they can be located in discharge areas, where they are sustained by discharging groundwater (Siegel, 1988a). Wetlands can also develop in areas where surface water is relatively stagnant (Winter, 1999).

The delicate balance between precipitation and evapotranspiration sustains wetlands; this makes them vulnerable to the effects of changes in land use in the surrounding areas, and to changes in climatic conditions (Clair, 1988; Covich *et al.*, 1997). Van der Kamp *et al.* (2003) state that the water balance of prairie wetlands is governed by the cold semi-arid climate. Annual potential evaporation usually ranges between 600 mm and 1000 mm, and exceeds annual precipitation, which typically ranges between 300 mm and 500 mm. During the generally long and cold winters, soils freeze to depths of 1 m or more. Winter snowfall accounts for less than 10 mm to 150 mm of water equivalent.

Wetland classification is difficult, complicated and the subject of much debate (Bridgham *et al.*, 1996). Historically, wetland classification has been based on topography, ontogeny, hydrology, water chemistry, and/or plant community composition (Bridgham *et al.*, 1996). Details on wetland classification are beyond the scope of this study, but can be found in Sjörs (1961); Moore and Bellamy (1974); Cowardin *et al.* (1979), Damman (1986); Glaser and Janssens (1986); and the National Wetlands Working Group (1988, 1997).

Zoltai (1988) provides an excellent description of bogs and fens. Each of these wetland types is briefly summarized here. Bogs are peat-covered wetlands, and are sustained by precipitation. Vegetation in bogs shows the effects of a high water table and a general lack of nutrients. The surface of a bog is often raised and therefore isolated from mineralized soil water. As a result, the surface waters of bogs are acidic and the upper peat layers are nutrient deficient. The pH of the groundwater is usually less than 4.6. Electrical conductivity values are also low (less than 80 $\mu\text{S}/\text{cm}$), due to the low concentrations of dissolved minerals. Bogs are often sources of groundwater recharge (Siegel, 1988b).

Like bogs, fens are peatlands characterized by a high water table. However, unlike bogs fens are fed by springs and are often located in groundwater discharge areas (Siegel, 1988b; Zoltai, 1988). Their associated recharge areas may be immediately adjacent or several kilometres away, depending on the scale of the flow system (Siegel, 1988b). Fens are typically more minerotrophic (mineral-rich) than bogs, because they are fed by discharging groundwater, enriched by dissolved upslope materials (Zoltai, 1988). For this reason, fens are able to support a diverse ecosystem and are ecologically valuable (Bateiaan *et al.*, 2003).

Fens can have a range of nutrient levels: some are mineral-rich and have high concentrations of calcium and magnesium, while others are extremely nutrient deficient (Batelaan *et al.*, 2003). However, most fens have moderate nutrient levels and are slightly acidic, with pH ranging from 5.5 to 6.0 (Zoltai, 1988). The nutrient concentrations in discharging groundwater have a significant effect on the vegetation found in fens. Fens can be classified by vegetation type. According to this classification scheme, there are three basic types of fens: graminoid fens without trees or shrubs, shrub fens, and tree fens. These three classes correspond to low, moderate and high levels of nutrients (Zoltai, 1988).

Fens fed by springs are often long, narrow, minerotrophic and characterized by open stands of sedges and a series of pools dammed by peaty ridges (Zoltai, 1988). These ridges may receive less spring water, and therefore develop a less minerotrophic vegetation. If the discharging spring water contains large amounts of dissolved solids, these fens can be locations of marl deposition (Zoltai *et al.*, 1988).

Based on the information presented in this chapter, it can be concluded that the Wagner Natural Area is a mineral-rich tree-fen composed of marl ponds, stands of black spruce and tamarack trees that hosts many common types of phreatophytes including: sedges, rushes, birch, poplar, and marsh marigold.

Chapter 3 Data Collection and Processing

3.1 Data Origin and Quality

Data used in this study came from a number of sources, including that published by Hydrogeological Consultants Ltd. (HCL) (1998a, 1998b), and Alberta Environment (2003). In addition, some drilling and water level monitoring was done in the WNA.

All of the data used to prepare this thesis is in NAD 83 10TM coordinates. Alberta Environment (2003) provided a digital elevation model (DEM), with a 25 m grid spacing.

Well logs used in this study were supplied by HCL. While well logs are available to the public from Alberta Environment, these reports are of varying degrees of quality and the well location is reported only to the nearest quarter section. Thus, the spatial resolution of the Alberta Environment data is not very high. HCL has improved upon the Alberta Environment database by georeferencing many of the wells with complete (detailed lithologic description, completion interval, and a static water level) well records (HCL, 1998a; 1998b).

Of the 9052 wells originally identified in the study area, 4249 had complete well records. Of the complete wells, 2953 were field verified and spatially referenced by HCL or the researcher. A global positioning (GPS) unit was used to determine the northings and eastings of the well. Of the 2953 georeferenced wells, 362 were constructed with completion intervals in both bedrock and surficial aquifers. Groundwater levels from these wells with multiple aquifer completion were not used, as groundwater levels measured in these wells would reflect the interaction of both bedrock and surficial heads.

The remaining 2591 wells (1135 surficial and 1456 bedrock) provided the data used to prepare the maps, cross-sections and model presented in this thesis. Figure 3.1 shows the distribution of the wells in the study area.

3.2 Preparation of Maps

Bedrock surface and surficial groundwater elevation maps presented in Chapter 4 were made using complete and georeferenced well records from HCL's database.

3.2.1 Bedrock Surface Mapping

Bedrock elevations were determined by subtracting the depth to bedrock from the surface elevation for each well that encountered bedrock. These elevations were then contoured using a computer-contouring program, Surfer 7 (Golden Software Inc, 1999). An automatic contouring technique was chosen over manual contouring simply because of the large number of data points used in this study.

Surfer 7 can use a variety of methods for producing contours. Kriging was used to develop the maps presented in this thesis. Kriging is a statistical interpolation method that works well with most data sets (Golden Software Inc., 1999). This method assumes the variable is a random function whose spatial correlation is defined by a variogram (Anderson and Woessner, 1992). A variogram is a function that describes the change in the variable with distance (Golden Software Inc, 1999). The default variogram and search radius of 2000 m was used to prepare the initial maps. The default variogram is a simple linear model and usually generates acceptable results (Golden Software Inc., 1999). After much experimentation with different search radii, it was found that a search

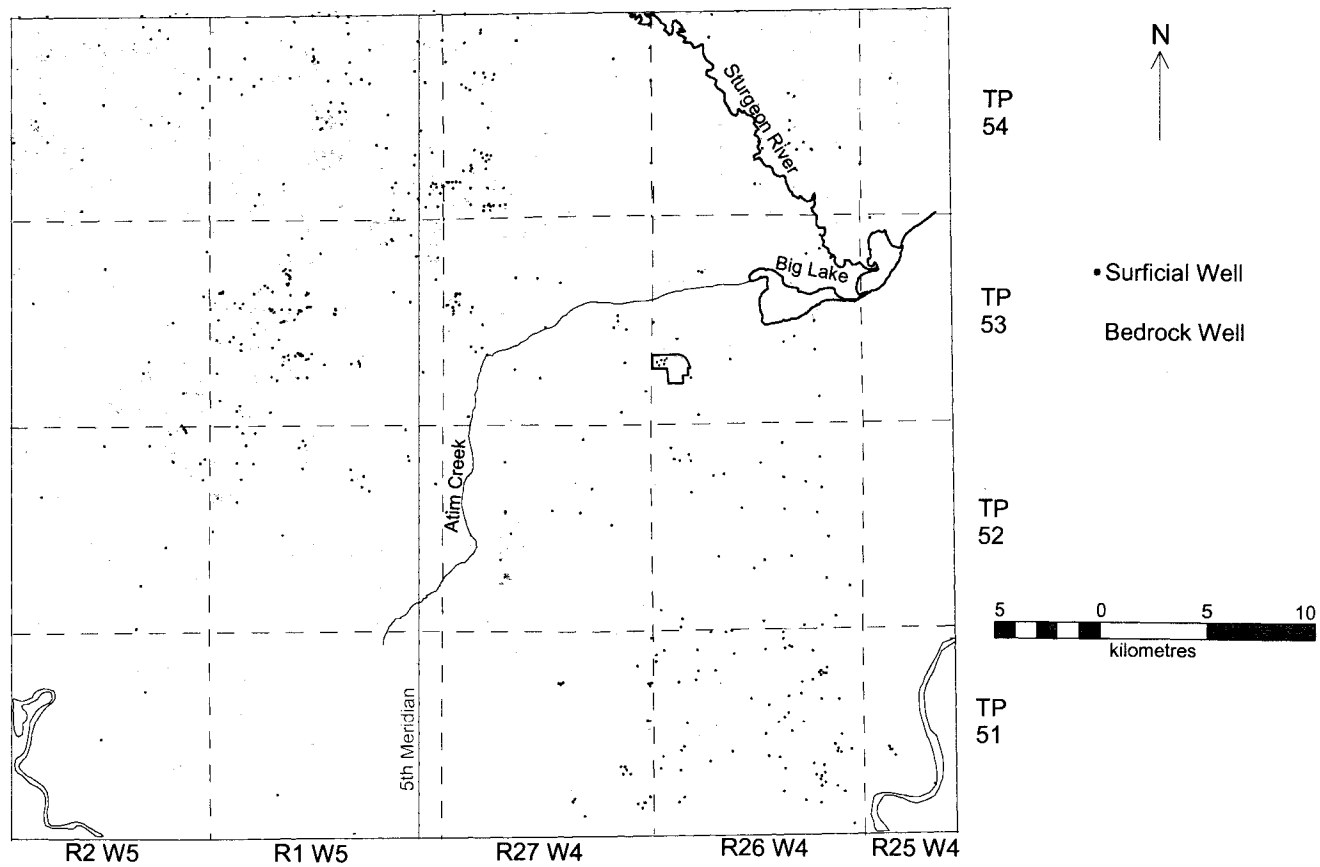


Figure 3.1 Map showing distribution of bedrock (1453 wells) and surficial (1127 wells) data

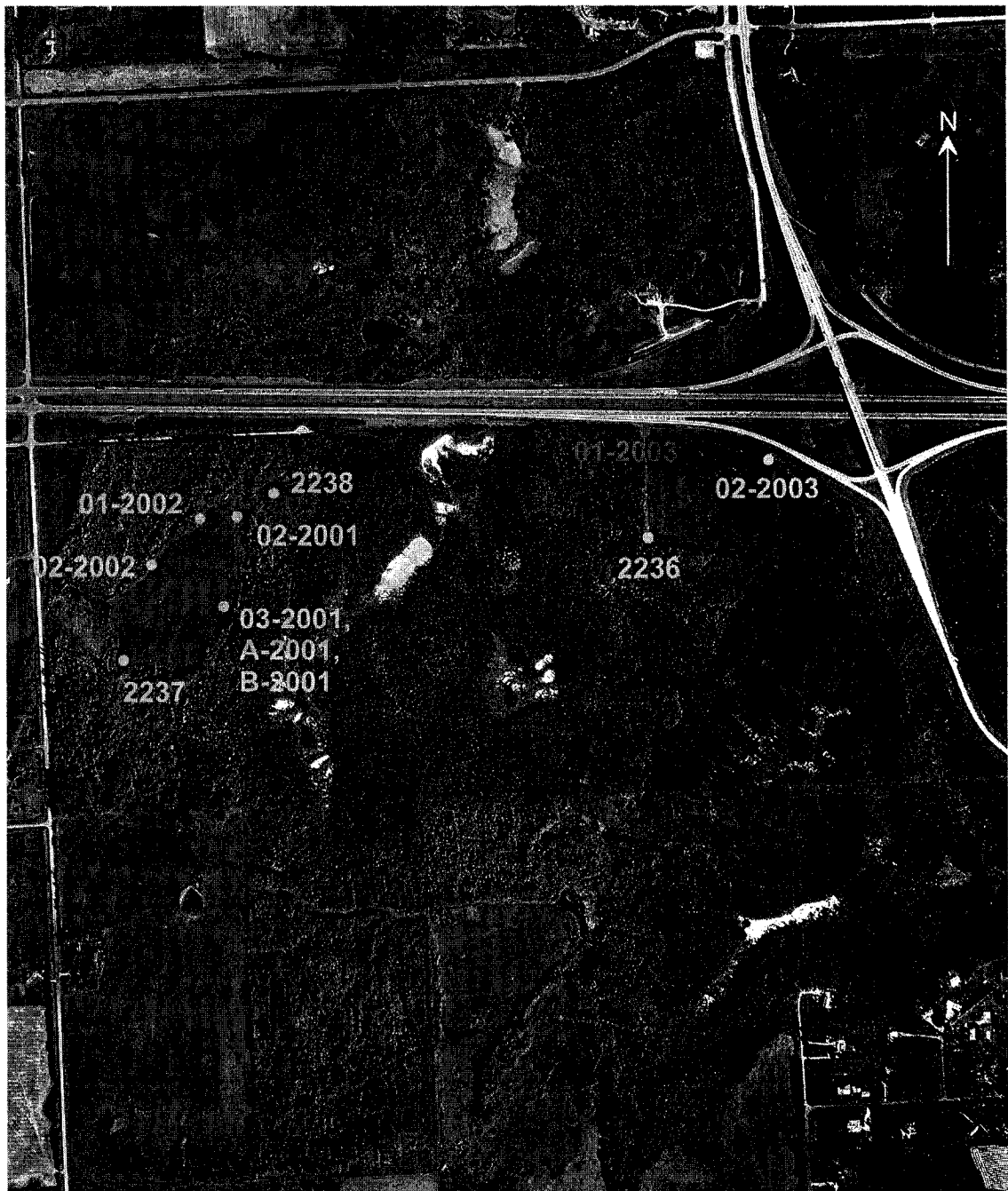
radius of 2000 m gave the most reasonable approximation. An interpretation was then applied to these maps produced with Surfer 7. Surfer data files were edited to reflect the interpretation, by adding or deleting data points, and by changing elevation values. The maps produced with the edited data files have smoother contours, and better-defined features than those initially made with Surfer 7. The bedrock surface map is presented and discussed in Chapter 4.

3.2.2 Groundwater Elevation Mapping in Surficial Sediments

Wells were classified as either surficial and bedrock based on the completion interval. Wells with a completion interval above the top of bedrock were classified as surficial wells; those with a completion depth below the top of bedrock as bedrock wells. Total head was calculated for each well by subtracting the static water level, measured from the top of the well casing, from the ground elevation. The groundwater elevation map was made using Surfer 7 to contour total hydraulic head. An interpretation was applied to this map using a method similar to that used to create the bedrock map.

3.3 Field Work

Alberta Environment installed three monitoring wells (2236, 2237, and 2238) in the Wagner Natural Area in 1985 (Figure 3.2). These wells were completed in the surficial sediments and shallow bedrock. During the course of this research project, three drilling programs were carried out in cooperation with the Northern Alberta Institute of Technology's (NAIT) hydrogeological field school in April of 2001, 2002 and 2003. During these programs, six groundwater monitoring wells, were completed in the surficial sediments (5 wells; 02-2001, 03-2001, 01-2002, 02-2002, 02-2003) and shallow bedrock (1 well; 01-2003), using a combination of mud-rotary and auger rigs (Figure



* Monitoring well completed in surficial sediments

* Monitoring well completed in bedrock



Figure 3.2 Locations of monitoring wells in the WNA, location of WNA shown in Figure 1.1 (airphotograph modified from UMA, 2000)

3.2). Additionally, two shallow monitoring wells (A-2001, B-2001) were installed by the researcher next to monitoring well 03-2001 to form a nest. Groundwater levels were monitored from January 2001 to January 2003. Typically, groundwater levels were measured on a weekly basis from April until November, and on a monthly basis for the remainder of the year. Borehole logs are in Appendix A.

Chapter 4 Physical Setting

4.1 Climate

The climate of the study area is continental (Kathol and McPherson, 1975). Continental climates are characterized by extreme disparities in summer and winter temperatures, and relatively low precipitation, which occurs mostly in the summer (Aguado and Burt, 2003). Summers are relatively warm, with an average daily temperature of 14 °C between May and September; winters are cold, with an average daily temperature of –7 °C between November and March (Environment Canada, 2004). Annual precipitation ranges between 300 and 640 mm, averaging 480 mm (Environment Canada, 2004). Seventy percent of the precipitation is in the form of low intensity rains between May and September (Bibby, 1974).

4.2 Surface Topography and Features

A broad valley that extends from Big Lake west to Stony Plain characterizes the study area. North and south of the valley, the land rises gently toward local topographic highs. To the west, the land is considerably more hummocky than the rest of the study area (Figure 4.1).

Within the study area, there are three geographically significant surface water features: Big Lake, Atim Creek and the Sturgeon River, in addition to many scattered wetlands (Figure 4.1). Big Lake is located in the topographic low in the northeast corner of the study area and has an average elevation of 650.6 m, but fluctuates between 650.0 m and 651.5 m (UMA, 2000). The Sturgeon River flows through Big Lake; it enters from

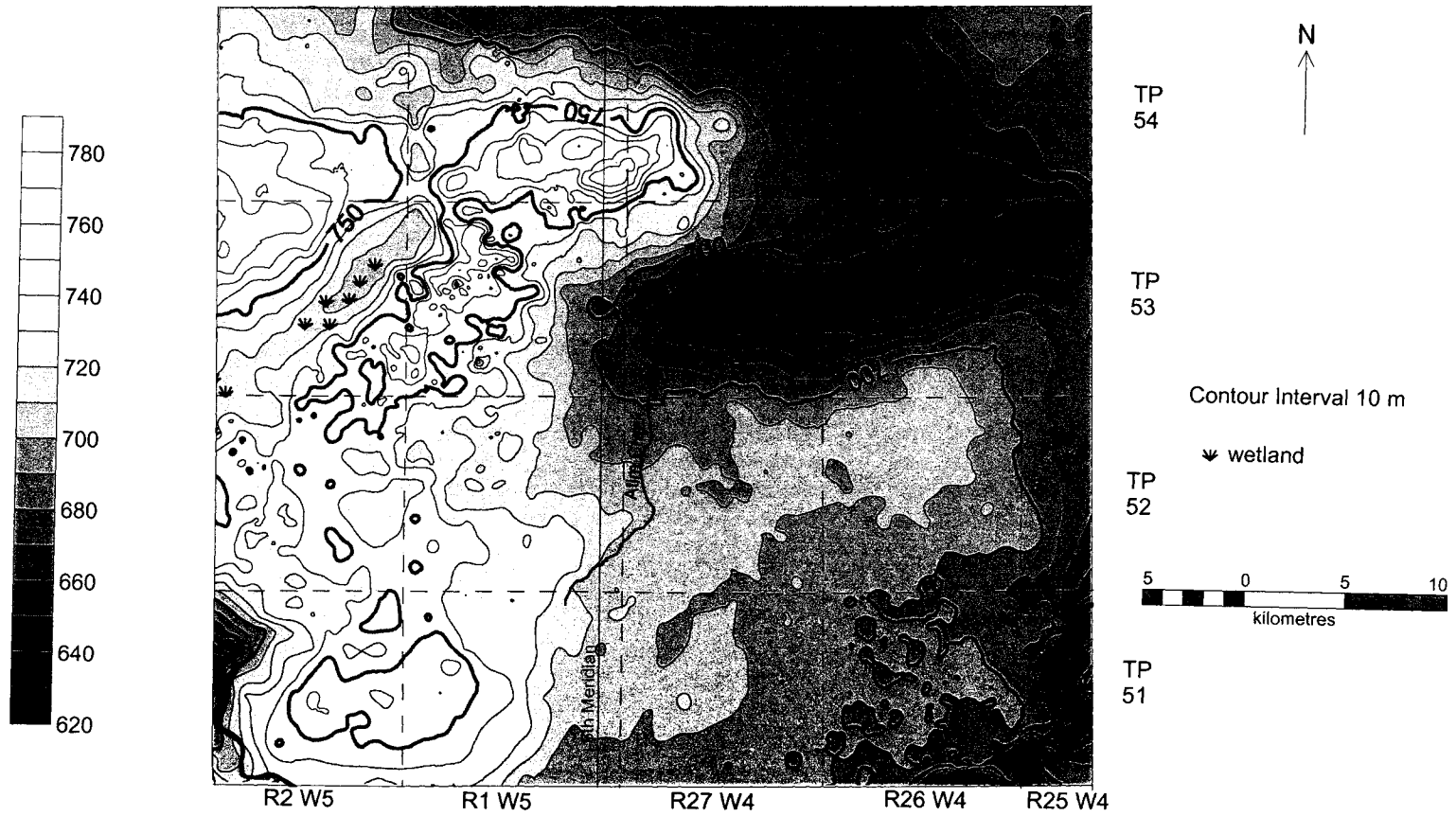


Figure 4.1 Ground surface elevation map, average elevation of Big Lake 650.6 m (UMA, 2000)

the northwest and exits from the northeast and flows toward St. Albert. Atim Creek also flows into Big Lake, though it originates in the southwest of the study area.

4.3 Geology

Figure 4.2 depicts a generalized stratigraphic column of the sediments found within the study area, and the following sections describe these sediments. Information is presented by deposit age, from oldest to youngest.

4.3.1 Bedrock

Near the surface, the bedrock is the poorly consolidated, Horseshoe Canyon Formation of Late Cretaceous age (Kathol and McPherson, 1975). It has a regional northwest-southeast strike and a dip of 1 in 300 to the southwest (Stein, 1993). The upper surface of the Horseshoe Canyon Formation was eroded extensively during the Tertiary and early Pleistocene (Kathol and McPherson, 1975). As a result its thickness ranges between 140 m and 190 m, averaging about 170 m (Carlson, 1967).

Bedrock Lithology

The Horseshoe Canyon Formation was deposited in a swampy deltaic environment, which was occasionally flooded by the sea (Stein, 1993). It is composed of fresh and brackish water sandstones, siltstones and shales (Irish, 1970). In addition, coal seams, concretionary ironstone and thin beds of bentonite are also present (Andriashek, 1988). The beds in Horseshoe Canyon Formation are lensoidal and extensively interbedded (Stein, 1993). Thus, the extremely variable nature of this formation makes it difficult to map individual beds, even over short distances (Kathol and McPherson, 1975).

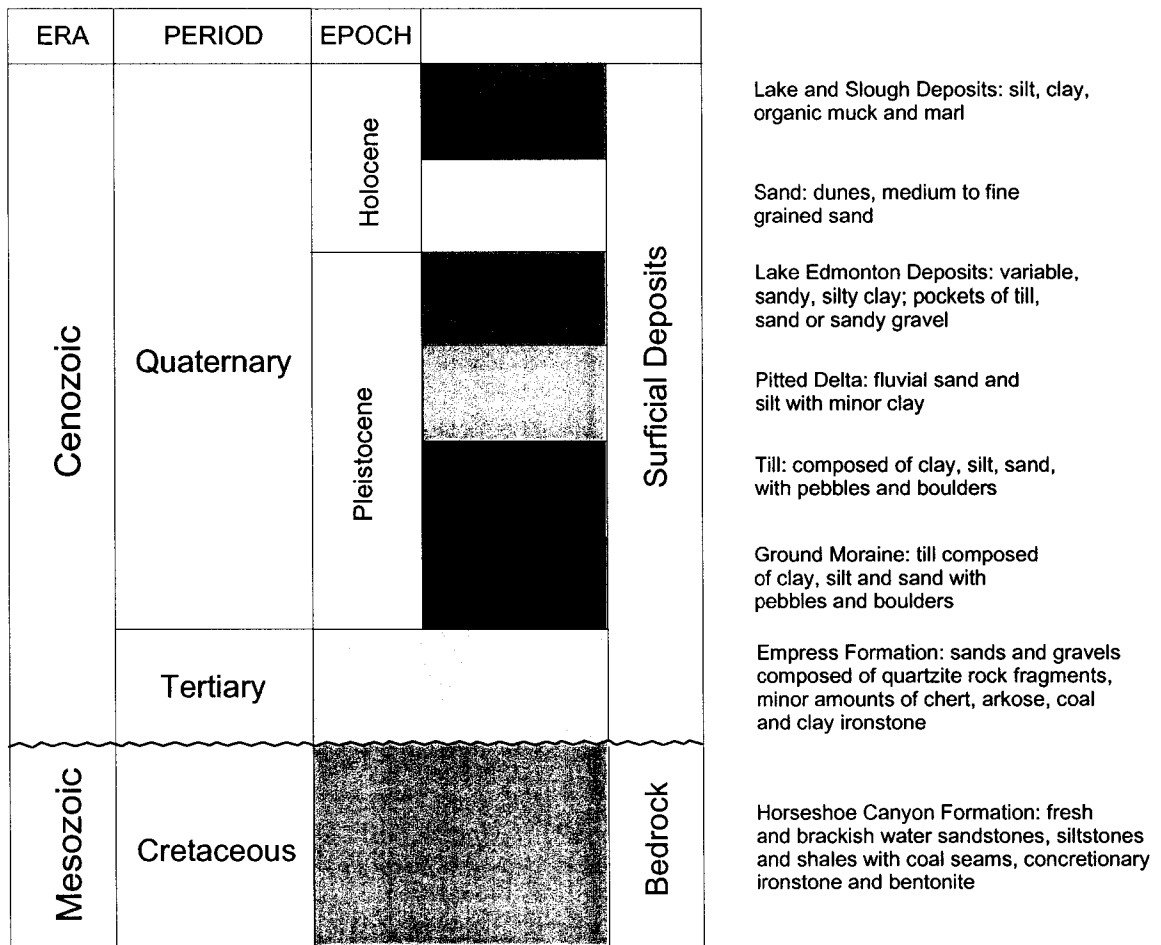


Figure 4.2 Stratigraphic column of sediments in the study area (Bayrock and Hughes, 1962; Kathol and McPherson, 1975; and Lehner, 1979)

Preglacial Valleys

A series of valleys developed as a result of erosional processes on the bedrock surface before glaciation. These preglacial valleys form a dendritic drainage pattern, in which the Beverly Valley is the major drainage feature (Figure 4.3). The Beverly Valley is up to 8 km wide, and approximately 60 m deep with gently sloping walls, and is filled with sands and gravels of the Empress Formation, till, and glacial Lake Edmonton deposits (Kathol and McPherson, 1975). It trended eastward from the eastern slopes of the Rocky Mountains (Stein, 1993). Within the study area, it drained the preglacial Onoway Valley from the north (Carlson, 1967) (Figure 4.3). The position of the Beverly Valley is expressed on the land surface by the topographic low that extends from north of Stony Plain to Big Lake (Kathol and McPherson, 1975) (Figure 4.1).

The Onoway Valley trends from northwest to southeast through the northeastern corner of the study area. The Onoway Valley is approximately 4 km wide and less than 40 m deep (Hydrogeological Consultants, 1998b) (Figure 4.3).

4.3.2 Surficial Deposits

Empress Formation

The preglacial sands and gravels of the Empress Formation line the bottoms of the buried valleys of the study area (Bayrock and Hughes, 1962). The gravels are composed of quartzite rock fragments, and minor amounts of chert, arkose, coal, and clay ironstone; the lithology of the sand is similar, but contains a higher percentage of local bedrock material (Kathol and McPherson, 1975). The Beverly Valley contains the greatest thickness of sands and gravels of the Empress Formation in the study area;

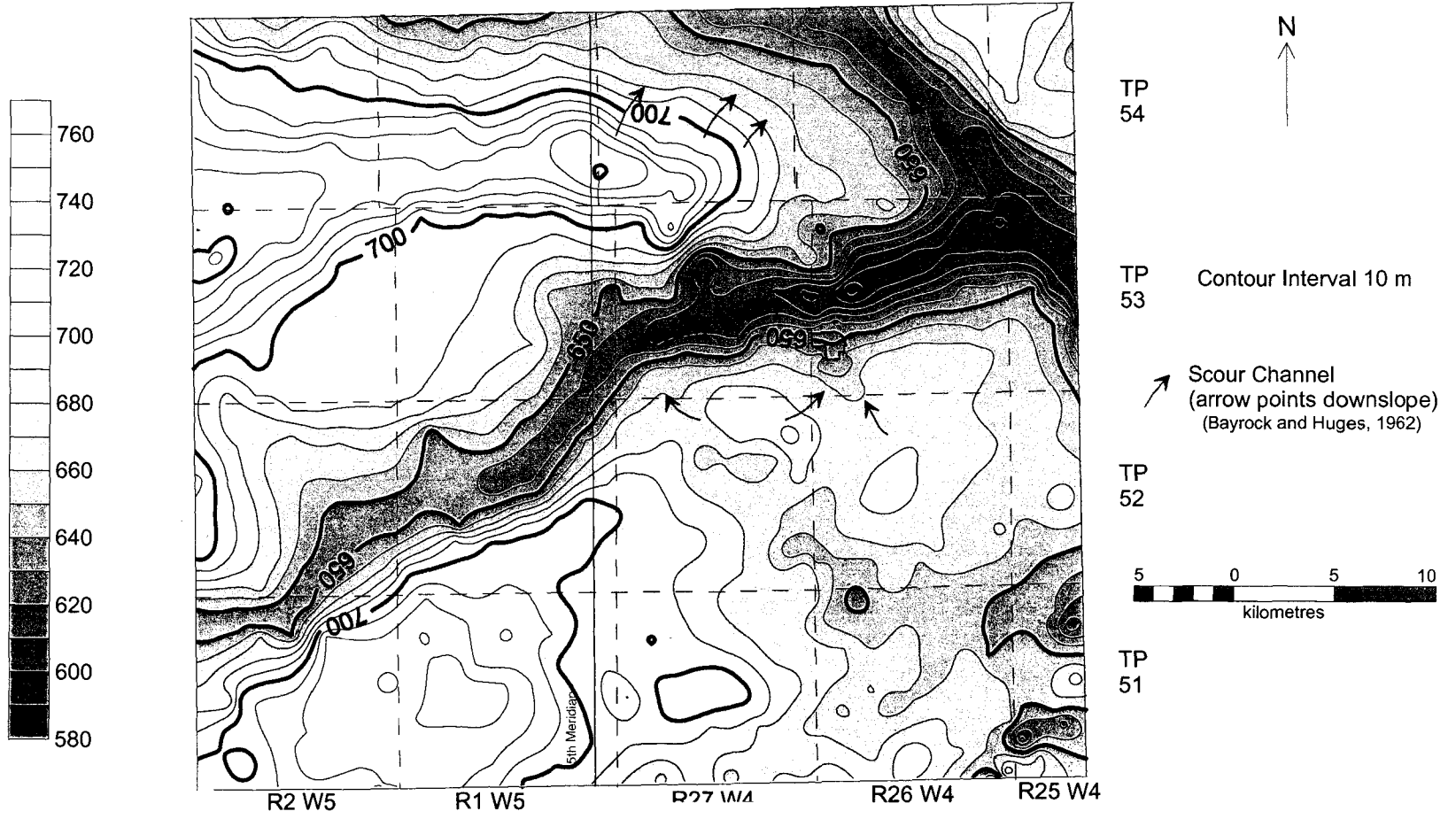


Figure 4.3 Bedrock surface elevations

approximately 15 m of fine-grained sand overlies as much as 5 m of gravel (Kathol and McPherson, 1975).

Lake Edmonton Deposits

Much of the study area is covered by proglacial Lake Edmonton deposits (Figure 4.4), which are composed of clay, silt, sand and gravel (Bayrock and Hughes, 1962; Andriashek 1988). The composition of the Lake Edmonton deposits is highly variable and can range from pure sand to pure clay (Bayrock and Hughes, 1962). The thickness of the Lake Edmonton deposits is variable, and ranges between a few metres to over 50 m. Approximately 20 m of Lake Edmonton deposits overlie the Beverly Valley (Andriashek, 1988).

The Lake Edmonton deposits were deposited by glaciofluvial meltwater in an ice-contact deltaic environment during the developing stages of Glacial Lake Edmonton, and are characterized by thin beds of clay, silt, sand, and gravel (Bayrock and Hughes, 1962; Andriashek 1988). Due to the nature of the depositional environment, the stratigraphy of the Lake Edmonton deposits is complicated and three-dimensional, making it difficult to trace individual beds over short distances and from one well to the next. This point is illustrated by Figures 4.5 to 4.7, which show south to north cross-sections through the study area. Locations of the wells shown in these cross-sections are listed in Appendix B.

Pitted Deltas

Some of the Lake Edmonton deposits contain significant amounts of sand, and are characterized by a hummocky topography; these deposits are known as pitted deltas

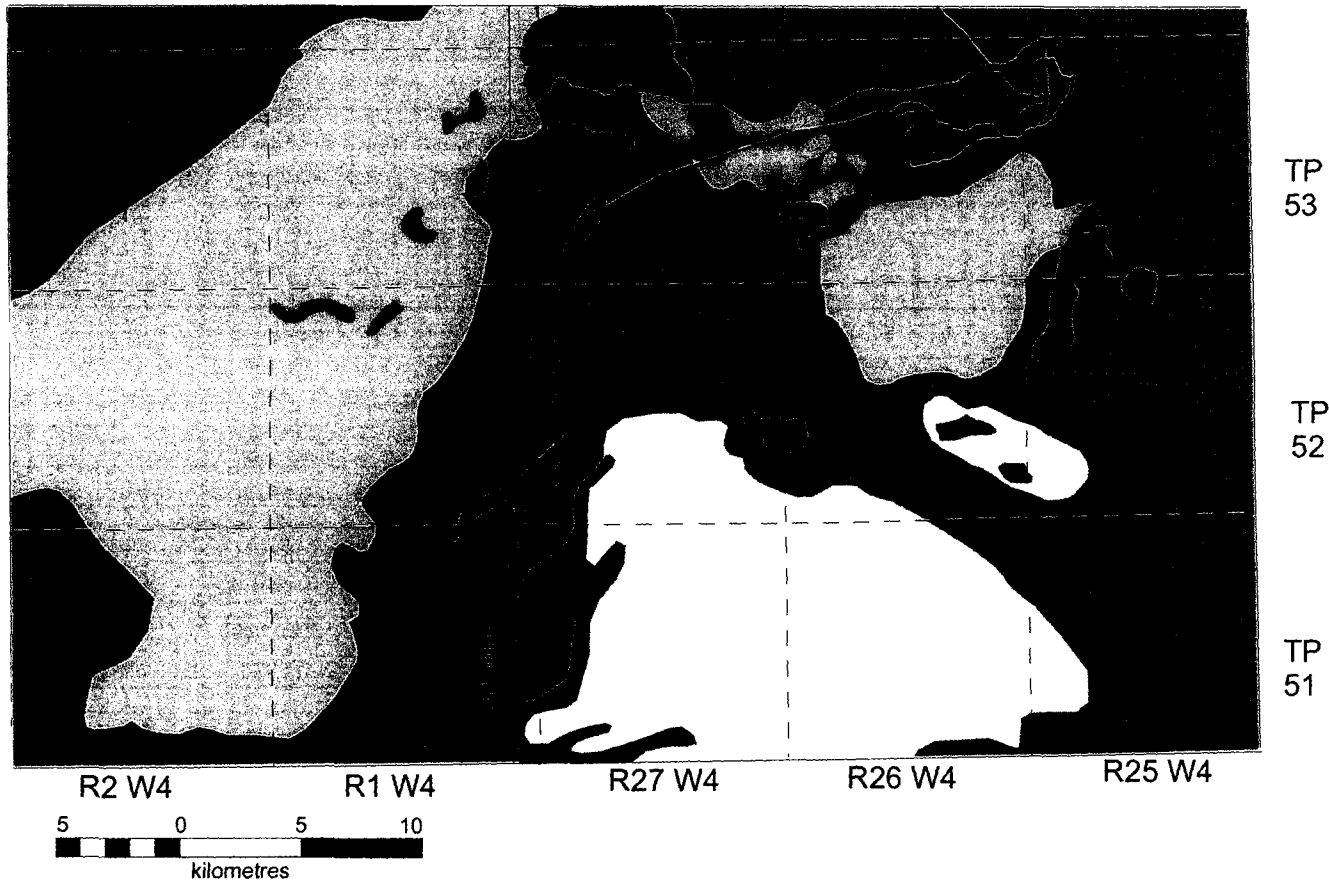


Figure 4.4 Surficial geology (adapted from Bayrock and Hughes, 1962; and Lehner, 1979) legend shown in Figure 4.2

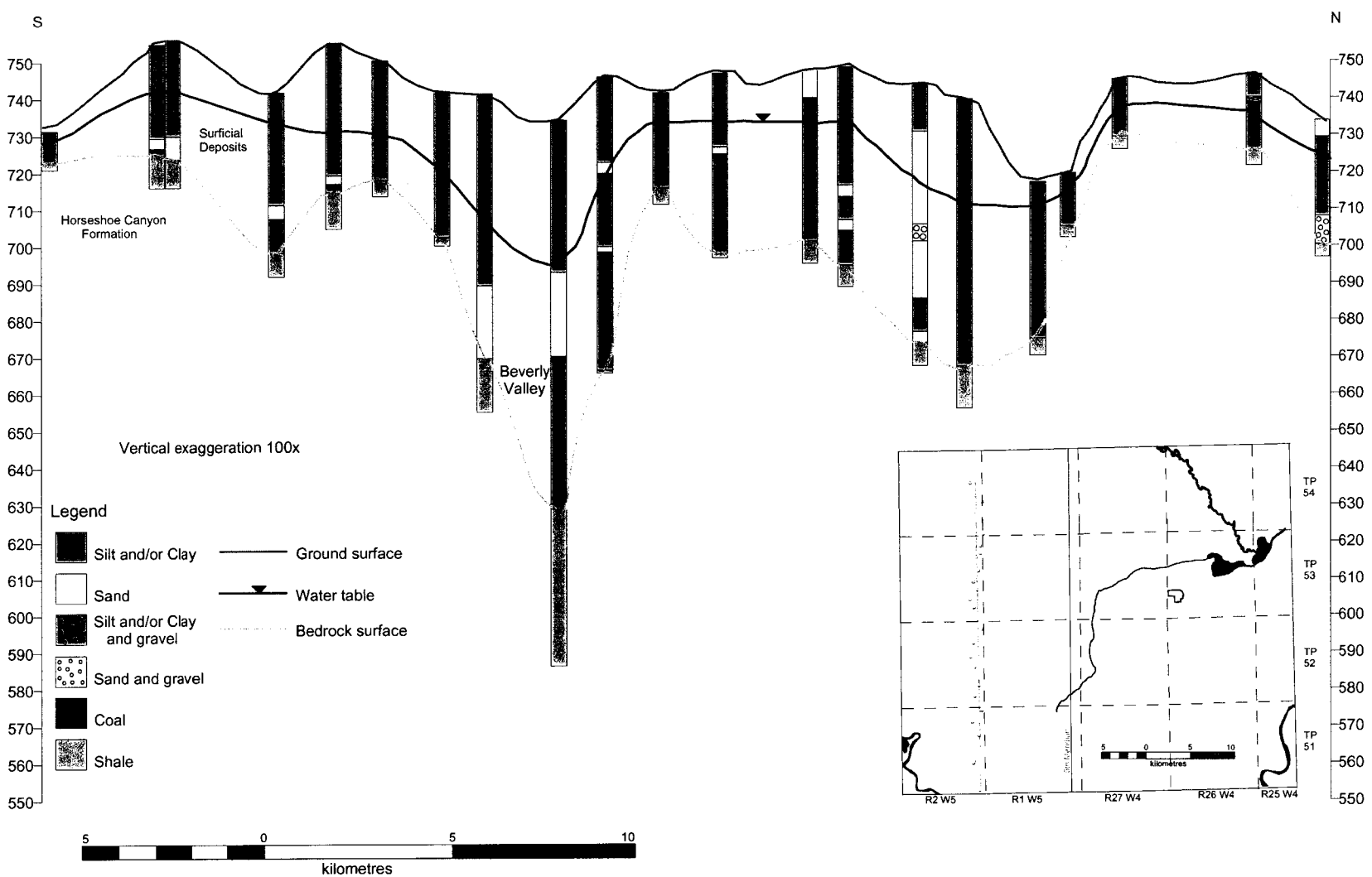


Figure 4.5 South to north cross-section through western side of study area (well locations in Appendix B)

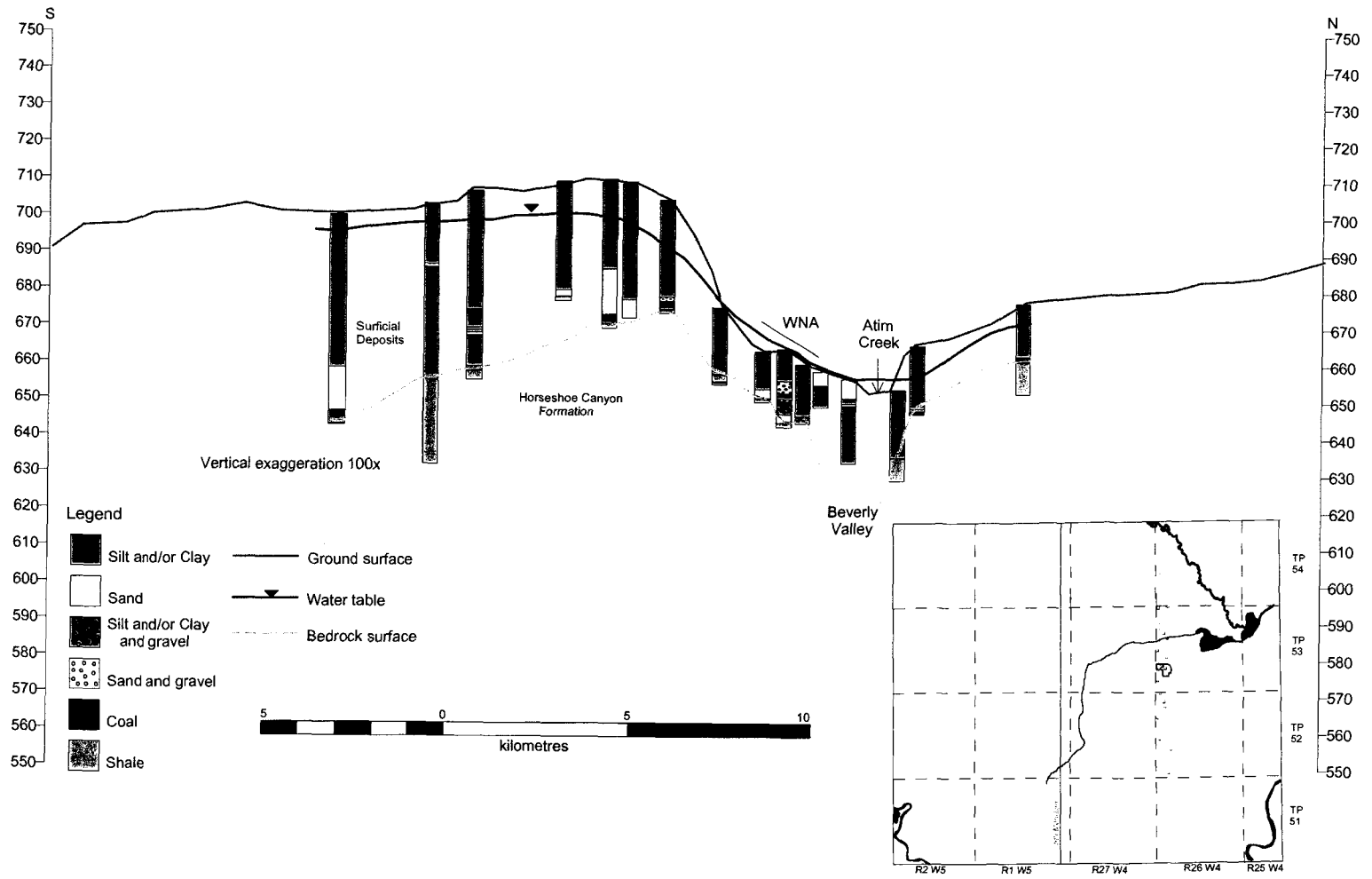


Figure 4.6 South to north cross-section through the WNA (well locations in Appendix B)

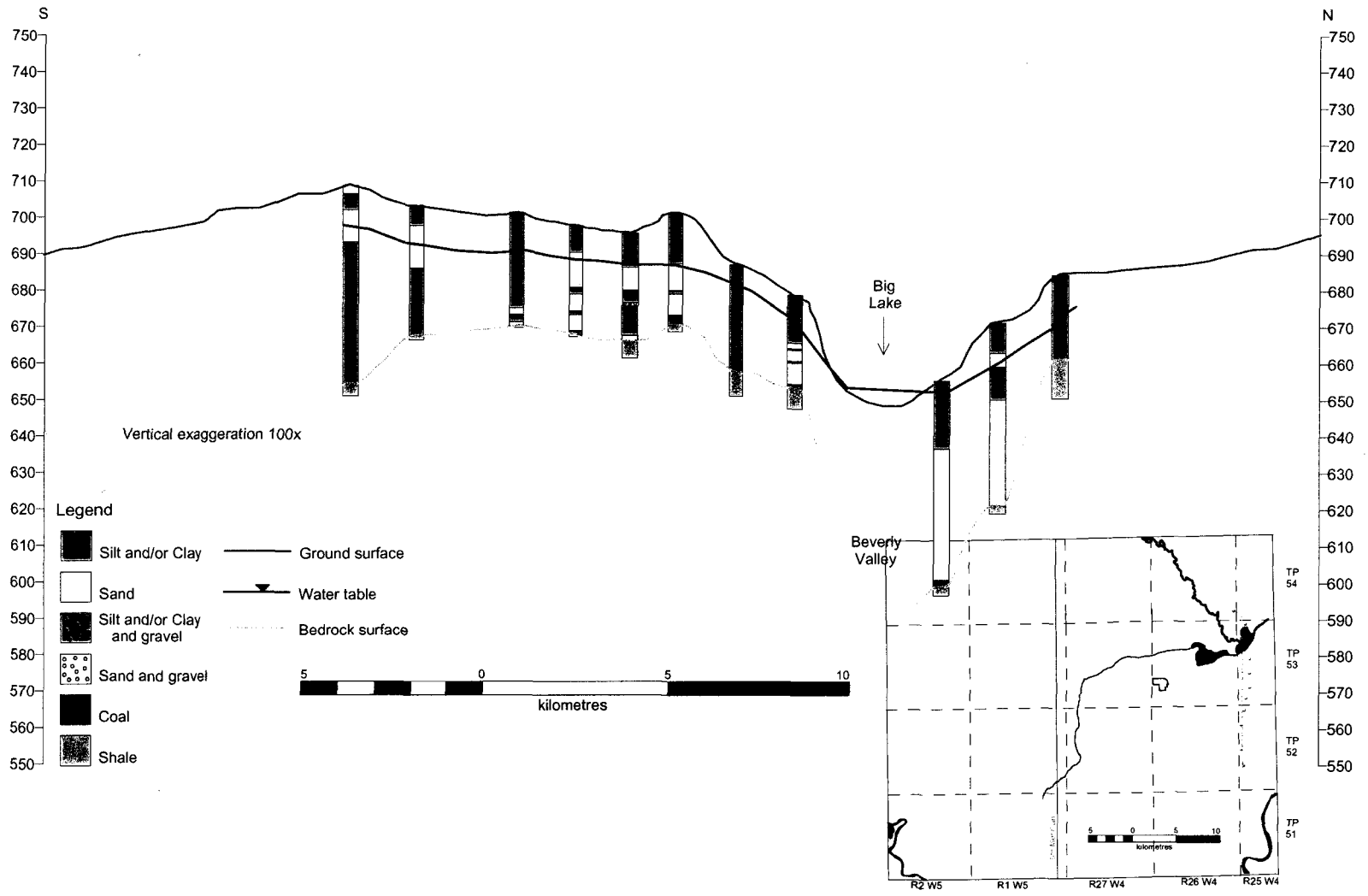


Figure 4.7 South to north cross-section through Big Lake (well locations in Appendix B)

(Bayrock and Hughes, 1962). Pitted deltas are localized composites of fine to medium grained sand, with thin beds of clay and silt. Beds of gravel and cobbles are also present. The pitted deltas are thought to have formed when large blocks of ice buried in glacio-deltaic sediments melted, producing a pitted or hummocky topography (Bayrock and Hughes, 1962). Within the study area, there are two large pitted deltas. One is located in the western portion; the other is located southeast of the Wagner Natural Area (TPs 51-53, Rgs 25-28). There are also a few small, localized pitted delta deposits north of the WNA (Figure 4.4).

The pitted delta southeast of the WNA is composed of more than 50 m of silt, sand and gravel (Andriashek, 1988). It is bounded on the east by a well-defined scour channel, and on the west by a poorly defined channel (Bayrock and Hughes, 1962; Figure 4.3).

The wetland, in which the WNA is located, is an extension of the poorly defined western scour channel (Bayrock and Hughes, 1962; Figure 4.3).

Till and ground moraine

Till and ground moraine are also found within the study area (Figure 4.4). Till is unsorted, unstratified sediment deposited by a glacier (Williams *et al.*, 1993). Tills in the Edmonton area are composed of approximately 40% sand, 30% silt, and 30% clay, and the amount of rock present is variable (Bayrock and Hughes, 1962). Ground moraine is a deposit of glacial till released beneath the ice sheet as the basal ice melts. It often has a hummocky form and is characterized by wetlands, ponds, and other indicators of poor drainage (Williams *et al.*, 1993).

4.3.3 Significant High Hydraulic Conductivity Deposits

Figure 4.8 shows an isopach map of total sand and gravel found in the surficial sediments. This map shows that significant amounts of sand are generally associated with buried valleys and pitted delta deposits. The Beverly and Onoway Valleys contain up to 30 m of sand and gravel in some places. Comparatively large amounts of sand are located in the areas mapped as pitted deltas on the west side of the study area, and southeast of the WNA.

4.4 Hydrogeology

4.4.1 Bedrock

Domestic water wells completed in the Horseshoe Canyon Formation typically produce 10 to 100 m³ of water per day (Hydrogeological Consultants Ltd, 1998a and 1998b).

The structure of the Cretaceous bedrock significantly influences the quality of groundwater in the study area. Average regional dip is to the southwest, and groundwater becomes increasingly mineralized and less potable down dip; therefore, wells southwest of Edmonton are generally confined to the shallow portions of the Horseshoe Canyon (Stein, 1993). Domestic wells are usually completed in the upper 90 m of this formation (Kathol and McPherson, 1975).

The Horseshoe Canyon Formation is characterized by sodium-bicarbonate and calcium-magnesium-bicarbonate type groundwaters, with concentrations of total dissolved solids ranging between 500 to 1000 mg/L (Stein, 1993).

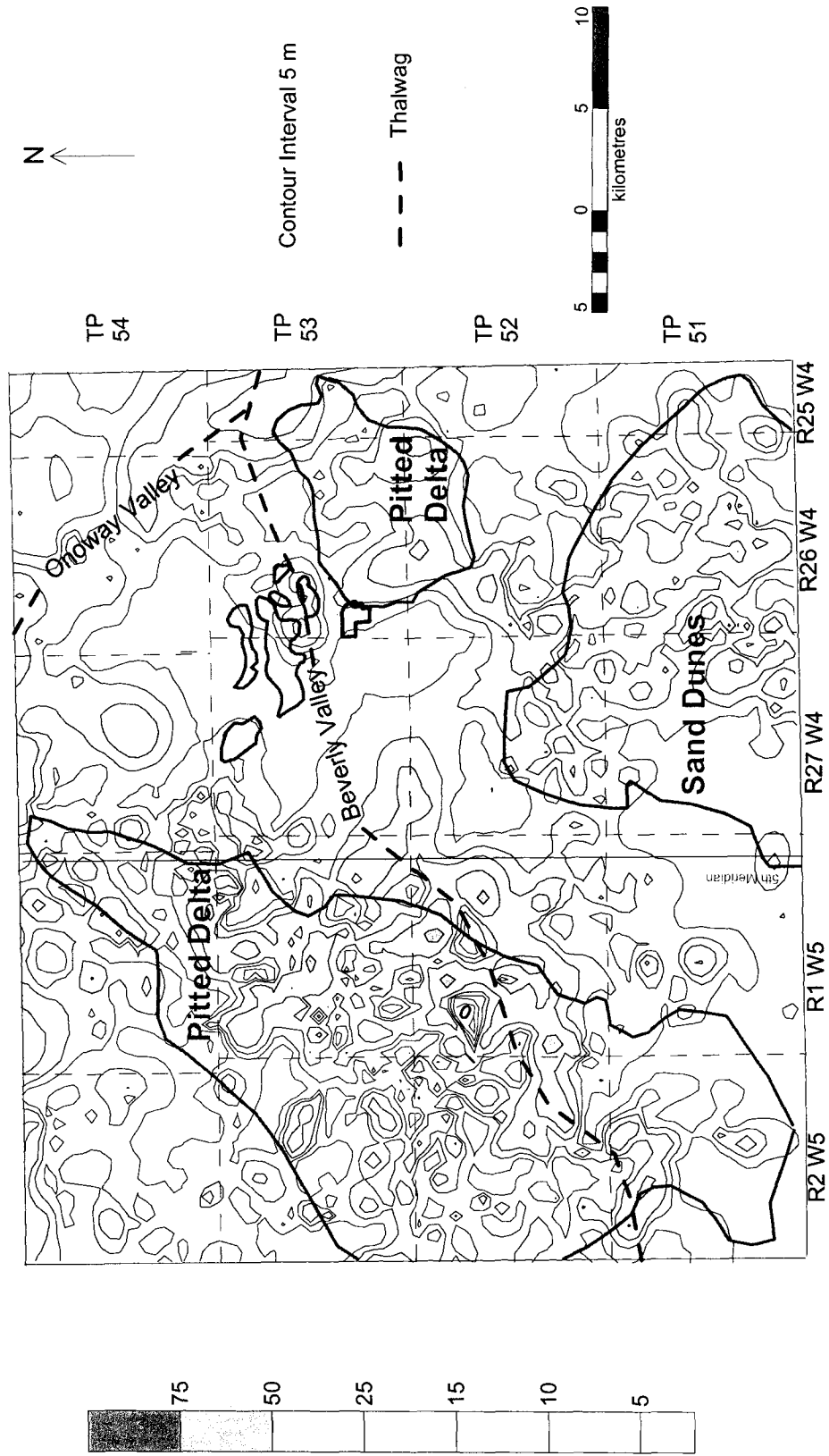


Figure 4.8 Isopach map of total sand and gravel in the surficial sediments

4.4.2 Surficial Deposits

The preglacial sands and gravels of the Empress Formation located at the bottom of the buried valleys are the most important and productive aquifers in the study area, because of their high permeability and low topographic position (Rutter *et al.*, 1998). The Beverly Valley (Figure 4.3) is the most important buried valley aquifer and can yield up to 650 m³ per day, making it a potential source of water for industry (Kathol and McPherson, 1975). The Onoway Valley (Figure 4.3) is also an important aquifer, and is reported to produce water at a rate of over 120 m³ per day (Stein, 1993).

Groundwater from the buried valley aquifers is of the calcium-magnesium-bicarbonate-type or of the sodium-bicarbonate-type (Stein, 1993). Concentrations of total dissolved solids range from less than 200 mg/L to over 1500 mg/L (Hydrogeological Consultants Ltd., 1998a and 1998b).

A number of shallow wells are completed within sand and gravel lenses of the overlying Lake Edmonton deposits. Wells completed in these deposits have variable production capacity because of the discontinuous nature of these aquifers (Stein, 1993), and their long-term yield depends on availability of groundwater recharge (Kathol and McPherson, 1975). Wells completed in the Lake Edmonton silts and clays can yield up to 40 m³ per day, and wells completed in the pitted delta deposits can yield between 40 and 150 m³ per day (Kathol and McPherson, 1975). Groundwater from the Lake Edmonton deposits is of the calcium-magnesium-bicarbonate-type or of the sodium-bicarbonate-type, and concentrations of total dissolved solids range from less than 500 mg/L to 1500 mg/L (Hydrogeological Consultants Ltd., 1998a and 1998b).

4.4.3 Groundwater Elevations in the Study Area

Figure 4.9 is a map of the groundwater elevations in the surficial deposits constructed from water well drillers' reports. The potentiometric surface closely resembles both the topographic and bedrock surfaces (Figure 4.10). Groundwater in the study area flows from areas of high topographic elevation to areas of lower topographic elevation; more specifically water tends to flow from the uplands to the Beverly Valley. Once groundwater reaches the Beverly Valley, it flows eastward out of the study area.

Regions of groundwater discharge are shown in Figure 4.11. Flowing wells and groundwater discharge, evidenced by wetlands, occur on the lower slopes and bottom of the Beverly Valley low. The flowing wells near the Wagner Natural Area (TP 53, R 27) are thought to result from significant and focused recharge in the pitted delta deposits southeast of the natural area (Alberta Environment, 1978).

4.4.4 Groundwater Elevations in the WNA

The WNA is located in a groundwater discharge area; evidenced by groundwater elevations at, near, or above the ground surface. Surficial groundwater elevations range between approximately 659 m and 663 m, and fluctuate approximately 1 m over the period of a year. Water levels tend to decrease in the fall and winter, and increase in the late spring and early summer (Figure 4.12).

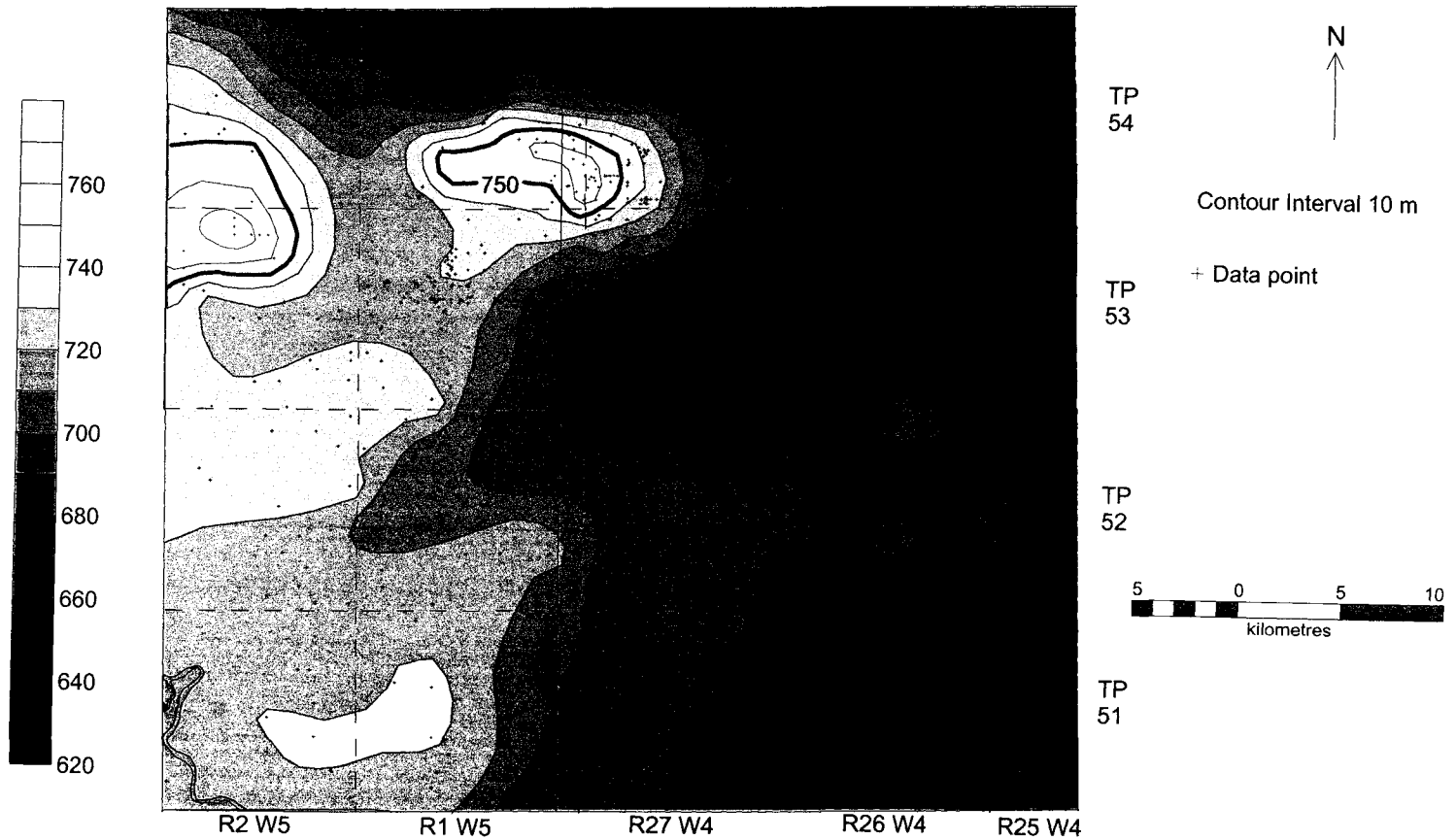


Figure 4.9 Groundwater elevations in the surficial sediments

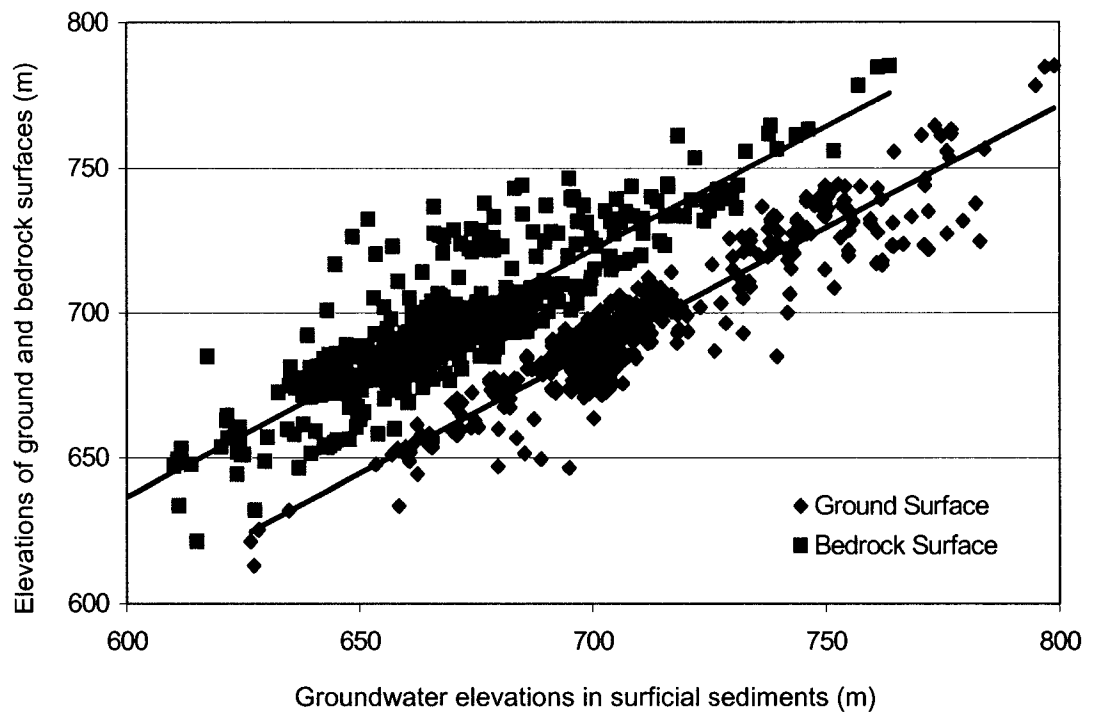


Figure 4.10 Graph showing the strong correlation of groundwater elevations in the surficial sediments to both ground surface and bedrock elevations

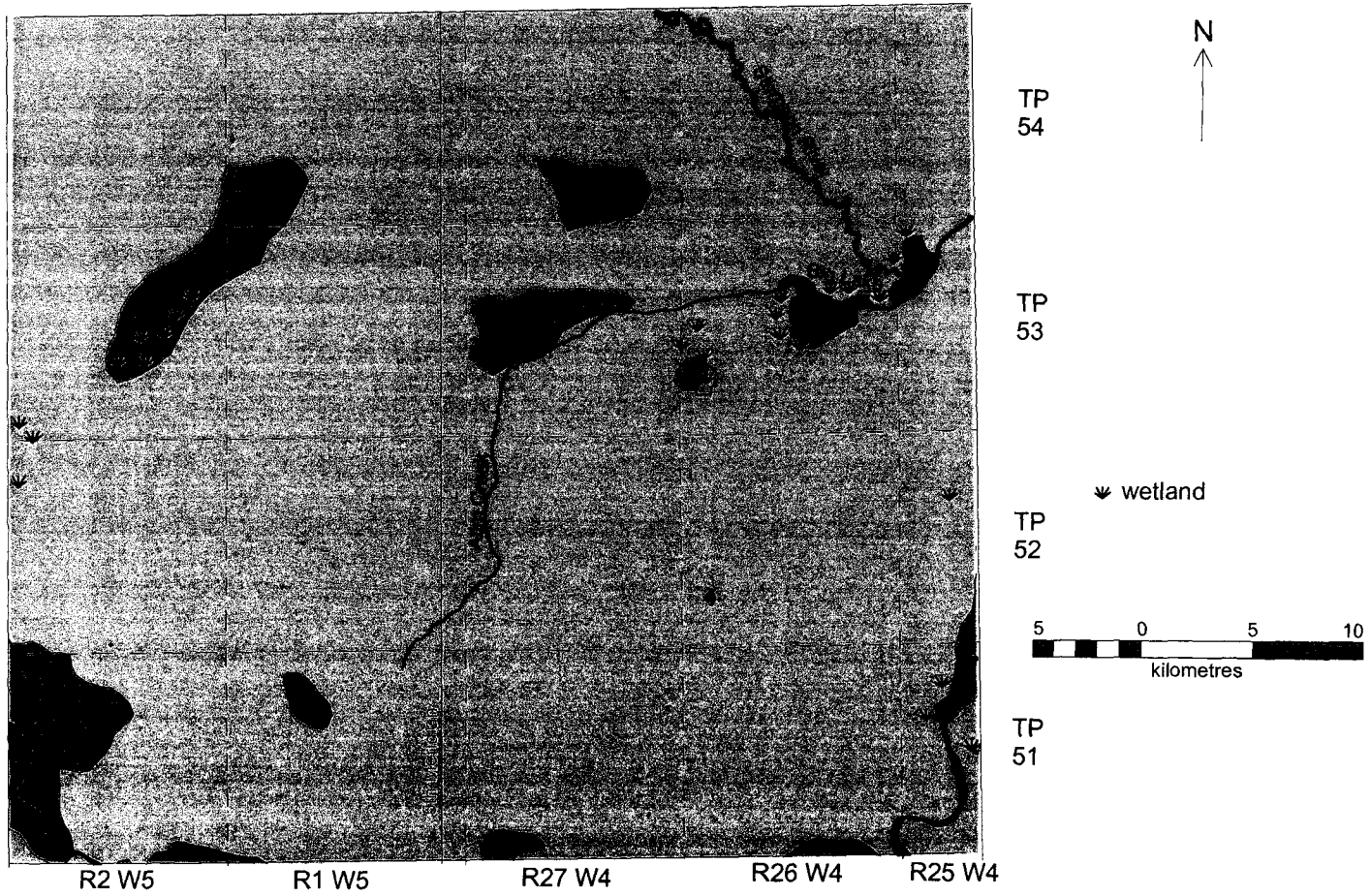


Figure 4.11 Map showing areas where groundwater elevations are above the land surface, these areas are shaded purple and coincide with locations of mapped wetlands

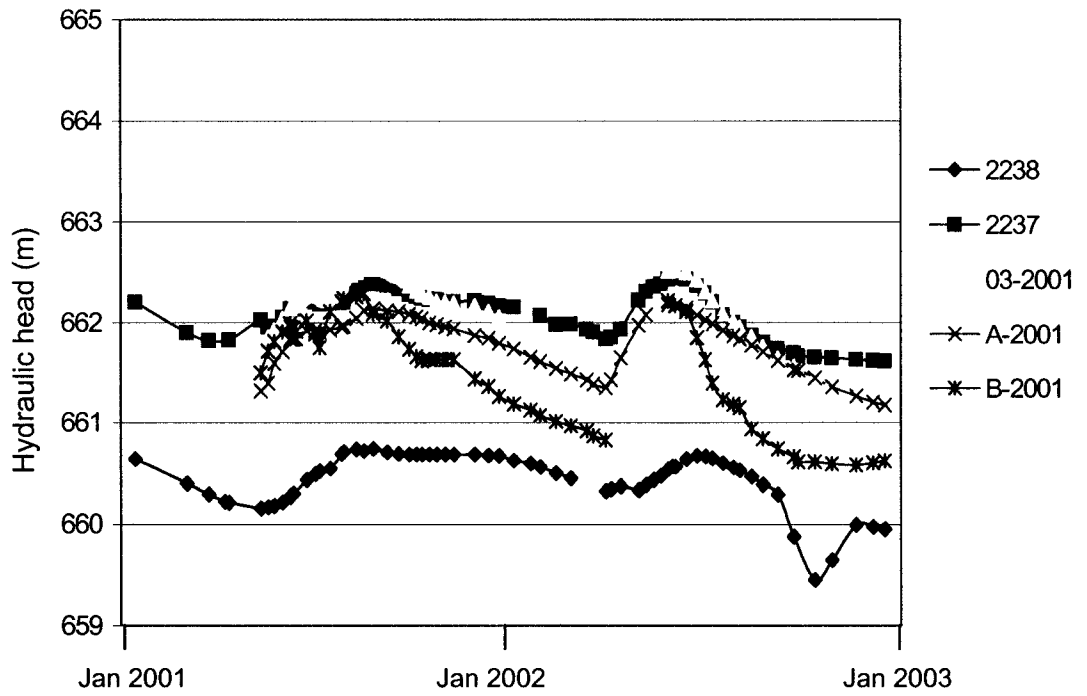


Figure 4.12 Hydrographs for monitoring wells in the WNA (monitoring well locations shown in Figure 3.2)

Chapter 5 Model Design and Calibration

This chapter is divided into two sections: (1) the design, and (2) calibration of the numerical model. Model results and sensitivity analysis are in the following chapter.

5.1 Model Construction

Groundwater models are mathematical representations of natural groundwater flow systems, and must be designed with care to ensure adequate representation of the natural system.

Constructing a numerical model involves (1) considering dimensionality and processes to be modeled, (2) choosing a steady state or transient representation of the natural system, (3) selecting a code, (4) designing a grid, (6) assigning material properties (e.g., hydraulic conductivity, porosity, storage coefficients) to the hydrostratigraphic units, and (6) assigning boundary conditions. The following is a discussion of the model design.

5.1.1 Dimensionality

A three-dimensional model was used to represent the natural system, because it was concluded that the distribution of surficial sediments (e.g., Lake Edmonton deposits, and Pitted Delta located near the WNA) likely has a significant influence on the WNA groundwater flow system.

5.1.2 A Case for Steady State Representation

Model design includes choosing either a steady state or transient representation of the natural groundwater flow system. The volume of water entering a system in steady state is equal to the volume of water leaving the system, and there is no change in storage

(Chapter 2). Conversely, in transient representations the volume of water entering the system is not necessarily equal to that leaving, and there can be a change in storage (e.g., temporal changes in hydraulic head or water table elevation).

A steady-state representation of the groundwater flow system around the WNA was chosen for the following reasons. First, groundwater basins can be represented as steady-state systems over long periods of time if there are no long-term trends in climate (Tóth: 1962; 1963). Second, seasonal fluctuations in the water table are not significant when compared to the vertical thickness of the system being simulated. The variation in the elevation of the water table over the course of a year at the WNA is approximately 1 m (Figure 4.12), and the average thickness of the surficial sediments in the study area is approximately 50 m. Thus, seasonal fluctuations account for a difference of less than two percent in elevation of the water table when compared to the average vertical thickness of the surficial sediments.

Third, surficial groundwater elevations in the study area have remained relatively constant for the past 40 years (Table 5.1). This was determined by comparing the water levels in surficial wells completed at the same depth, in the same section or nearby sections. Seasonal effects and differences in elevation were considered when making this comparison. Groundwater levels in the surficial sediments have probably not been affected significantly by wells, because much of the extracted water is returned via septic fields and irrigation. Thus, the amount of groundwater removed from the system is approximately equal to the amount returned.

Well Location	Ground Elevation (m)	Hydraulic Head (m)	Date Well Drilled	Depth to water (m)	Change in depth to water (m)
SW 22-51-26-W4	701	680	01 September 1964	21	0
SW 22-51-26-W4	700	679	18 March 2000	21	0
SE 25-52-2-W5	738	732	01 June 1968	6	0
SE 25-52-2-W5	738	732	10 January 2000	6	0
SW 18-53-25-W4	693	683	10 April 1968	10	0
SW 18-53-25-W4	694	684	05 October 2000	10	0
SW 13-53-26-W4	698	692	28 September 1968	6	-1
SW 12-53-26-W4	699	692	12 September 2000	7	-1
NE 26-53-26-W4	657	651	29 September 1965	6	-1
NH 26-53-26-W4	653	646	03 May 2003	7	-1

Table 5.1 Groundwater levels in some representative sections over last 40 years

5.1.3 Code

The United States Geological Survey's three-dimensional, finite-difference groundwater flow code MODFLOW 2000 (Harbaugh, *et.al.*, 2000) was selected to construct the model, because it is a well documented and frequently used groundwater modelling code that allows for three-dimensional representation of groundwater systems (Anderson and Woessner, 1992). Visual MODFLOW, Version 2.6 (Waterloo Hydrogeologic Software Inc., 1996) was used as the pre- and post-processing environment for the modelling.

A detailed discussion on finite difference models and MODFLOW is beyond the scope of this thesis, but can be found in McDonald and Harbaugh (2000), and Anderson and Woessner (1992). Briefly, MODFLOW incorporates first-order finite difference approximations to discretize the area to be modeled into a three-dimensional array of grid cells. Each grid cell is assigned a hydraulic conductivity and porosity. Boundary

conditions are assigned at select grid cells, and fix either the hydraulic head in the cell, or the flux of water across the cell. Using the finite difference method, the groundwater flow equation is solved for each grid cell to calculate the hydraulic head at the centre of each grid cell. Depending on the number of grid cells in a model, there may be hundreds of thousands of equations. These equations, and the boundary conditions are assembled into a global matrix representing the entire domain, and a solver, or mathematical program is used to solve this large system of equations iteratively.

Several different solvers are available to solve MODFLOW models. The BiCGSTAB-P Matrix Solver (Waterloo Hydrogeologic Software Inc., 1996) was used in the development of this model. A head change criterion for convergence of 0.01 m, and a residual criterion for convergence of 0.0001 m were chosen after a sensitivity analysis. Additionally, a relaxation factor of 0.1 was necessary to attain convergence, as numerical oscillations were problematic due to the wetting and drying of cells during the solution process.

A relaxation factor is a coefficient that controls the change in hydraulic head in successive iterations. Estimates of hydraulic head in the iterative solution process can be under-relaxed, exact, or over-relaxed. Under-relaxation is when the relaxation factor ranges between 0.0 and 1.0. Over-relaxation is when the relaxation factor ranges between 1.0 and 2.0. Under-relaxation is useful for non-linear equations, and can reduce oscillations by reducing the head change calculated in successive outer iterations. Reducing oscillations makes a solution more stable, and increases the probability of convergence.

5.1.4 Grid Design

A grid results from the discretization of the domain along the x, z, y axes into individual grid cells, and is the foundation of the numerical model. Poor grid design can cause numeric oscillations and other grid artifacts (Anderson and Woessner, 1992). Therefore it is crucial to construct a grid that is tailored to meet the requirements of the problem at hand.

Model Domain

The model domain was defined by the locations of physical features, groundwater divides, and flow lines (Figure 5.1). Groundwater divides located at topographic highs in the northern part of the study area (TPs 53 and 54, R 2 W5 and TP 54 R 27 W4 to R1 W5), define the northern boundaries of the model. Between these two highs is a topographic low (TPs 53 and 54, R1 W5), and in this low area, the model boundary is parallel to groundwater flow. The western boundary of the model is largely based on interpreted flow lines. Groundwater flow is focused from the north and south toward the Beverly Valley. The southern boundary of the model follows a southwest-northeast oriented groundwater divide. Localized groundwater divides and flow lines define the southeastern corner of the domain (TP 52 R 26 W4). At TP 53 R25 W4, the model boundary follows a flow line northeast toward the Beverly Valley. The northeastern boundaries of the domain are perpendicular to the Beverly and Onoway Valleys (TP 53 and 54 R 25 and 26 W4).

The domain is relatively large: it is approximately 43 km (x-axis) by 26 km (y-axis), and covers an area of about 675 km². Superimposing the rectangular grid directly onto the problem domain would leave a large number of cells inactive. Inactive cells are cells in

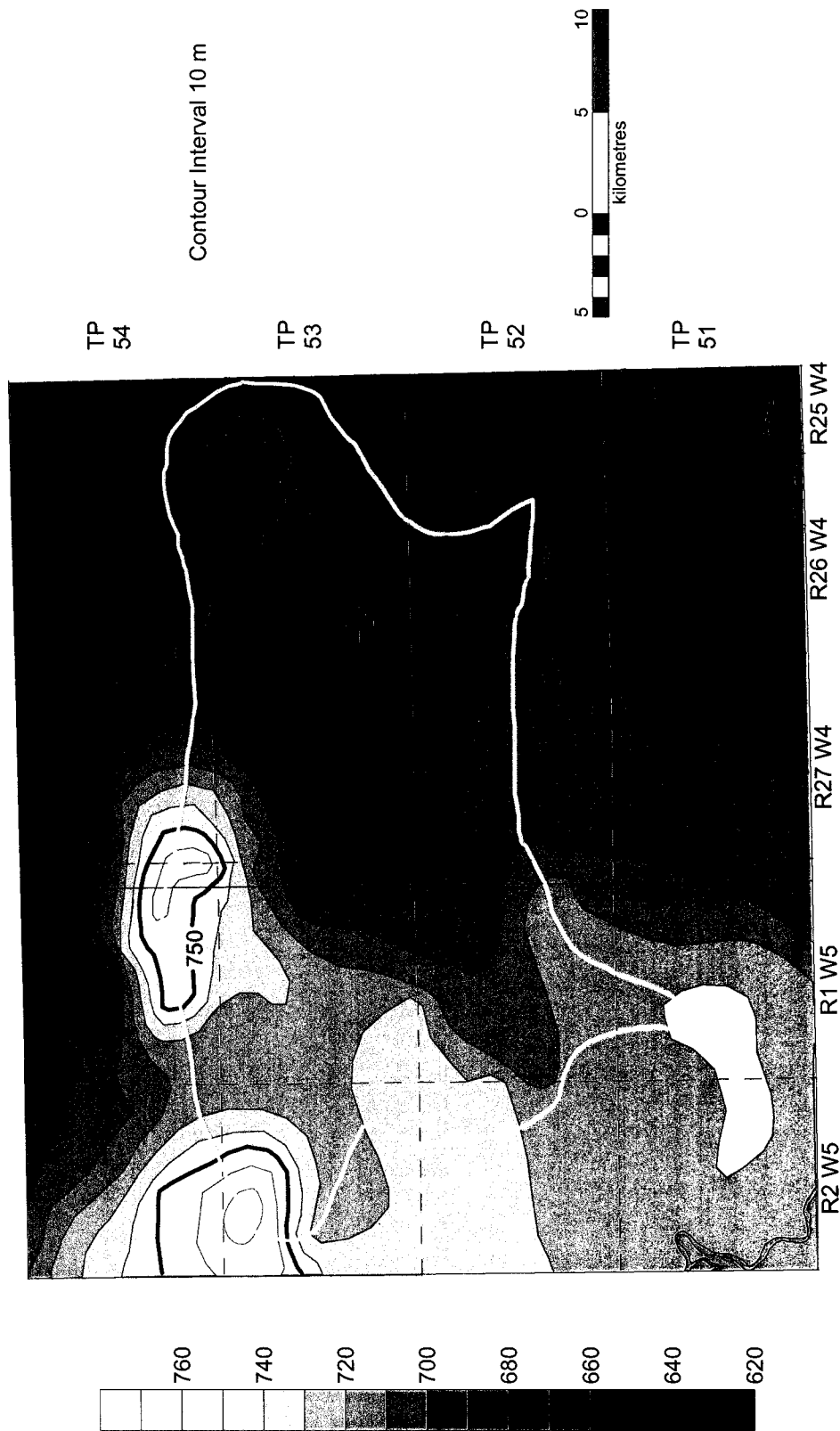


Figure 5.1 Model domain superimposed over map of groundwater elevations in the surficial sediments

which hydraulic head and/or flux are not calculated. Therefore the grid was rotated 24° west of north to match the orientation of the domain's x-axis.

Discretization

Discretization involves dividing the model domain into discrete units, or grid cells.

Aspect ratio is a useful concept to describe the degree of discretization. In isotropic media, aspect ratio is the ratio between the maximum and minimum dimensions of a grid cell. In anisotropic media, aspect ratio is defined as:

$$AR = \frac{K_x / \Delta x}{K_z / \Delta z} \quad (5.1)$$

where:

K_x is hydraulic conductivity along the x-axis

Δx is the length of the grid cell along the x-axis

K_z is hydraulic conductivity along the z-axis

Δz is the length of the grid cell along the z-axis

An aspect ratio of 1:1 is ideal in homogeneous, isotropic cases, because uniform discretization of the problem domain yields the most accurate results (Anderson and Woessner, 1992). For most regional-scale domains, an aspect ratio of 10:1 is acceptable (Anderson and Woessner, 1992). The ground and bedrock surfaces slope steeply in the vicinity of the Beverly Valley. For this reason, the problem domain was discretized finely. Experiments with different levels of discretization led to a grid design with 224 rows by 328 columns by 8 layers, for a total of 587,776 finite-difference cells (Figures 5.2 and 5.3). Grid cells are of constant length and width, although the length

and width are not equal. Figure 5.2 shows an outline of the grid and model domain, and the locations of the WNA, Big Lake, Atim Creek and Sturgeon River. Because individual grid cells are very small compared to the size of the domain, a rectangle representing a 10 by 10 block of grid cells is shown for scale.

Elevations for the top of the model domain (top of Layer 1) were interpolated from a digital elevation model with a grid spacing of 25 m. Within the model domain, the ground surface elevation ranges between 640 m and 780 m. A constant elevation of 590 m defines the base of the model (bottom of Layer 8). This elevation was chosen to allow a minimum of 20 m between the base of the Beverly Valley and the lower model boundary to minimize boundary effects from the base of the model. The top of layer 5 is defined by the interpreted bedrock surface (Chapter 3), which was imported from Surfer 7 (Golden Software, 2001). Cell height in layers 1 to 5 is equal and dependant on the thickness of the surficial sediments (Figure 5.3). Cell height in layers 6 to 8 is equal and dependant on the difference between the elevation of the bedrock surface and the base of the model.

Model cell dimensions are approximately 130 m (x-axis) by 120 m (y-axis) by an average of 5 m (z-axis). When a horizontal hydraulic conductivity of 10^{-5} m/s and a vertical hydraulic conductivity of 10^{-6} m/s are considered, the average aspect ratio is approximately 3:1. This value is well within the acceptable limits prescribed by the literature for a model of this size.

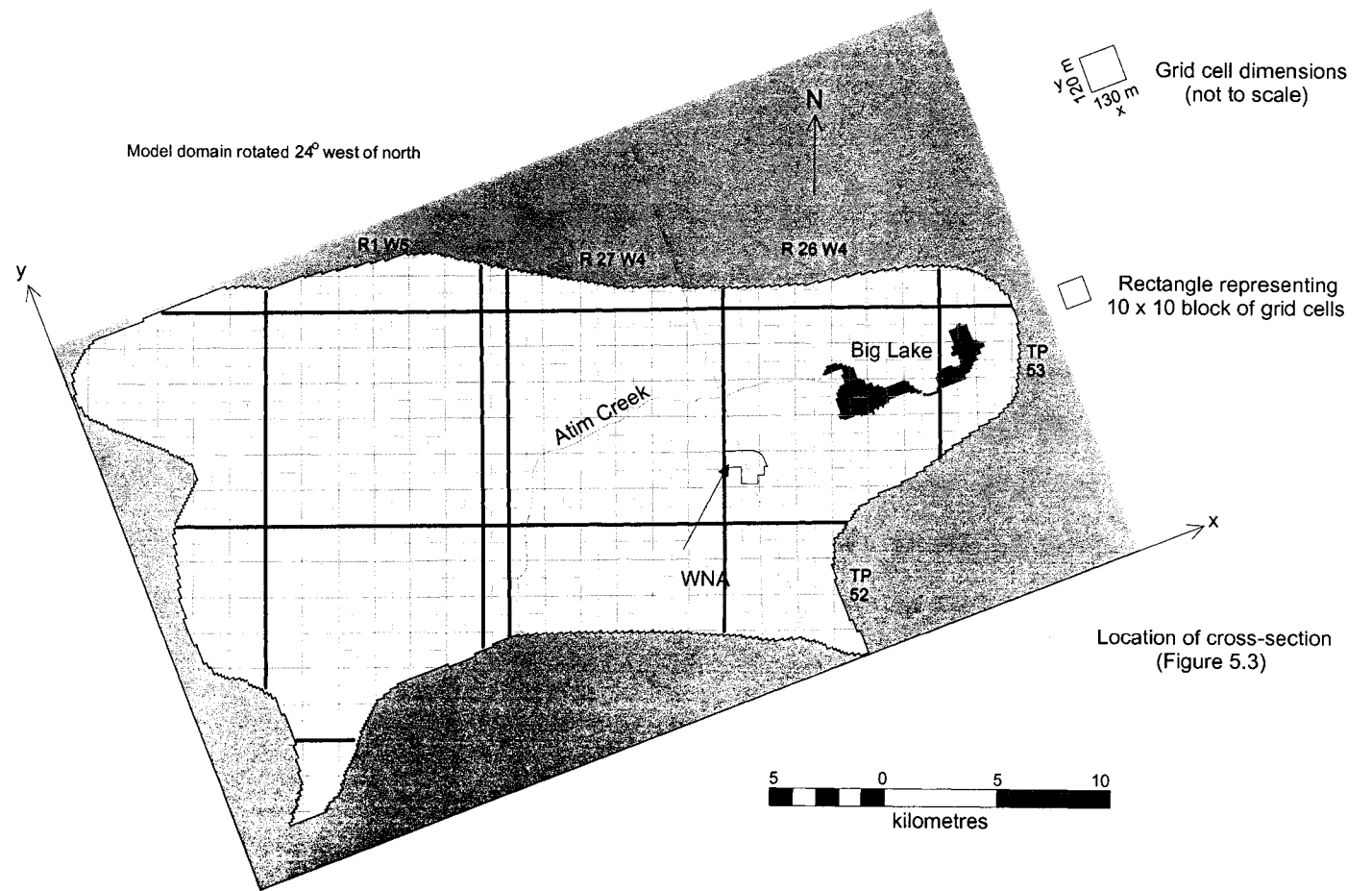


Figure 5.2 Plan view of model domain (grey area inactive), with township, range and quarter section boundaries superimposed, red line shows location of cross-section shown in Figure 5.3

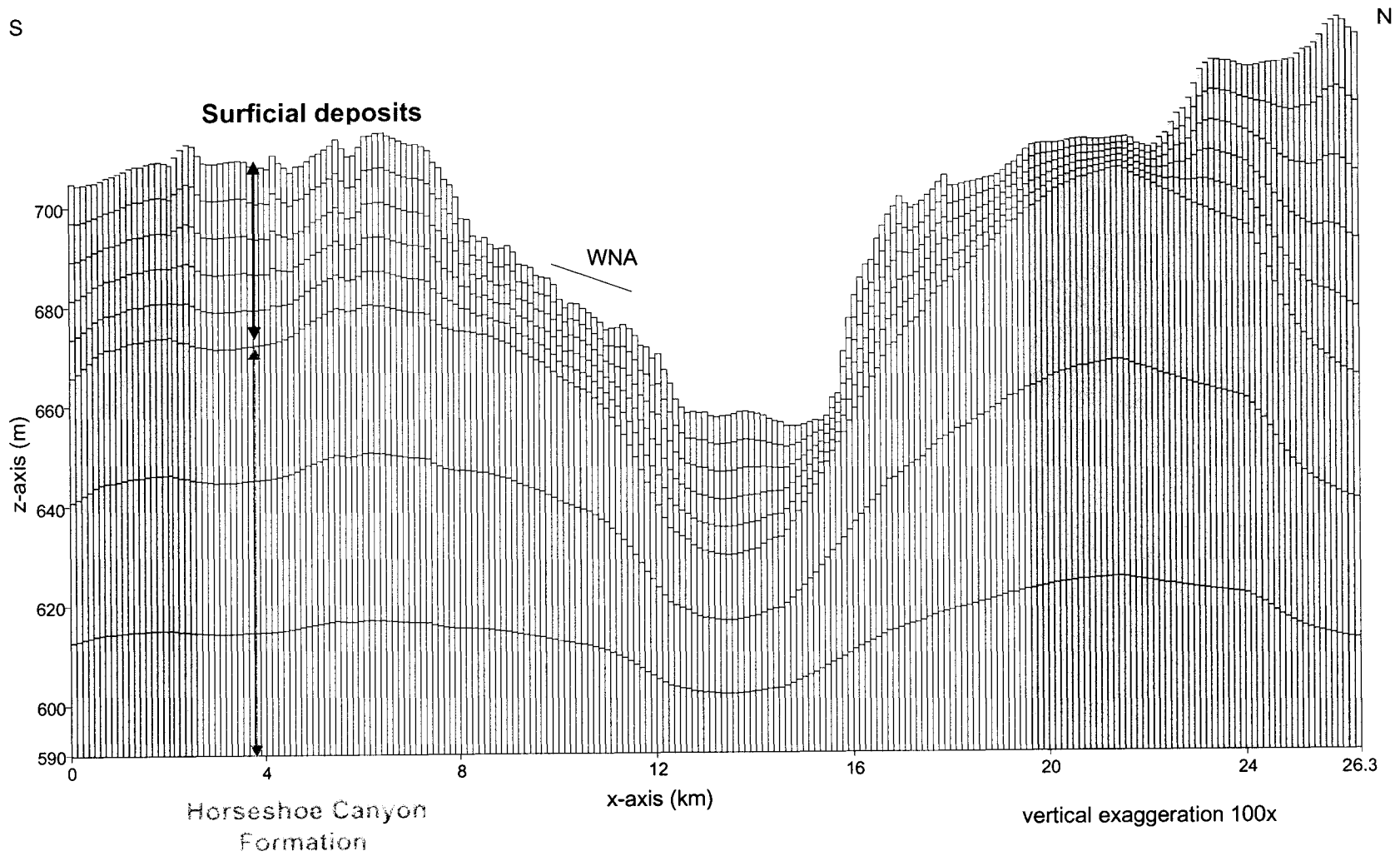


Figure 5.3 Sample cross-section through grid (grey cells inactive), location of cross-section shown in Figure 5.2

5.1.5 Hydrostratigraphic Units

Developing a numerical model involves mapping hydrostratigraphic units to grid cells and assigning material properties (e.g., hydraulic conductivity, porosity, storage coefficient) to the cells to approximate the natural flow system. Due to the regional scale of the model, the discontinuous nature of beds in the surficial sediments, the geology was simplified to include only seven hydrostratigraphic units. These units are the large-scale mapped features presented and discussed in Chapter 4, and are briefly summarized again here.

The relatively impermeable bedrock of the Horseshoe Canyon Formation forms the base of the study. The Beverly Valley, which trends from west to east in the centre of the domain, is incised into the bedrock. Sands and gravels of the Empress Formation line the bottom of the Beverly Valley. This channel-fill is composed of two units: a lower unit composed of up to 5 m of gravel and sand, and an upper unit composed of approximately 15 m of sand. Thick Lake Edmonton deposits composed of silt, sand and clay cover the channel-fill in the Beverly Valley and blanket the bedrock on the valley flanks and uplands. A large localized pitted delta deposit is located in the western region of the study area. Smaller pitted delta deposits area also located near the WNA. Till is found in the northwestern corner of the area modeled, and ground moraine is found in the north-central area.

Figures 5.4 to 5.6 illustrate how the surficial sediments were represented in the model. The Lake Edmonton deposits, pitted deltas, till and ground moraine extend from the ground surface to the top of bedrock (Layers 1 to 5). Where the Beverly Valley is present, layer 5 was used to represent the lower sand and gravel unit, and layer 4 was

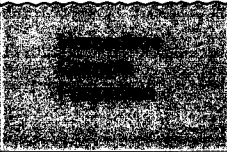
ERA	PERIOD	EPOCH	Hydrostratigraphic unit and model layer	Calibrated horizontal hydraulic conductivity values (m/s)	Hydraulic conductivity estimates for sediments in the study area (Kathol and McPherson, 1975) (m/s)	Generic hydraulic conductivity estimates for different sediments (Domenico and Schwartz, 1998) (m/s)	
Cenozoic	Quaternary	Holocene		not represented in model			
			Sand				
		Pleistocene		Layers 1 to 5	1×10^{-5}	Sand $10^{-3} - 10^{-4}$ Silt $10^{-6} - 10^{-7}$ Clay $<10^{-6}$	Fine sand $2 \times 10^{-7} - 2 \times 10^{-4}$ Medium sand $9 \times 10^{-7} - 5 \times 10^{-4}$ Coarse sand $9 \times 10^{-7} - 6 \times 10^{-3}$
				Pitted Deltas (east and west) (Layers 1 to 5)	East 4×10^{-5} West 5×10^{-5}	Sand $10^{-2} - 10^{-4}$ Silt $10^{-5} - 10^{-7}$	
				Layers 1 to 5	2×10^{-6}	$10^{-5} - 10^{-8}$	Silt $1 \times 10^{-9} - 2 \times 10^{-5}$ Clay $1 \times 10^{-11} - 5 \times 10^{-9}$
		Layers 1 to 5	8×10^{-8}	$<10^{-6}$	Till $1 \times 10^{-12} - 2 \times 10^{-6}$		
Tertiary	Empress Formation	Upper Beverly Valley (Layer 4) and Lower Beverly Valley (Layer 5)	Upper 1×10^{-4} Lower 1×10^{-3}	Sand $10^{-2} - 10^{-4}$ Gravel $>10^{-2}$	Gravel $3 \times 10^{-4} - 3 \times 10^{-2}$		
Mesozoic	Cretaceous		Layers 6 to 8	1×10^{-9}	Sandstone $10^{-5} - 10^{-6}$ Siltstone $<10^{-4}$ Shale $<10^{-5}$	Sandstone $3 \times 10^{-10} - 6 \times 10^{-6}$ Shale $1 \times 10^{-13} - 2 \times 10^{-9}$	

Figure 5.4 Hydrostratigraphic units in numerical model, and calibrated and reported hydraulic conductivity values (calibrated values implement a horizontal to vertical anisotropy ratio of 10)

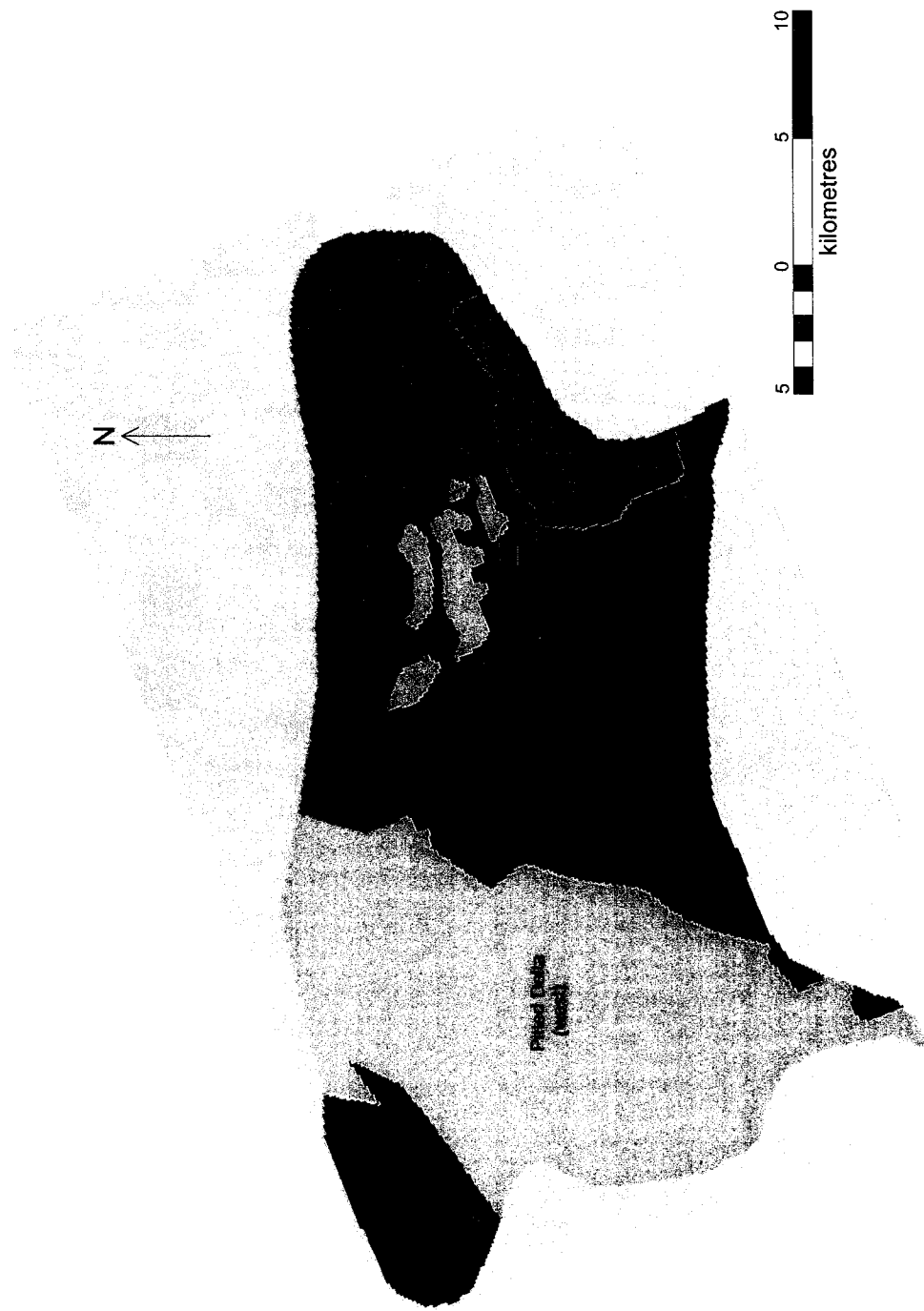


Figure 5.5 Plan view of model domain showing distribution of hydrostratigraphic units in layers 1 to 3

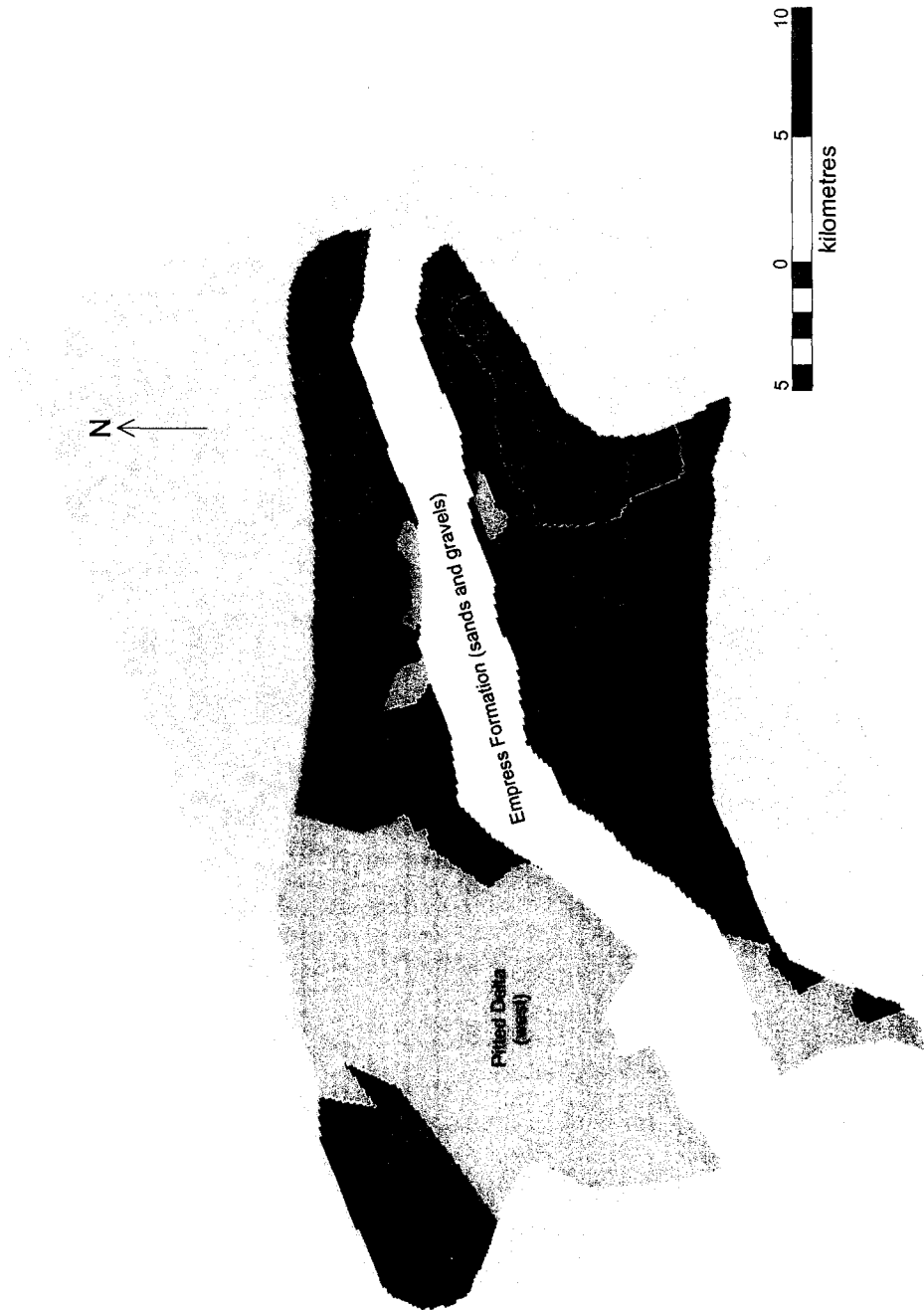


Figure 5.6 Plan view of model domain showing distribution of hydrostratigraphic units in layers 4 and 5

used to represent the upper sand unit of the Beverly Valley. The combined average thickness of layers 4 and 5 in the vicinity of the Beverly Valley ranges between 15 and 20 m. Layers 6 to 8 were used to represent the bedrock.

5.1.6 MODFLOW Layer Types

When constructing a model in MODFLOW it is necessary to specify a “type” for each layer in the model. Layer type determines how transmissivity is calculated and the value of the storage coefficient. A steady-state model was constructed, and for this reason storage coefficients are not required. In the model, Layer 1 is a MODFLOW *Type 1* layer, which represents unconfined conditions. In *Type 1* layers, transmissivity is calculated from the saturated thickness and hydraulic conductivity.

Layers 2, 3 and 4 are MODFLOW *Type 3* layers. *Type 3* layers represent both confined and unconfined conditions. In *Type 3* layers, transmissivity is calculated from the saturated thickness and hydraulic conductivity. Vertical leakage from grid cells above is limited if the overlying unit becomes unsaturated.

Layers 5 through 8 are MODFLOW *Type 0* layers. *Type 0* layers represent confined conditions; transmissivity is fixed.

5.1.7 Boundary Conditions

Once the three-dimensional grid has been designed, and the hydrostratigraphic units have been specified, boundary conditions can be defined. Boundary conditions are a mathematical description of the heads or fluxes along the boundaries of the model

domain. There are three types of boundary conditions used in groundwater flow models (Anderson and Woessner, 1992):

1. Specified hydraulic head (Dirichlet)
2. Specified flux (Neumann), and
3. Head dependant flux (Cauchy or mixed)

It is extremely important to select the correct boundary conditions in a steady state model because the boundaries determine the flow pattern (Anderson and Woessner, 1992).

The model was designed with specified flux, head dependant flux, and specified head boundary conditions (Figure 5.7). The application and assumptions behind these conditions is described in further detail below.

Big Lake and the Beverly Valley were represented with specified head nodes (Dirichlet condition). Atim Creek was not represented, because it is an intermittent creek that is heavily influenced by discharge from the Town of Stony Plain (UMA, 2000). The Sturgeon River was not represented in this model, because its location is not evident in the hydraulic head distribution shown in Figure 5.1. Constant head nodes at Big Lake were assigned a value of 650.6 m (average elevation of Big Lake; UMA, 2000).

The Beverly Valley enters the domain on the west side and exits on the east side (Figure 5.7). Specified head nodes were used to represent the Beverly Valley on the east and west edges of the domain. The head at the western boundary was set to 725 m asl, a value derived from groundwater levels interpreted from drillers' logs. Hydraulic head

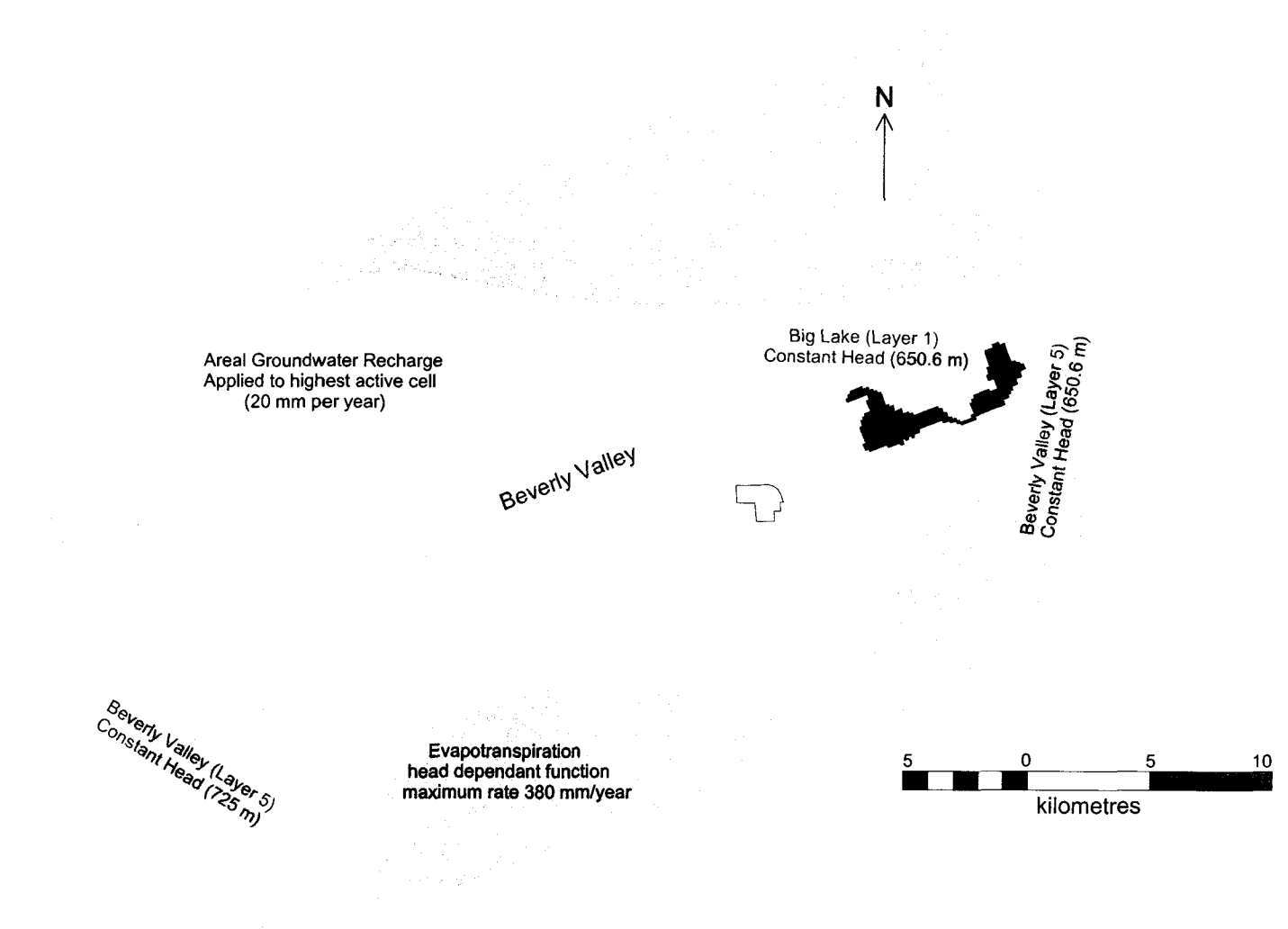


Figure 5.7 Boundary conditions implemented in the model

along the eastern boundary was set to 650.6 m asl, the same value used for Big Lake. Making the head equal in these two features, forces groundwater to flow horizontally across the eastern boundary of the model domain.

Groundwater Recharge

Areal groundwater recharge was applied as a constant flux (Neumann condition) to the highest active cells over the entire upper surface of the model. Absolute rates of recharge are uncertain, but have been estimated on the Canadian prairies. Van der Kamp and Hayashi (1998) found that recharge rates to regional aquifers on the prairies range from 2 to 45 mm per year, averaged over the area of the catchments. Hayashi *et al.* (1998) found that recharge rates for a wetland near Saskatoon ranged between 1 and 3 mm per year. Recharge rates are frequently estimated as a percentage of total annual precipitation. As a rule of thumb, about five percent of total precipitation may become recharge (Schwartz and Zhang, 2003, pg 25). On the Canadian Prairies, recharge rates are estimated to range between 0.5 and 9 percent of total annual precipitation (Meyboom 1966, 1967a; Meyboom *et al.*, 1966). Using these percentage estimates, recharge rates in the study area would range between 2 and 43 mm per year.

Within the study area, there have been two studies on recharge rates. Farvolden (1963) estimated a recharge rate of 2 percent of the total precipitation, or approximately 9.5 mm, for an area located between Townships 50 and 51, and Ranges 25 and 26, west of the fourth meridian. This estimated recharge rate is likely lower than the average recharge rate over the study area, because the study area has significantly more high hydraulic conductivity sediments at the surface than the area Farvolden studied.

Hydrogeological Consultants Ltd. (HCL) estimated a recharge rate of approximately 10 percent of the total precipitation, or 47 mm, for an area extending from Township 53 to the Beverly Valley, and from Range 25 to Range 27, west of the fourth meridian (Alberta Environment, 1978). This estimate of recharge is likely higher than the average rate of recharge over the study area because the area studied by HCL has significantly more high conductivity material near the surface than the study area as a whole. A recharge rate of 20 mm per year, approximately five percent of total annual precipitation, was assumed. This value falls within the range of recharge rates presented above.

Evapotranspiration

Groundwater discharge was simulated using evapotranspiration. In MODFLOW, evapotranspiration is represented as a linear, head dependant function (Cauchy condition). The rate of evapotranspiration is dependant on the depth of the water table below ground surface (Figure 5.8).

Generally, in MODFLOW the rate of evapotranspiration varies linearly from 0 mm/year at the extinction depth to a maximum rate when the elevation of the water table in a cell is equal to the elevation of the land surface.

Studies have been conducted on evapotranspiration rates in western Canada and the United States; however no data are available on actual evapotranspiration rates within the study area. Su *et al.* (2000) measured evapotranspiration from an upland (333.4 mm per year) and wetland (549.7 mm per year) on the Canadian prairies. Barr *et al.* (2000)

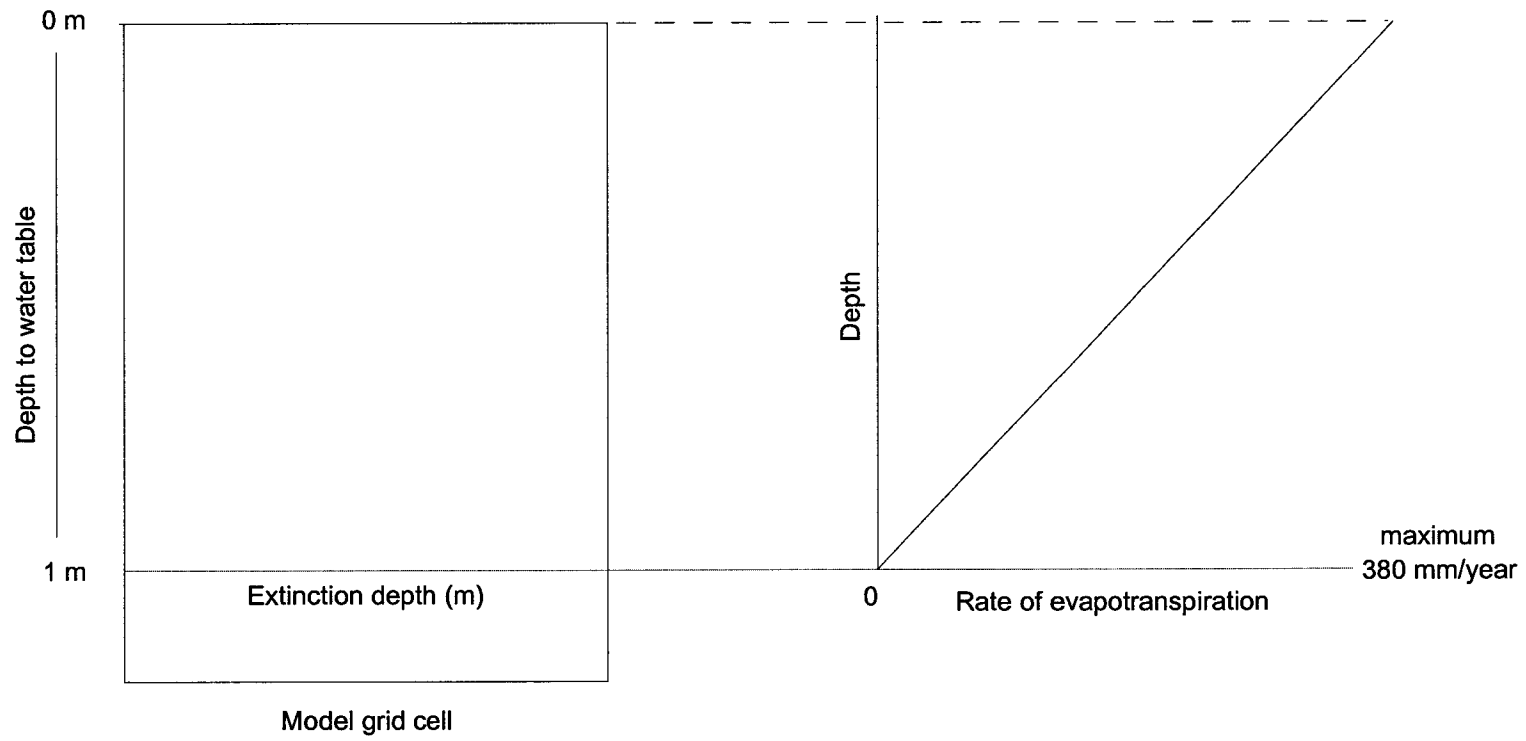


Figure 5.8 Representation of evapotranspiration function

measured evapotranspiration of 760 mm per year in a mature aspen forest in western Canada.

In the numerical model, a maximum rate of evapotranspiration (380 mm per year) was obtained from calibration. The maximum rate of evapotranspiration occurred when the elevation of the potentiometric surface was equal to or above the elevation of the ground surface. An extinction depth of 1 m was used, as soil moisture loss due to evapotranspiration at depths of less than 1 m is negligible in the study area (Feng, 2003)

5.2 Model Calibration

Model calibration involves making changes to input parameters, within reasonable ranges, until model results match field observations. Calibration can be done manually by trial-and-error or with parameter estimation codes (Anderson and Woessner, 1992).

5.2.1 Calibration Targets and Associated Errors

Calibration points are required for model calibration and allow quantitative comparison of simulated heads to observed heads at specific locations in the model. When using calibration points to calibrate a model, a calibration target is specified. A calibration target quantifies the allowable discrepancy between simulated and observed heads. Using field groundwater level measurements as calibration targets in a model has inherent errors. There are several sources of error associated with field measurements, including: measurement errors, scaling effects, transient effects and interpolation errors. The following is a discussion of these error types.

Measurement Errors

Measurement errors stem from the accuracy of the water level measuring device, the operator, and the spatial description of the water well location. Generally, these errors are on the order of centimetres; however, the magnitude of these errors tends to increase with regional surveys (Anderson and Woessner, 1992). The greatest single source of error in water level measurements in this study is the ground surface elevation estimate. Ground surface elevations were determined from a DEM with a 25 m grid spacing. In relatively flat lying areas, ground surface elevation estimates introduce errors on the order of a few metres. On the other hand, in areas where the elevation changes quickly over short distances, such as along a valley wall, the error may be on the order of several metres. In addition, water levels are generally measured from the top of the well casing. Most water well records do not report the height of the well casing above the ground surface. As a result, errors stemming from the casing height will also be introduced. These errors are usually on the order of one metre.

Errors also stem from the discretization in the model. While the DEM has a grid spacing of 25 m, the model has a grid spacing of approximately 125 m. Thus, the ground surface estimates in the model are even coarser than those from the DEM. Therefore, in regions of steep topography, simulated hydraulic head values may have induced error on the order of several metres.

Scaling Effects

Scaling effects are errors resulting from the small-scale heterogeneities that are not represented in the model, because they fall below the scale of discretization (Anderson

and Woessner, 1992). Point field values may not be representative at the cell scale or the regional scale.

Water level data can also introduce scaling effects. Numerical models require point measurements of hydraulic head. However, most domestic water wells in the study area have long screen intervals, usually several metres. Thus, water level measurements from wells with long screens may not represent the point measurement, which is required for the model (Anderson and Woessner, 1992).

Transient Effects

Transient effects are introduced to the model by using field water level measurements. Water levels in the field are affected by seasonal and long-term changes in climate. Seasonal and climatic changes can produce fluctuations in hydraulic head on the order of several metres (Maathuis, 2000).

Interpolation Errors

The position of wells used as calibration points in a groundwater model should coincide with the location of nodes in the model. In the case of MODFLOW, well screens should be located at the centre of a cell. If well locations do not coincide with the nodal positions, linear interpolation is used by Visual MODFLOW to calculate hydraulic head at that point from surrounding nodes. Increasing the level of discretization decreases the distance between nodes, and reduces interpolation error.

5.2.2 Calibration Points and Target

Eighteen calibration points were selected (Figure 5.9). Data were derived from drillers' reports (Table 5.2). Wells chosen for calibration points were evenly distributed over the whole domain and had the following characteristics:

- Completed in the surficial sediments
- Good spatial accuracy (x,y,z)
- A reported static water level
- Lithologic information
- A location that coincided closely to the centre of a cell in the model
- Screen intervals which were limited to a single layer of the model, and therefore a single hydrostratigraphic unit

A calibration target of +/- 3 m was used in this study. This corresponds to about two percent of the total vertical thickness of the model, and approximately 5% of the average vertical thickness of the surficial sediments.

5.2.3 Calibration Process

Model calibration was achieved through a trial-and-error process. Calibration involved making small changes in material properties, within the constraints of literature values (Kathol and McPherson, 1975; Domenico and Schwartz, 1998) (Figure 5.4), and those estimated by the researcher. Average horizontal and vertical hydraulic conductivity values were calculated from well log data (1127 wells) for model layers 1 to 5. The process used to estimate hydraulic conductivity is described in the following section.

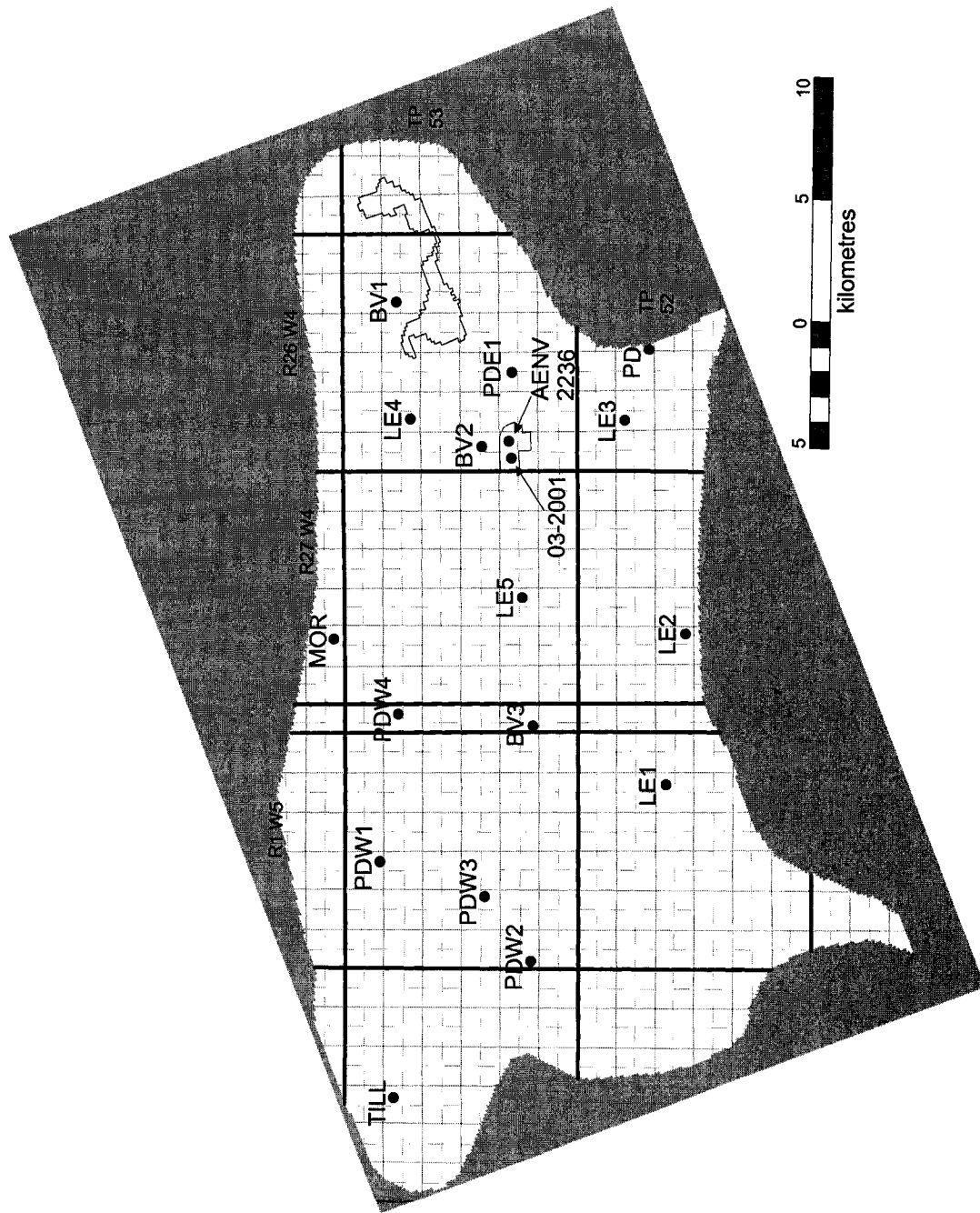


Figure 5.9 Locations of calibration points in model domain

In addition to adjusting hydraulic conductivity values of the hydrostratigraphic units, the maximum rate of evapotranspiration varied to improve the correspondence between the mapped (Figure 4.9) and simulated heads. Throughout the entire calibration process the recharge rate (20 mm per year) was held constant.

Initially, calibration was done visually, by comparing the simulated heads to Figure 4.9, which was imported into the model as a spatially referenced image file. When simulated heads matched mapped heads closely, the model was then further refined using the calibration points presented in the previous section.

Estimating Hydraulic Conductivity

Representative hydraulic conductivity values and anisotropy ratios were estimated from well logs for each of the surficial hydrostratigraphic units. Because the surficial model layers (1 to 5) are of an equal thickness at a point, the depth to bedrock in each of the 1127 wells was divided by five, giving the thickness of each model layer at a particular well location. The fraction of clay, silt, sand, and gravel was then calculated for each of these 5 layers from the well logs.

Once the fraction of clay, silt, sand, and gravel was calculated for each layer, the average horizontal and vertical conductivities were calculated for each layer using hydraulic conductivity estimates from Domenico and Schwartz (1998). Horizontal hydraulic conductivity was calculated using the weighted arithmetic mean. Vertical hydraulic conductivity was calculated using the weighted harmonic mean (Fetter, 1994).

The wells were then classified by hydrostratigraphic unit, and the geometric average horizontal and vertical hydraulic conductivity was calculated for each hydrostratigraphic unit to determine representative values of hydraulic conductivity, and anisotropy.

Point Name	Location	Elevation (m)	Head (m)	Screen Length (m)	Date Well Completed
LE1	NE 23-52-1-W5	715	709	1.52	22 February 1996
LE2	SE 20-52-27-W4	714	708	2.74	20 December 1979
LE3	NW 29-52-26-W4	712	701	1.52	09 July 1994
LE4	SW 29-53-26-W4	667	664	1.22	12 July 1977
LE5	SE 9-53-27-W4	681	680	1.52	25 August 1993
BV1	NW-26-53-26-W4	664	650	2.44	29 September 1965
BV2	SE 18-53-26-W4	658	656	2.74	17 July 1979
BV3	SW12-53-28-W4	692	694	1.53	17 November 1995
PDE1	NW 9-53-26-W4	679	677	1.53	30 March 1990
PDE2	NW 27-52-26-W4	715	698	1.53	16 November 1994
PDW1	SE 33-53-1-W5	741	719	1.53	16 September 1991
PDW2	SW 7-53-1-W5	772	721	1.52	15 October 1992
PDW3	SE 17-53-1-W5	749	722	1.52	14 August 1995
PDW4	SE 25-53-28-W4	720	710	1.22	10 December 1978
TILL	NE 28-53-2-W5	773	761	1.22	14 September 1994
MOR	SE 5-54-27-W4	750	738	1.22	11 October 1973
03 -2001	WNA	663	662	1.52	11 April 2001
AENV - 2236	WNA	666	664	1.22	24 November 1983

Table 5.2 Wells used as calibrations points in the numerical model

Chapter 6 Model Results and Sensitivity Analysis

6.1 Results

The following sections describe the calibrated parameter values, simulated hydraulic head distribution and model water balance.

6.1.1 Parameter Values

Due to the regional scale of the study, model parameters were based on literature values. Figure 5.4 lists typical hydraulic conductivity ranges for various sediment types, estimates of hydraulic conductivity for sediments within the study area, and hydraulic conductivity values used in the calibrated model.

6.1.2 Hydraulic Head Distribution and Groundwater Flow

Numerical simulations produced predicted heads in the domain. Figures 6.1 through 6.3 show the calibrated hydraulic heads in layers 1, 3 and 5 of the model (surficial deposits). The head distribution in each of the layers is very similar. Hydraulic heads range from 650 m to 780 m over the domain, and are higher in the uplands located along the north and south perimeters of the model than in the central area occupied by the topographic low that reflects the location of the buried Beverly Valley (TP 53, R25-27 W4).

Interpretation of Figures 6.1 to 6.3 suggests that groundwater recharge occurs in the highlands in the west and along the north and south perimeters of the model domain. Groundwater recharging in the highlands flows downward to the Beverly Valley, which occupies the central portion of the domain. Once groundwater reaches the Beverly

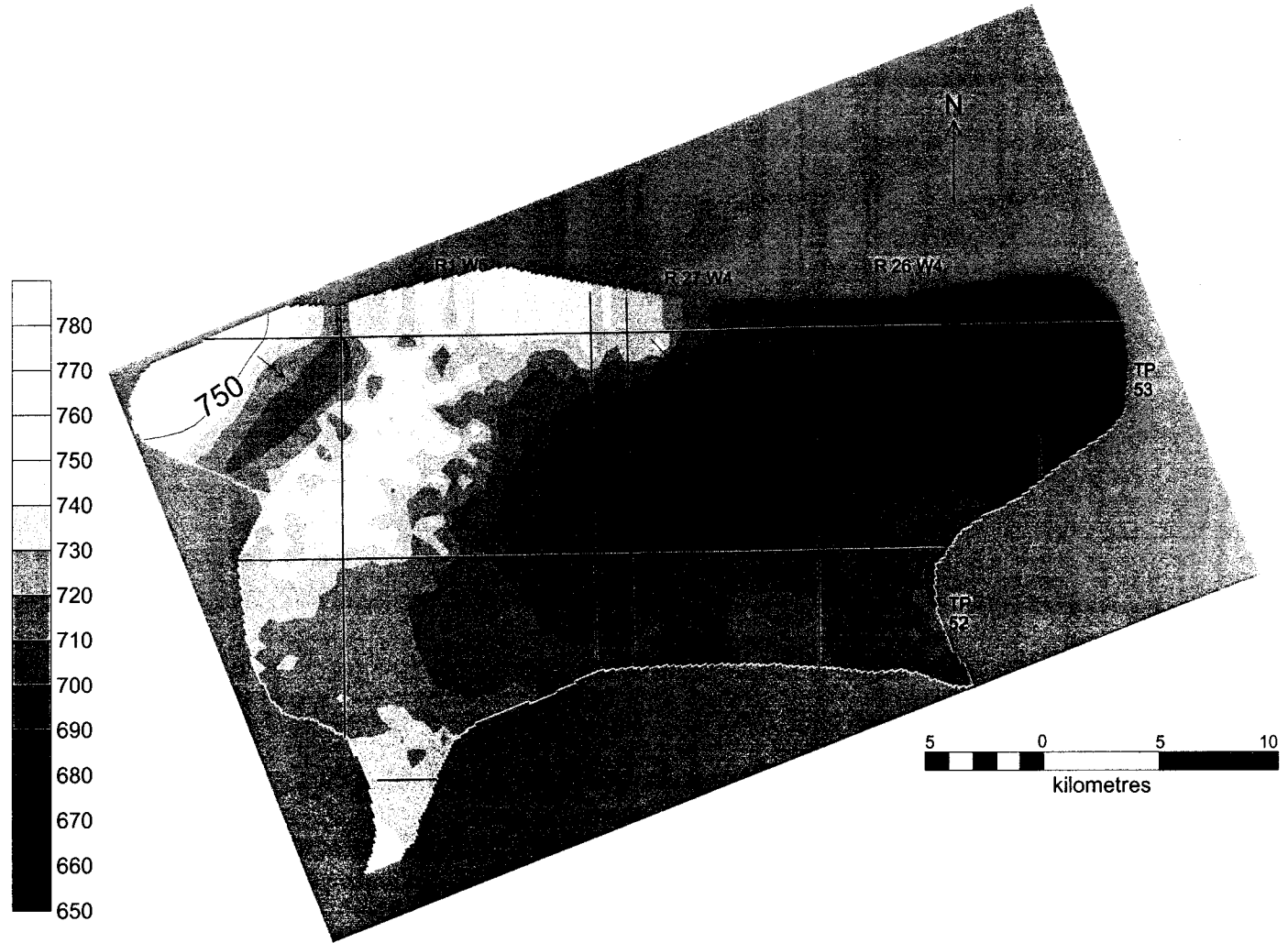


Figure 6.1 Calibrated hydraulic head in layer 1 (10 m contour interval), arrows show direction of groundwater flow

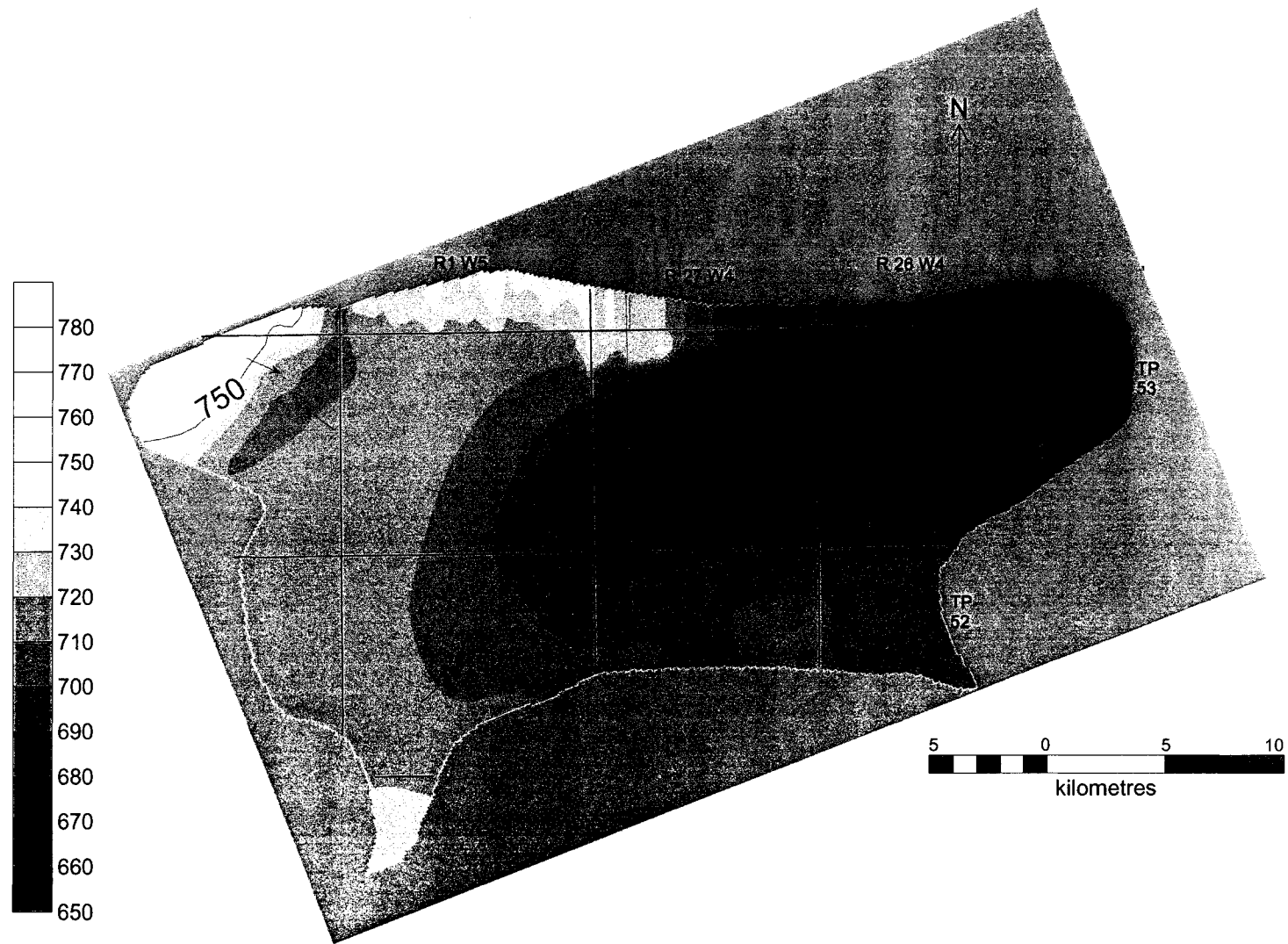


Figure 6.2 Calibrated hydraulic head in layer 3 (10 m contour interval), arrows show direction of groundwater flow

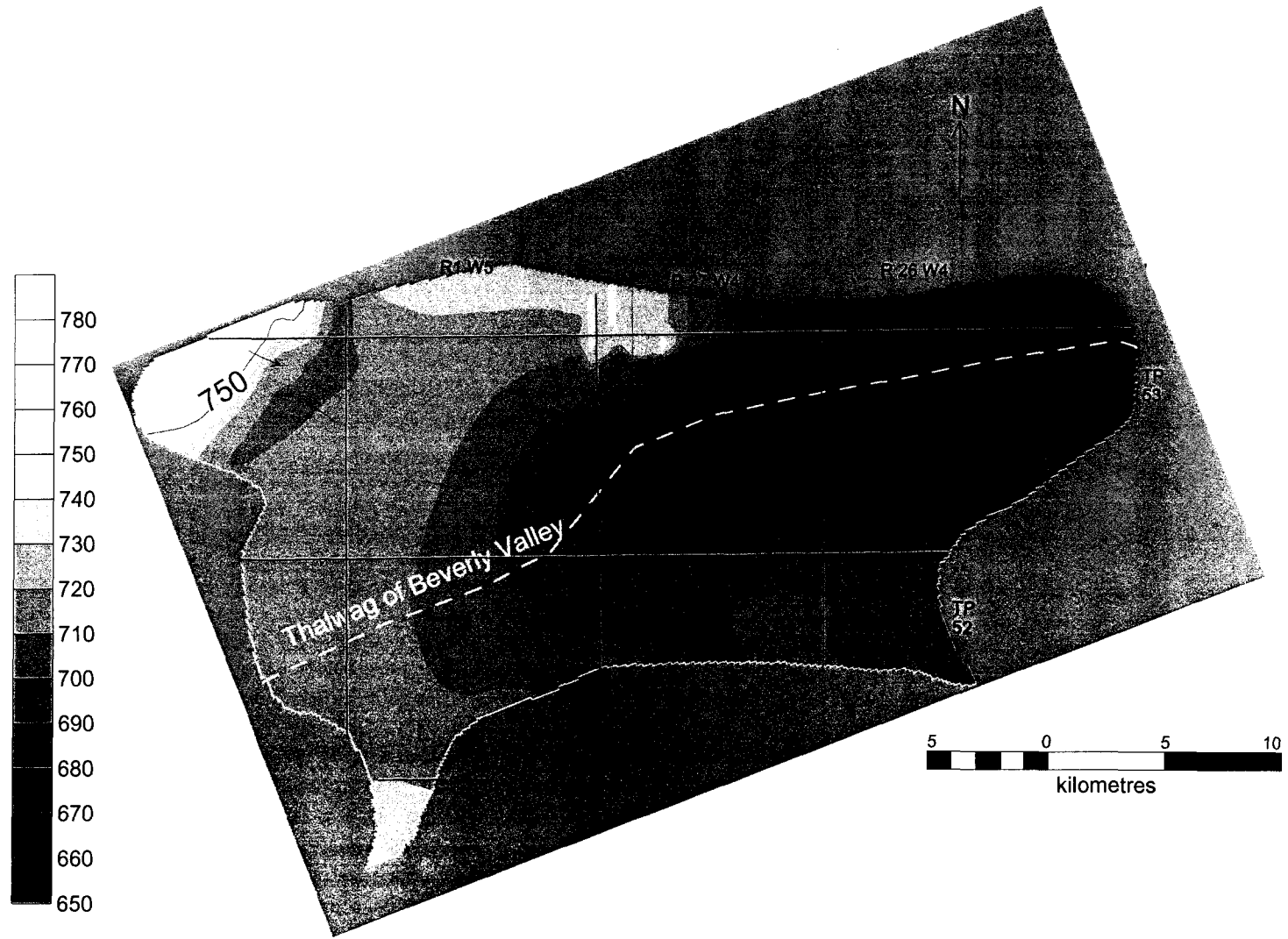


Figure 6.3 Calibrated hydraulic head in layer 5 (10 m contour interval), arrows show direction of groundwater flow

Valley it flows eastward toward the edge of the model domain. These figures also show that groundwater flow is focused toward a topographic low located in the northwest corner of the model domain (TP 53, R2 W5).

Figure 6.4 shows areas of the model where the water table is above the land surface, and groundwater is discharged. The model predicts groundwater discharge in the western part of the domain (TP 53, R2 W5), along the bottom and flanks of the topographic low that reflects the position of the Beverly Valley (TP 53, R 25-27 W4), in the WNA, and in the area occupied by Atim Creek. These results are consistent with the locations of mapped surface water features and groundwater discharge areas (Figure 4.10).

From the model results, it appears that the scour channel mapped by Bayrock and Hughes (1962) may have a significant influence on the hydrological conditions near the WNA. Groundwater discharge occurs to the southwest of the WNA (TP 53, R 27 W4) in the area that coincides with the location of the scour channel. Bayrock and Hughes proposed that the wetlands in this area may be an extension of this scour channel. Modelling results suggest that this may be the case.

6.1.3 Groundwater Velocities

Figures 6.5 through 6.7 show logarithmic plots of groundwater velocities in layers 1, 3 and 5. These plots show groundwater velocities are generally higher in the relatively high hydraulic conductivity units (Pitted Deltas, and Beverly Channel), and lower in the lower hydraulic conductivity units (Till, Ground Moraine). Groundwater velocities are

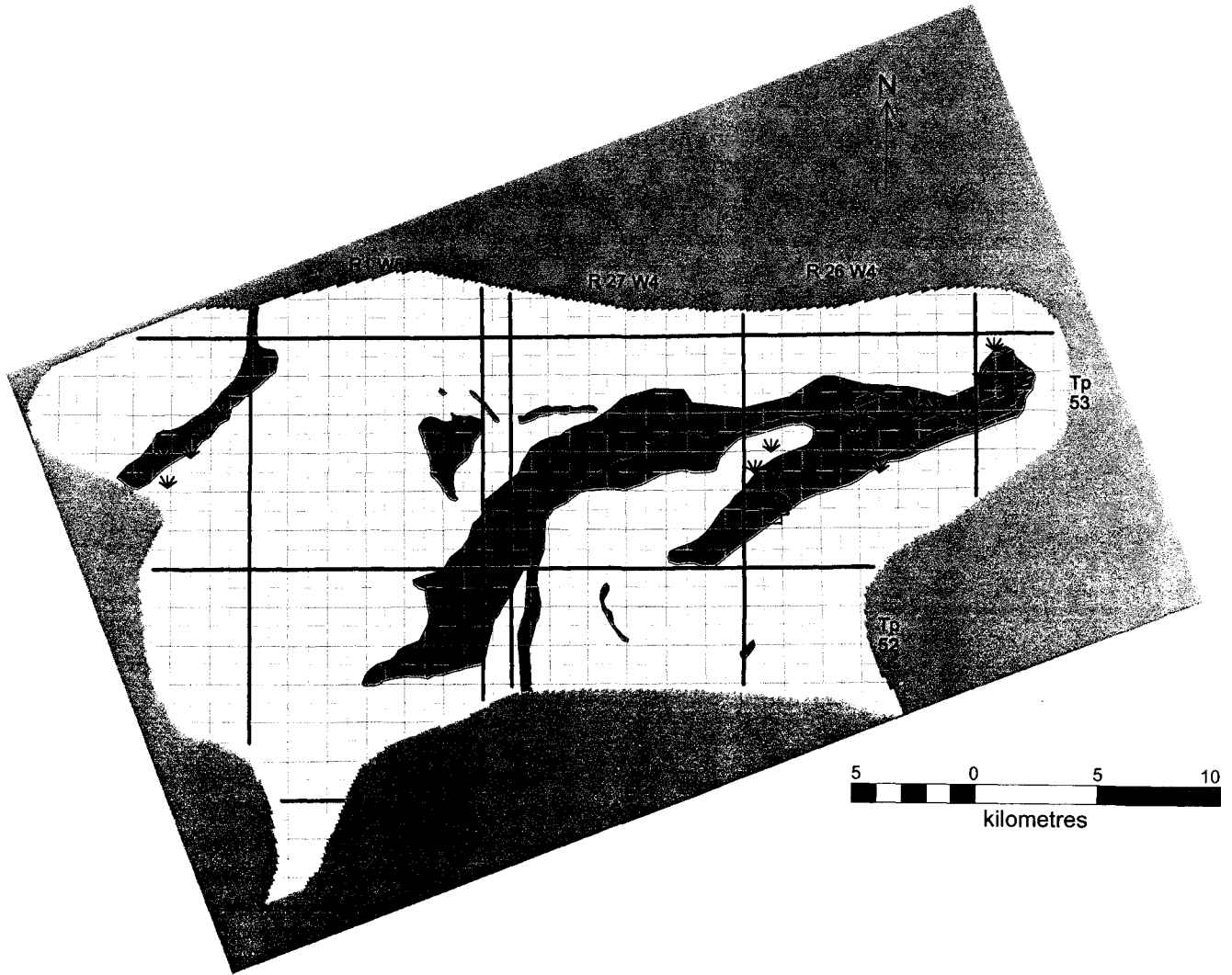


Figure 6.4 Locations of groundwater discharge areas in the calibrated model, locations of Atim Creek, Big Lake and wetlands (Figure 4.11) are shown for comparison

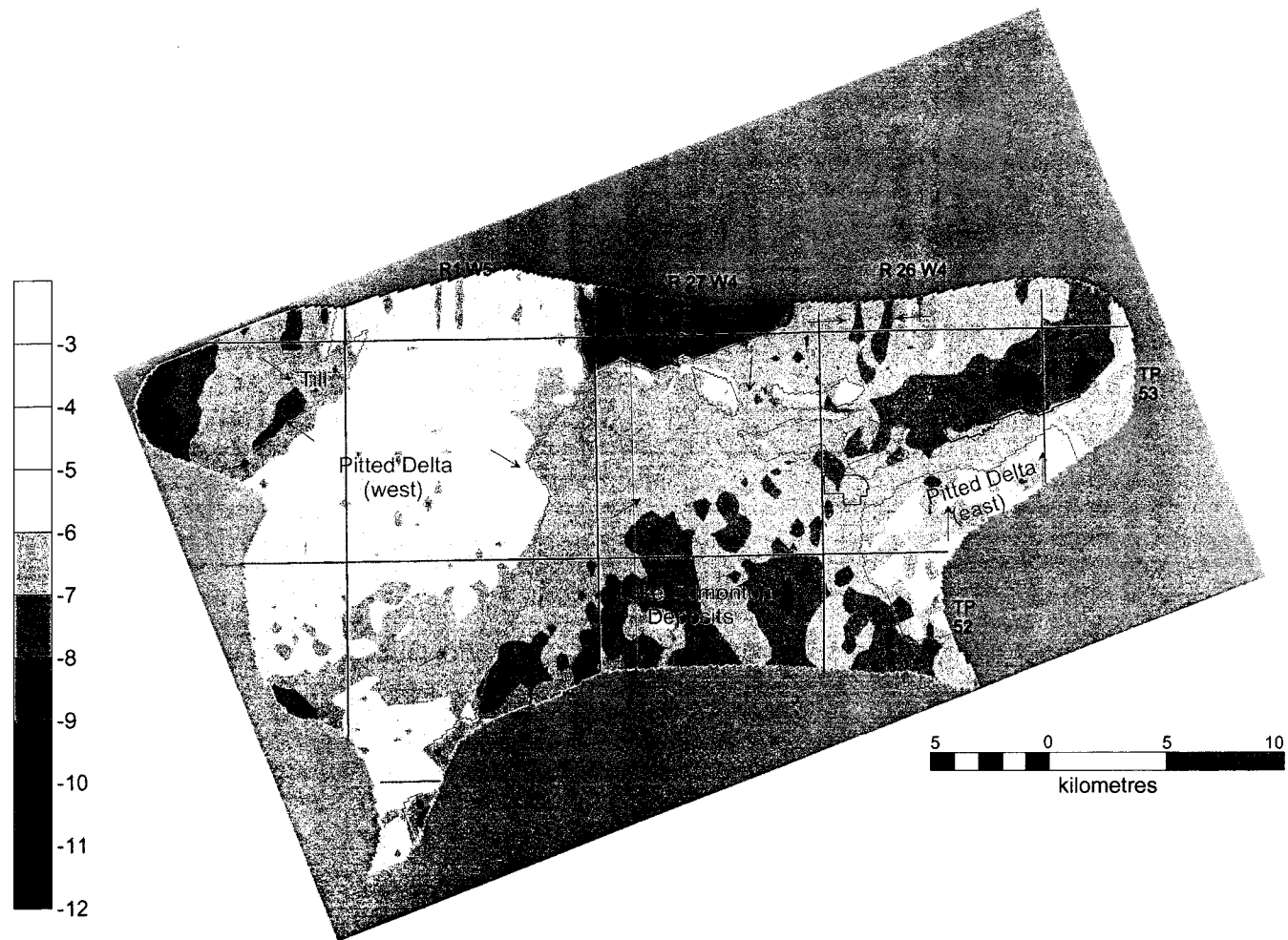


Figure 6.5 Logarithmic map of horizontal groundwater velocities (m/s) in layer 1 of calibrated model, blue arrows show direction of groundwater flow, boundaries of hydrostratigraphic units shown in grey

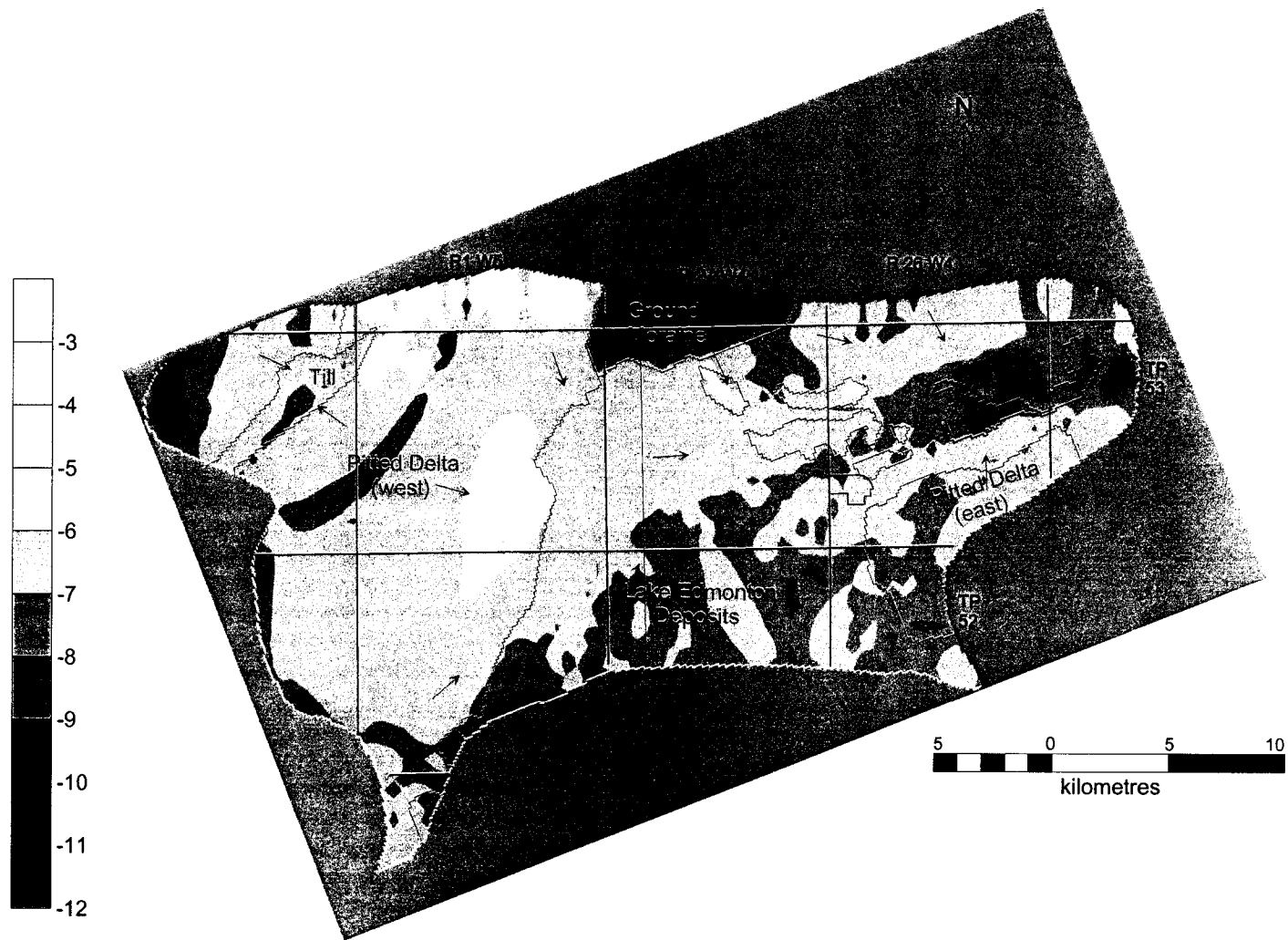


Figure 6.6 Logarithmic map of horizontal groundwater velocities (m/s) in layer 3 of calibrated model, blue arrows show direction of groundwater flow, boundaries of hydrostratigraphic units shown in grey

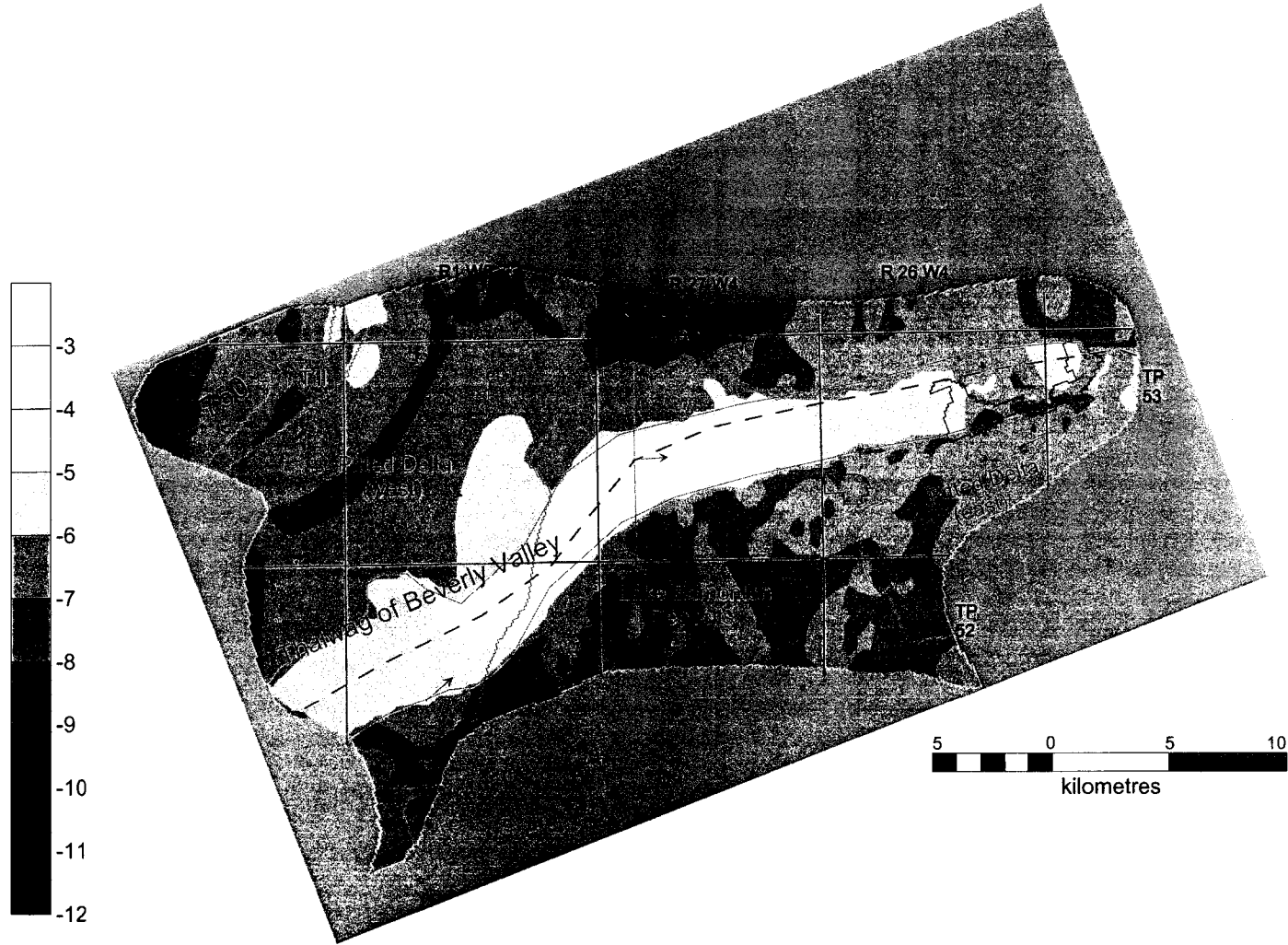


Figure 6.7 Logarithmic map of horizontal groundwater velocities (m/s) in layer 5 of calibrated model, blue arrows show direction of groundwater flow, boundaries of hydrostratigraphic units shown in grey

greatest in the Beverly Channel and are approximately 10^{-7} to 10^{-3} m/s (0.01 to 90 m/day). Groundwater velocities in the vicinity of the WNA range between approximately 10^{-8} to 10^{-5} m/s (0.001 to 1 m/day).

6.1.4 Model Water Balance

The total water balance for the model is presented in Table 6.1. Constant head nodes on the western edge of the model that represent the Beverly Valley input 8.5×10^{-2} m³/s of groundwater. By the time the groundwater in the Beverly Valley exits the model, the flux through this channel is 3.9×10^{-3} m³/s. Model evapotranspiration, which simulates both seepage at the surface and evapotranspiration, occurs at a rate of 2.8×10^{-1} m³/s in the discharge area, located in the central topographic low (TP52 to TP 53, R25 W4 to R1 W5). Evapotranspiration from the central discharge area accounts for approximately 70 percent of all discharge in the model. Evapotranspiration from the discharge area located in the northwest of the model (TP 53, R1 to R2 W5), the WNA, and Big Lake accounts for approximately five, one and three percent of total evapotranspiration, respectively.

6.2 Evaluation of Calibration

6.2.1 Methods

While there is no standard convention for evaluating calibrated models (Anderson and Woessner, 1992), there are several measures of error that are commonly used to evaluate error in a model with respect to a calibration dataset. These measures of error include: residuals, mean error (ME), mean absolute error (MAE), root mean square error (RMS), and normalized root mean square error (NRMS).

	Recharge	Constant Head (in)	Model "Evapotranspiration"	Constant Head (out)
Beverly Valley (west)	0	8.54×10^{-2}	0	0
Beverly Valley (east)	0	0	0	3.9×10^{-3}
Big Lake	1.3×10^{-3}	2.2×10^{-5}	1.24×10^{-2}	3.36×10^{-2}
Discharge Area (central)	3.86×10^{-2}	0	2.83×10^{-1}	0
Discharge Area (west)	6.8×10^{-3}	0	1.96×10^{-2}	0
WNA	1.4×10^{-3}	0	3.9×10^{-3}	0
Model Total	3.87×10^{-1}	8.55×10^{-2}	4.34×10^{-1}	3.86×10^{-2}
Total Input	4.73×10^{-1}			
Total Output	4.73×10^{-1}			
Percent Discrepancy	-0.01			

Table 6.1 Water balance for calibrated model (m^3/s)

Residual

The difference between observed heads and simulated heads is termed the residual. Negative residuals indicated that simulated heads are greater than the observed, and positive residuals indicate that simulated heads are less than the observed heads.

Mean Error

Mean error quantifies the average error between observed hydraulic head (h_o) and simulated hydraulic head (h_s) for a given set of calibration points (of size n). Positive and negative differences are averaged when calculating mean error. These differences may cancel each other out, and for this reason mean error is not a preferred method for

evaluating calibrated models. A positive mean error indicates that simulated heads are generally less than observed heads. A negative mean error indicates that simulated heads are generally greater than observed heads (Anderson and Woessner, 1992).

$$ME = \frac{1}{n} \sum_{i=1}^n (h_o - h_{s,i}) \quad (5.1)$$

Mean Absolute Error

The Mean Absolute Error is the average of the absolute value of the residuals. In this calculation, the absolute values of the residual heads are determined prior to averaging; therefore positive and negative residuals cannot cancel each other out. For this reason, the MAE is a better method to assess the difference between simulated and observed heads (Anderson and Woessner 1992).

$$MAE = \frac{1}{n} \sum_{i=1}^n |(h_o - h_{s,i})| \quad (5.2)$$

Root Mean Square Error

The root mean square (RMS) error is the square root of the average of the squared differences between the observed and simulated heads. The RMS is the best error estimate available if the errors are normally distributed (Anderson and Woessner, 1992).

$$RMS = \sqrt{\frac{1}{n} \sum_{i=1}^n (h_o - h_{s,i})^2} \quad (5.3)$$

6.2.2 Evaluation of the Calibrated Model

The calibrated model was evaluated both qualitatively and quantitatively. Qualitative evaluation of the model involved comparing the general head distribution predicted by the model to the mapped directions shown in Figure 4.9. Quantitative evaluation of the model involved comparing the difference between simulated hydraulic heads at

calibration points. Figure 6.8 shows a graph of the correlation between observed and simulated heads for the calibration points. The black line on the graph represents a perfect calibration, where simulated heads are equal to observed heads. The red lines running parallel to the black line represent the limits of the calibration target, ± 3 m or 5% of the average thickness of the surficial sediments. Data points that lie within the red lines are within 3 m of the observed values, while points lying outside this zone are not.

Simulated heads at four of the calibration points exceeded the calibration target, and include LE1, LE3, LE5, which are located in the area of Lake Edmonton deposits, and MOR, which is located in the area of ground moraine. Of the points unsuccessfully calibrated, LE1 most closely matched the observed head, and was within 3.2 m. MOR was calibrated to within 3.5 m, and LE5 was calibrated to within 4.5 m of the observed heads. LE3 was most sensitive to changes in conductivity during the calibration process, and the most difficult to match to the observed head. The simulated head at LE2 was 4.9 m greater than the observed head. While these observation points exceed the calibration target, when the regional scale of this model and the inherent measurement, scaling and interpolation errors are considered, this model reproduces observed heads very well.

The ME calculated for the model is 0.022 m. The positive value indicates that simulated hydraulic heads are generally less than observed heads. The near zero value indicates that the negative and positive residuals nearly cancel each other out. This suggests that the simulated heads are generally not skewed too high or too low, when compared to the observed heads. Figure 6.8 supports this; calibration points are evenly distributed on

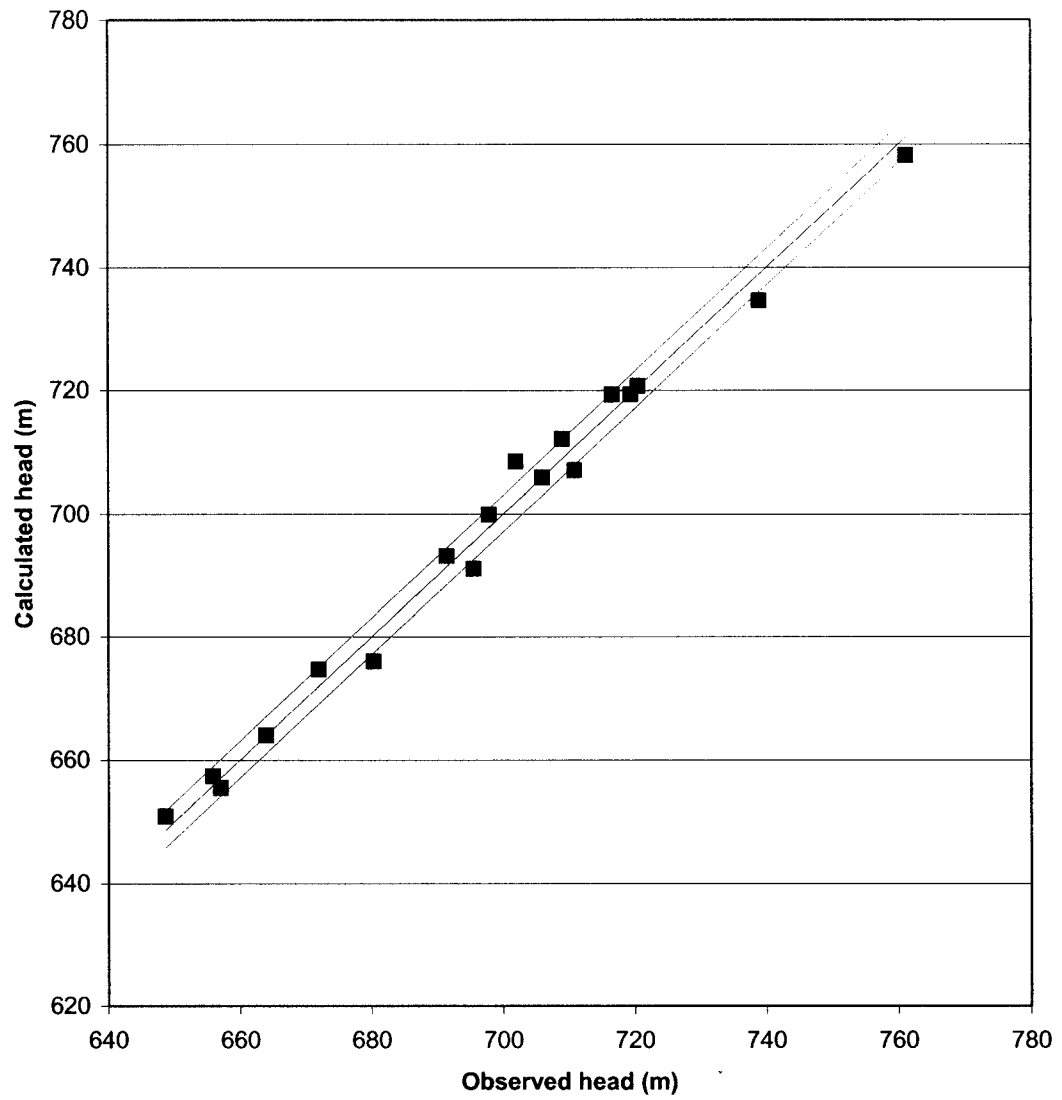


Figure 6.8 Simulated heads versus observed heads, black line represents perfect calibration, red lines show limits of calibration target (± 3 m), blue squares are data points

either side of the line. The MAE and RMS were 1.84 m and 2.35 m, respectively. These values fall below the calibration target of 3 m, indicating that simulated heads match observed heads closely. Table 6.2 shows the residuals for each of the 18 calibration points. Simulated heads in the WNA were within 0.6 m of the observed value at 03-2001 and within 0.1 m of the observed value at AENV-2236. This difference between simulated and observed head is negligible in a model of this scale.

Point Name	Observed Head (m)	Simulated Head (m)	Residual (m)
LE1	709	712.1	-3.1
LE2	708	708.5	-0.5
LE3	701	705.9	-4.9
LE4	664	663.9	0.1
LE5	680	676.0	4.0
BV1	650	650.8	-0.8
BV2	656	657.3	-1.3
BV3	694	693.1	0.9
PDE1	677	674.7	2.3
PDE2	698	699.9	-1.9
PDW1	719	719.3	-0.3
PDW2	721	720.7	0.3
PDW3	722	719.3	2.7
PDW4	710	707.1	2.9
TILL	761	758.2	2.8
MOR	738	734.5	3.5
03-2001	663	662.4	0.6
AENV-2236	666	666.1	-0.1

Table 6.2 Residuals for calibration points used in the numerical model

6.3 Sensitivity Analysis

The sensitivity analysis is an important component in the evaluation of a numerical model. There is an inherent uncertainty in any calibrated numerical model, resulting from the uncertainty in the estimates of aquifer parameters, fluxes and boundary

conditions (Anderson and Woessner, 1992). Sensitivity analyses involve identifying and varying parameters having a significant effect on simulated results to determine the model's sensitivity to changes to a particular parameter.

Values of hydraulic conductivity values used in the calibrated model depend on a recharge rate of 20 mm per year, this value is the average of literature estimates. During the calibration process it was found that increasing or decreasing the recharge rate necessitated increasing or decreasing the hydraulic conductivity values. Since evapotranspiration is a head dependent function that depends on both hydraulic conductivity and recharge, the rate of evapotranspiration is essentially a fitting parameter. Therefore, during the calibration process any changes made to hydraulic conductivity or recharge in the calibration process required changes to the evapotranspiration rate. Thus, the parameters having the greatest effect on the calibrated model are recharge and hydraulic conductivity. For this reason, the sensitivity analysis focused on the model's sensitivity to variations in hydraulic conductivity and recharge.

The sensitivity analysis performed on this model involved varying hydraulic conductivity values by one order of magnitude. In addition, because reasonable recharge rates for the study area range between three and ten percent of total annual precipitation (Chapter 2), the sensitivity analysis involved decreasing recharge from the calibrated case of five percent to three percent, and increasing recharge to ten percent of total annual precipitation. The sensitivity analysis is divided into 2 main sections: (1) effects of varying hydraulic conductivity, and (2) effects of varying recharge.

6.3.1 Effects of Varying Hydraulic Conductivity

The calibrated model was composed of eight hydrostratigraphic units, or hydraulic conductivity zones. These zones include the: Bedrock (HSC), Lake Edmonton Deposits (LE), Pitted Delta (west) (PDW), Pitted Delta (east) (PDE), Till, Ground Moraine (MOR), Upper Beverly Valley (UBV), and Lower Beverly Valley (LBV). As part of the sensitivity analysis, hydraulic conductivity was increased and decreased by one order of magnitude in each of these units. The effects of varying hydraulic conductivity on RMS error, and on evapotranspiration rates in the WNA and the discharge area are discussed below.

RMS Error

RMS error is a measure of error between simulated and observed heads. RMS is a particularly useful method of comparing simulated heads in the sensitivity analysis to the simulated heads in the base case, because in a model of this scale, visual comparison of hydraulic head contours is not effective. Small changes in head distribution are not obvious. For this reason, the discussion on hydraulic heads centres on changes in RMS.

Figure 6.9 shows percent change in RMS plotted against increasing or decreasing hydraulic conductivity by one order of magnitude. From this plot, it can be seen that increasing the hydraulic conductivity of the Lake Edmonton deposits (LE) by one order of magnitude produces the greatest change in RMS (266 percent). This suggests that the model is extremely sensitive to increasing the hydraulic conductivity of the Lake Edmonton deposits. The model was also very sensitive to increasing the hydraulic conductivity of the Pitted Delta east (PDE) and decreasing the conductivity of the Pitted Delta west (PDW), and resulted in 160 and 170 percent changes in RMS, respectively.

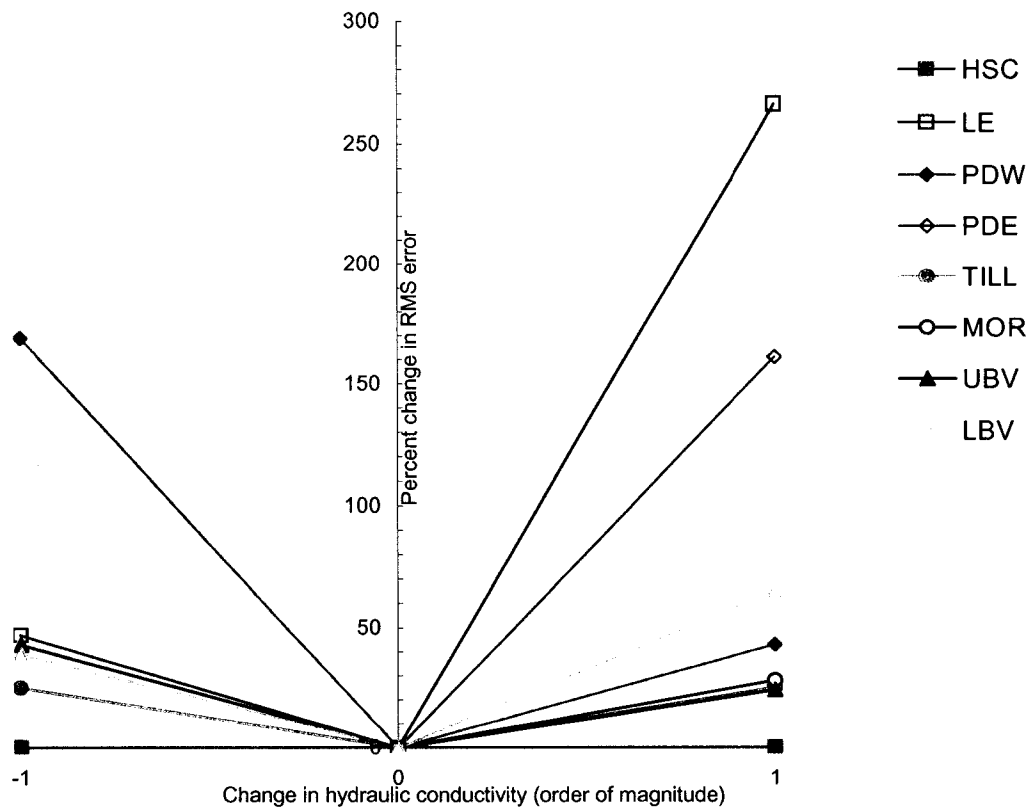


Figure 6.9 Changes in RMS error resulting from increasing and decreasing hydraulic conductivity of different hydrostratigraphic units by one order of magnitude

The model was less sensitive to changes in the other units and extremely insensitive to changes in bedrock hydraulic conductivity. Changes to bedrock hydraulic conductivity had little effect on the model, because groundwater flow occurred primarily in the surficial sediments (layers 1 to 5).

Evapotranspiration Rates in the Central Discharge Area

Figure 6.10 shows that increasing the hydraulic conductivity of the Lower Beverly Valley has the greatest effect on the evapotranspiration rate in the central discharge area (Figure 6.4; TP 52 to 53, R25 W4 to R1 W5), and results in a decrease of about 140 percent. The rate of evapotranspiration was moderately sensitive to increasing the hydraulic conductivity of the Lake Edmonton Deposits, and resulted in a decrease of approximately 30 percent. Decreasing the hydraulic conductivity of the Upper and Lower Beverly Valley also had a moderate effect on the model and resulted in increases of 50 percent and 38 percent, respectively. Rates of evapotranspiration in the discharge area were extremely insensitive to varying the hydraulic conductivity of the Horseshoe Canyon, Till, and Ground Moraine.

Evapotranspiration Rates in the WNA

Figure 6.11 shows percentage change in evapotranspiration in the WNA plotted against increasing or decreasing hydraulic conductivity by one order of magnitude. This graph shows that increasing the hydraulic conductivity of the Lake Edmonton Deposits produces the greatest change in evapotranspiration, and results in a decrease of about 85 percent. Decreasing the hydraulic conductivity of the Pitted Delta (west) produced the second greatest change in evapotranspiration in the WNA, and resulted in an increase of approximately 65 percent. Increasing the hydraulic conductivity of the Till

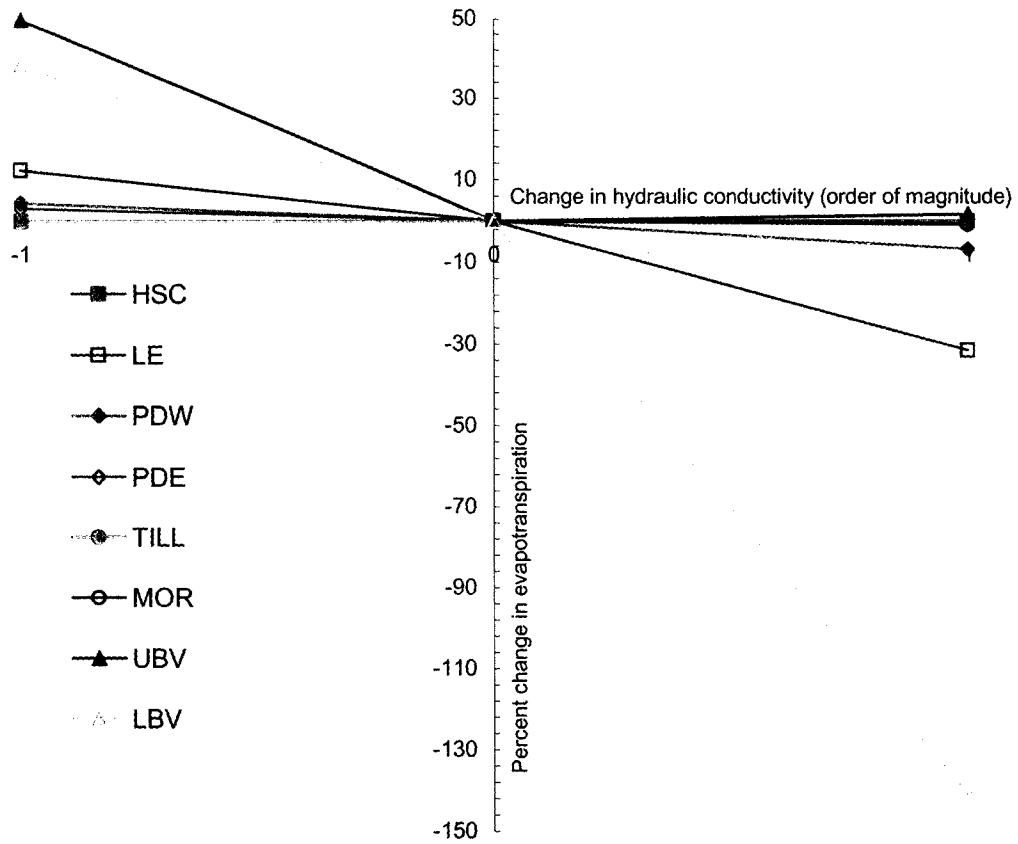


Figure 6.10 Changes in evapotranspiration in the central discharge area (TP 52 to 53, R25 W4 to R1 W5) resulting from changes in hydraulic conductivity of the different hydrostratigraphic units by one order of magnitude

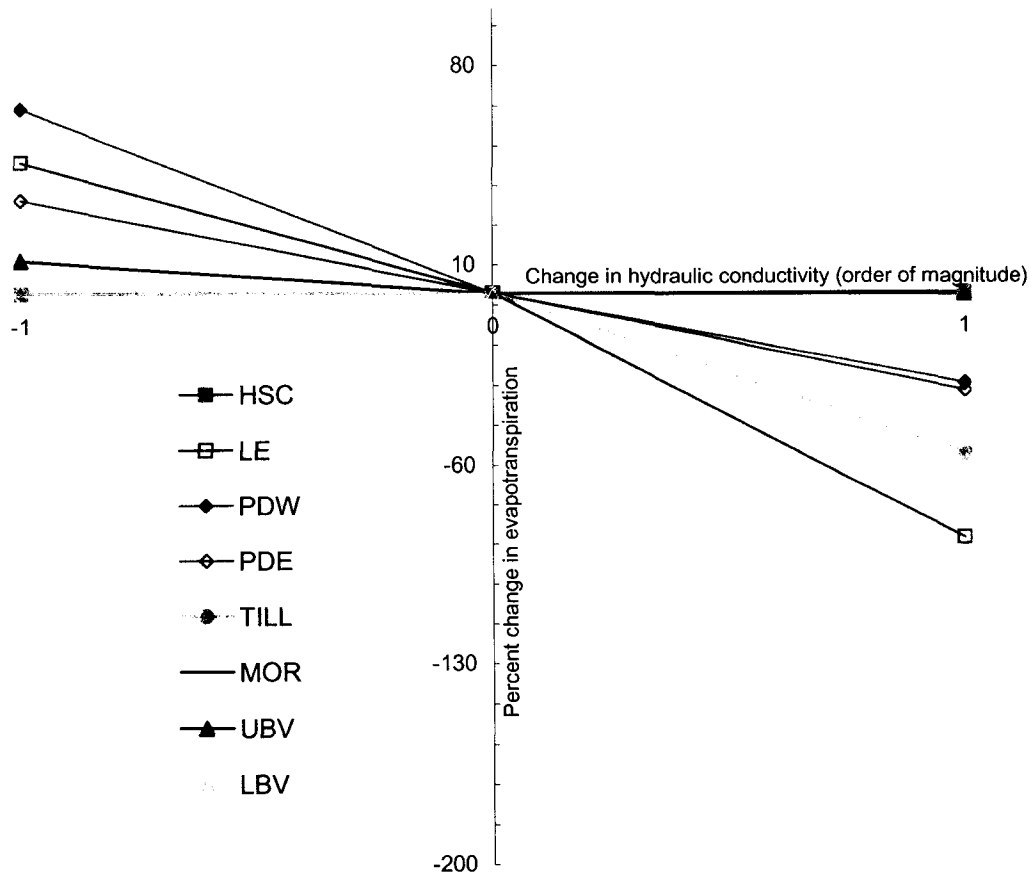


Figure 6.11 Changes in evapotranspiration in the WNA resulting from changing the hydraulic conductivity of different hydrostratigraphic units by one order of magnitude

also produced a significant change, a decrease of about 55 percent. Decreasing the hydraulic conductivities of the Till, Lower Beverly Valley, and increasing the conductivities of the Ground Moraine and Upper Beverly Valley produced changes of less than two percent. Neither increasing nor decreasing the hydraulic conductivity of the bedrock affected the evapotranspiration rate in the WNA.

6.3.2 Effects of Varying Recharge

Recharge was also evaluated in the sensitivity analysis. Recharge estimates range between 3 and 10 percent of total annual precipitation (Chapter 2). In the sensitivity analysis, the rate of recharge was decreased to 10 mm per year, approximately 3 percent, and increased to 40 mm per year, approximately 10 percent. Figure 6.12 shows the percent change in RMS error, rates of evapotranspiration in the WNA and discharge area when the recharge rate is varied.

Decreasing the recharge rate from 20 mm per year to 10 mm per year increased the RMS error by about 45 percent (3.75 m). Increasing the recharge rate to 40 mm per year also increased the RMS error by about 80 percent (5.08 m).

Of the parameters varied, increasing and decreasing recharge had the greatest effect on the rate of evapotranspiration in the WNA. Increasing recharge to 40 mm/year increased the evapotranspiration by almost 140 percent. Decreasing recharge by a factor of two to 10 mm/year resulted in a decrease in the evapotranspiration rate by approximately 55 percent.

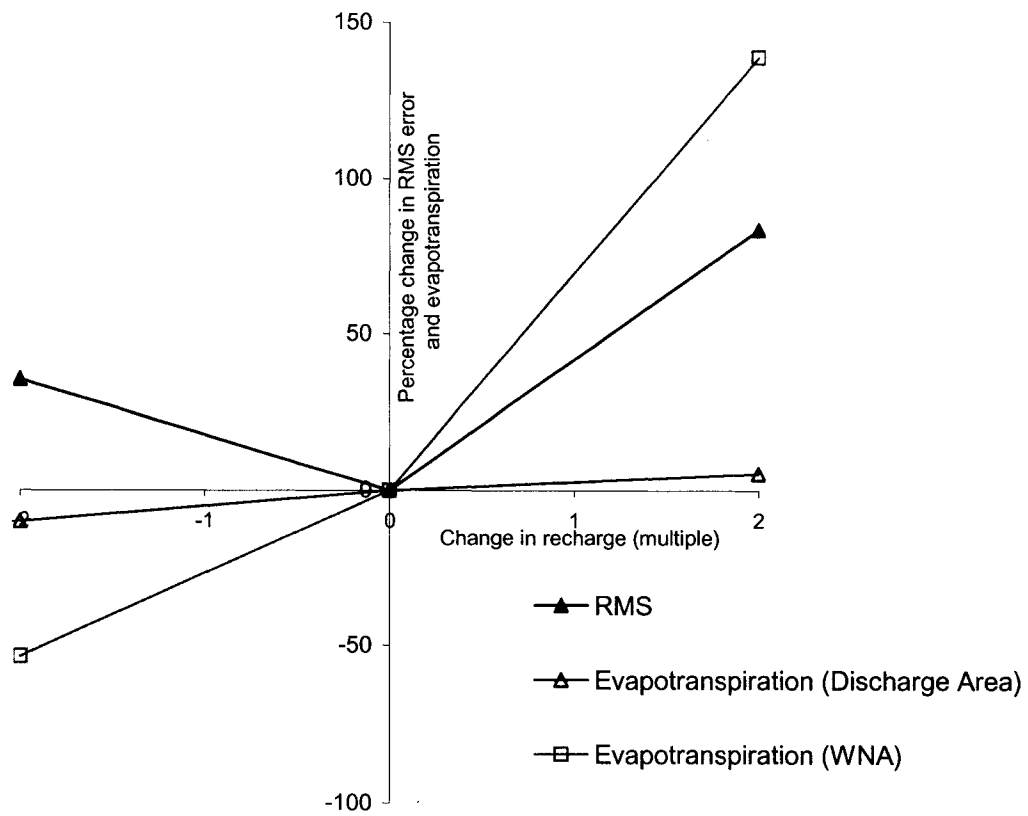


Figure 6.12 Changes in RMS error, and evapotranspiration rates resulting from changes in recharge

Similar effects were observed on the rate of evapotranspiration in the central discharge area (TP 52 to 53, R 25 W4 to R1 W5), although these changes were less significant. Increasing recharge resulted in an increase of approximately 10 percent in the rate of evapotranspiration, while decreasing recharge resulted in a decrease of approximately 5 percent.

6.3.3 Discussion

The calibrated model represents observed hydraulic heads well; this is supported by a MAE and RMS of 1.84 m and 2.35 m, respectively. These values fall below the calibration target of 3 m. Simulated heads in the WNA were within 0.6 m of the observed value at 03-2001 and within 0.1 m of the observed value at AENV-2236. This difference between simulated and observed head is negligible in a model of this scale, and may result from measurement errors, scaling effects and interpolation errors.

The model is extremely sensitive to the relation between hydraulic conductivity, recharge, and evapotranspiration, and the calibrated parameter values are based on a recharge rate of 20 mm per year. From the calibration process it is known that decreasing the recharge rate in the model would require hydraulic conductivity values to be decreased, and increasing the recharge rate would require the hydraulic conductivity values to be increased. In addition, because the rate of evapotranspiration is a head dependant function, decreasing the evapotranspiration rate in the model would require the hydraulic conductivity values to be increased, and vice-versa.

Results of the sensitivity analysis indicate that the model is more sensitive to changes in certain parameters than others. Increasing the hydraulic conductivity of the Lake Edmonton deposits had the greatest effect on RMS error. The model also showed

significant increases in RMS error when the hydraulic conductivities of the Pitted Delta (west), and the Pitted Delta (east) were increased and decreased, respectively.

Rates of evapotranspiration in the discharge area that occupies the topographic low in the central portion of the study area were most affected by increasing the hydraulic conductivity of the upper Beverly Valley. Moderate changes were observed when the hydraulic conductivities of the Lake Edmonton deposits and Upper and Lower Beverly Valley were increased, and decreased, respectively. Evapotranspiration rates in the WNA were most sensitive to decreasing the hydraulic conductivity of the Lake Edmonton deposits.

Overall, it appears that varying the hydraulic conductivities of the Lake Edmonton deposits, and the Pitted Deltas (east and west) produce the greatest effects on the model.

Chapter 7 Location of WNA Recharge Area and Effects of Reduced Recharge on Groundwater Levels in the WNA

This chapter presents the results of the particle-tracking which was used to locate the WNA recharge area, and the results of the scenarios in which recharge in the WNA recharge area was reduced.

7.1 Location of the WNA Recharge Area

This section is subdivided into three sections. The first describes how the WNA recharge area was delineated, the second presents the location of the WNA recharge area, and the third discusses the time required for water to travel from the WNA recharge area to the WNA.

7.1.1 Particle-tracking Method

One of the objectives of this study was to delineate the WNA recharge area. Once the MODFLOW model was calibrated, MODPATH (Pollock, 1989) was used to delineate the WNA recharge area. MODPATH is a particle-tracking program, which uses MODFLOW solutions to determine the advective pathway of water through the flow system.

Particles can be tracked either forward or backward from any location in a model.

Forward tracking traces a particle from its point of origin to a sink (e.g., well, or lake);

backward tracking traces a particle to its recharge area or capture zone.

It is good practice to start particles at the water table to ensure the accuracy of generated path lines (Anderson and Woessner, 1992). However, Visual MODFLOW

places particles at the centre of a grid cell by default, and does not accommodate starting particles on the water table. This short-coming was compensated for by first electronically drawing the profile of the simulated water table onto the grid before manually placing particles in the water table.

A combination of both backward tracking from the WNA to its recharge area, and forward tracking from the recharge area to the WNA was used to delineate the recharge area. Particles were first tracked backward from the WNA to the recharge area to delineate the recharge area. Then particles were placed in the WNA recharge area and tracked forward to the WNA to confirm the location of the recharge area. Porosity for all surficial units was assumed to be 30 percent.

7.1.2 Location of the Recharge Area

The results of the particle tracking analysis indicate that the WNA recharge area occupies a linear area trending from the northwest of 24-052-27-W4 to the west half of 05-053-26-W4, and includes a portion in the southeast of the WNA (Figure 7.1). The blue lines on the figure show the advective pathway of groundwater flowing from the WNA recharge area to the WNA. The model delineates the location and shape of the recharge area more precisely than that proposed by Prosser (1982).

7.1.3 Particle Travel Time

The time required for particles to travel from the recharge area to the WNA ranges up to 800 years, averaging 100 years. There is a substantial difference in particle travel time, because the time required depends in part on the distance from the point of recharge to

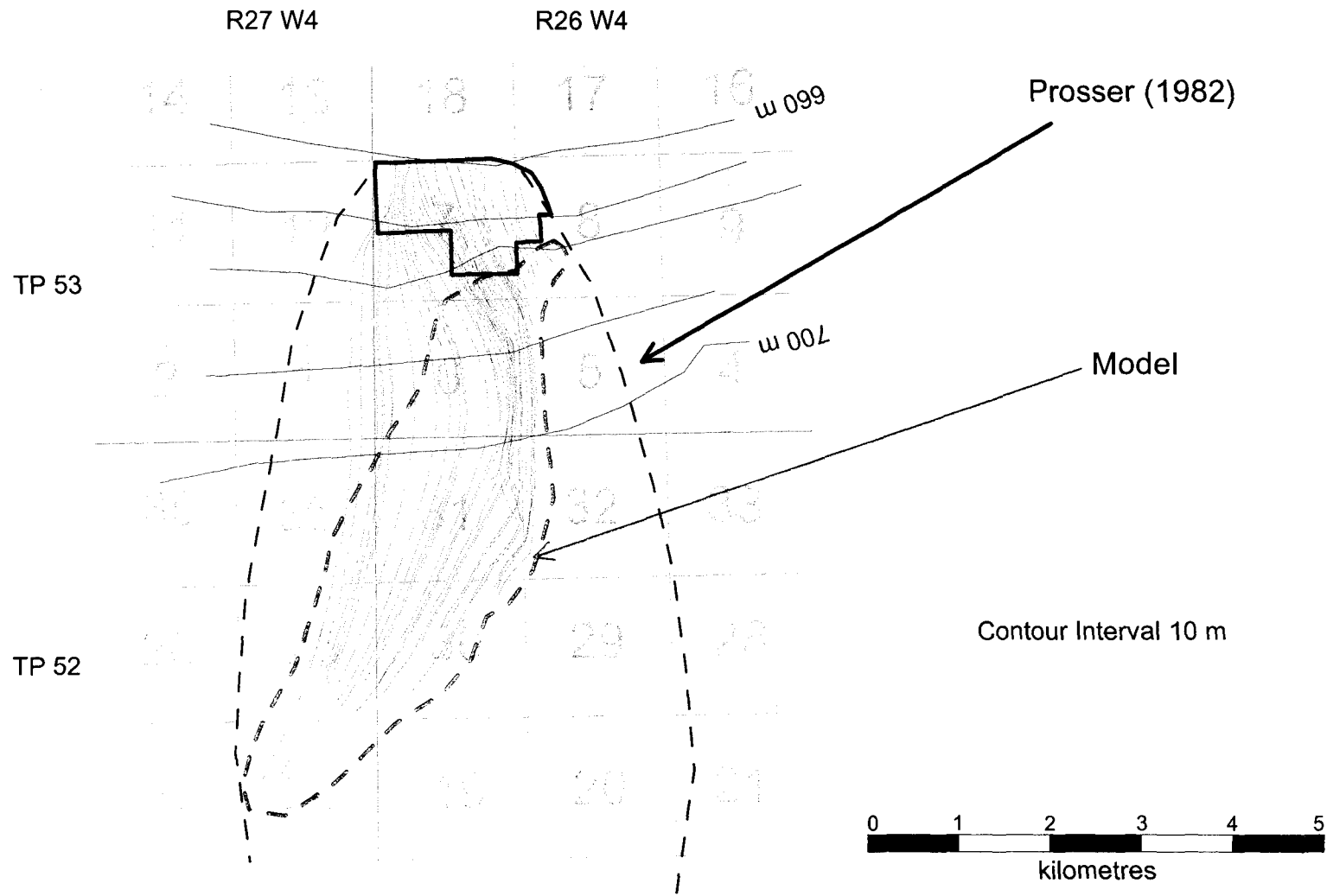


Figure 7.1 Location of WNA recharge area predicted by the model and proposed by Prosser (1982), blue lines are advective pathlines, section numbers in grey

the WNA. Recharge occurs over a large area from the WNA extending to as far as 7.5 km to the southwest (Figure 7.1).

7.2 Sensitivity Analysis

In Chapter 6, it was shown that the calibrated model is most sensitive to changes in the hydraulic conductivities of the Lake Edmonton deposits, and the Pitted Delta (east).

Because one of the objectives of this study was to determine the location of the WNA recharge area, a sensitivity analysis was performed on the calibrated model to determine the effect of changing certain parameters on the location of the recharge area. The findings of this sensitivity analysis are presented below.

7.2.1 Effects of Varying Hydraulic Conductivity

Location of the Recharge Area

Decreasing the hydraulic conductivity of the Lake Edmonton Deposits had a significant effect on the location of the recharge area, and caused it to move northward, closer to the WNA. In contrast, increasing the hydraulic conductivity of the Lake Edmonton Deposits caused the recharge area to move farther south, to the model boundary.

Decreasing the hydraulic conductivity of the Pitted Delta (west) did not significantly change the general location of the recharge area, but did affect the shape causing it to spread eastward. Decreasing the hydraulic conductivity of the Pitted Delta (east) moved the recharge area eastward, while decreasing conductivity moved the recharge area westward. Increasing the hydraulic conductivity of the Lower Beverly Valley also influenced the location of the recharge area and caused it to expand to the west. These changes in the location of the recharge area are summarized on Figure 7.2.

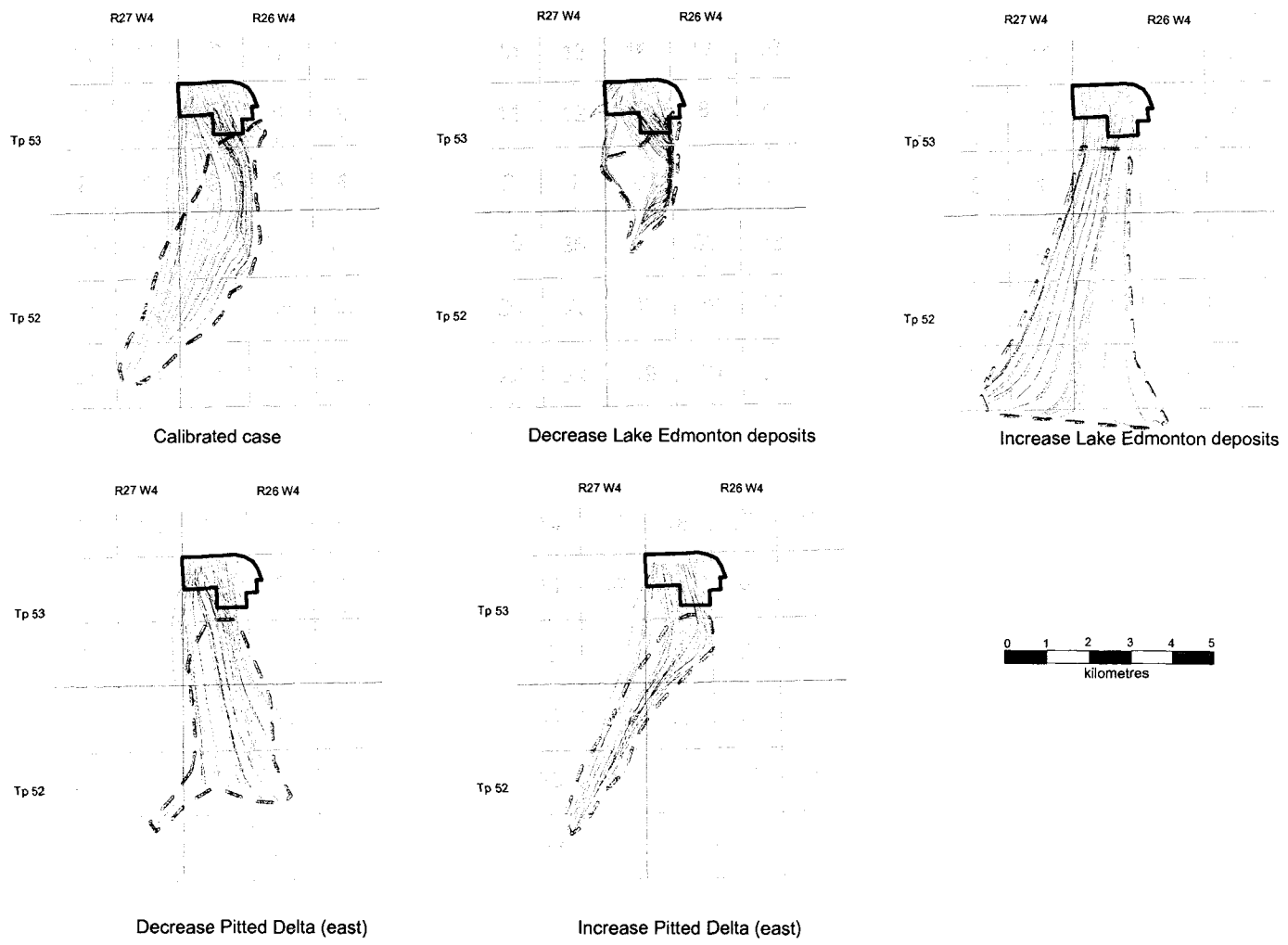


Figure 7.2 Sensitivity of the location of the WNA recharge area to increasing and decreasing hydraulic conductivity of the Lake Edmonton deposits, and Pitted Delta (east), blue lines show advective pathlines and red dashed line delineates recharge area

Average Particle Travel Time

Figure 7.3 shows percentage change in maximum time required for particles to travel from the recharge area to the WNA. Negative values indicate that the average travel time is greater than in the calibrated case.

Figure 7.3 shows that particle travel time was most sensitive to decreasing the hydraulic conductivity of the Lake Edmonton Deposits, and resulted in a 100 percent increase in travel time. Similarly, decreasing the hydraulic conductivity of the Pitted Delta (west) and increasing the conductivity of the Lower Beverly Valley resulted in an increase in travel time of 27 and 24 percent, respectively. In contrast, decreasing the hydraulic conductivity of the Pitted Delta (east) results in a decrease in travel time of approximately 30 percent. Increasing the hydraulic conductivity of the Lake Edmonton Deposits, Upper Beverly valley, and Ground Moraine resulted in moderate increases in travel time, less than 15 percent. Varying the hydraulic conductivity of the Horseshoe Canyon Formation had no effect on average particle travel time or the location of the recharge area.

7.3 Reduced Recharge Scenarios

Prosser (1982), and Spencer (1990) identified development in the recharge area resulting in a reduction in recharge as the greatest threat to the WNA. Thus, the calibrated model was used to evaluate the effects of reduced recharge on groundwater elevations in the WNA. Recharge was reduced by 25 percent (to 15 mm per year), 50 percent (to 10 mm per year), and by 100 percent over the area shown in Figure 7.4.

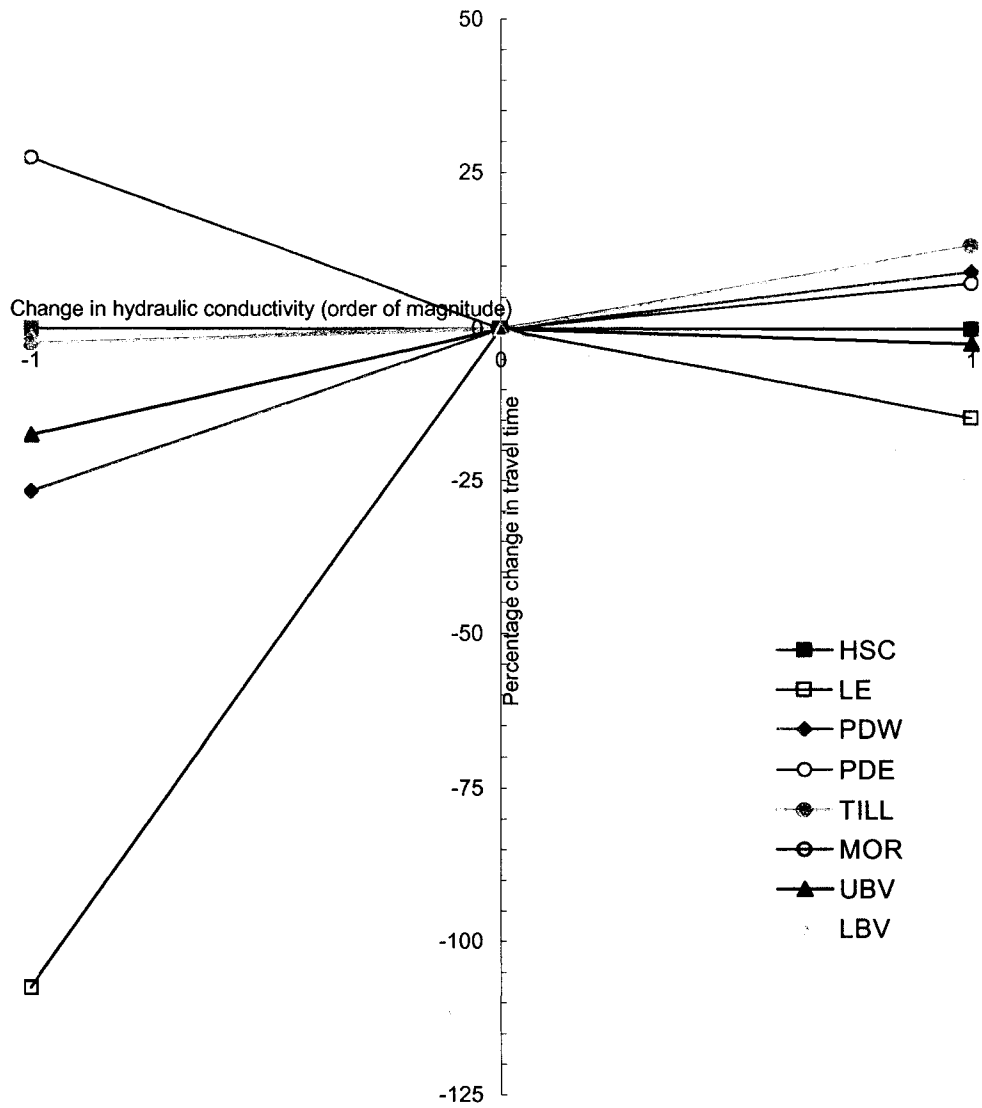


Figure 7.3 Percentage change in time required for water to travel from the WNA recharge area to the WNA resulting from increasing and decreasing hydraulic conductivity of different units by one order of magnitude

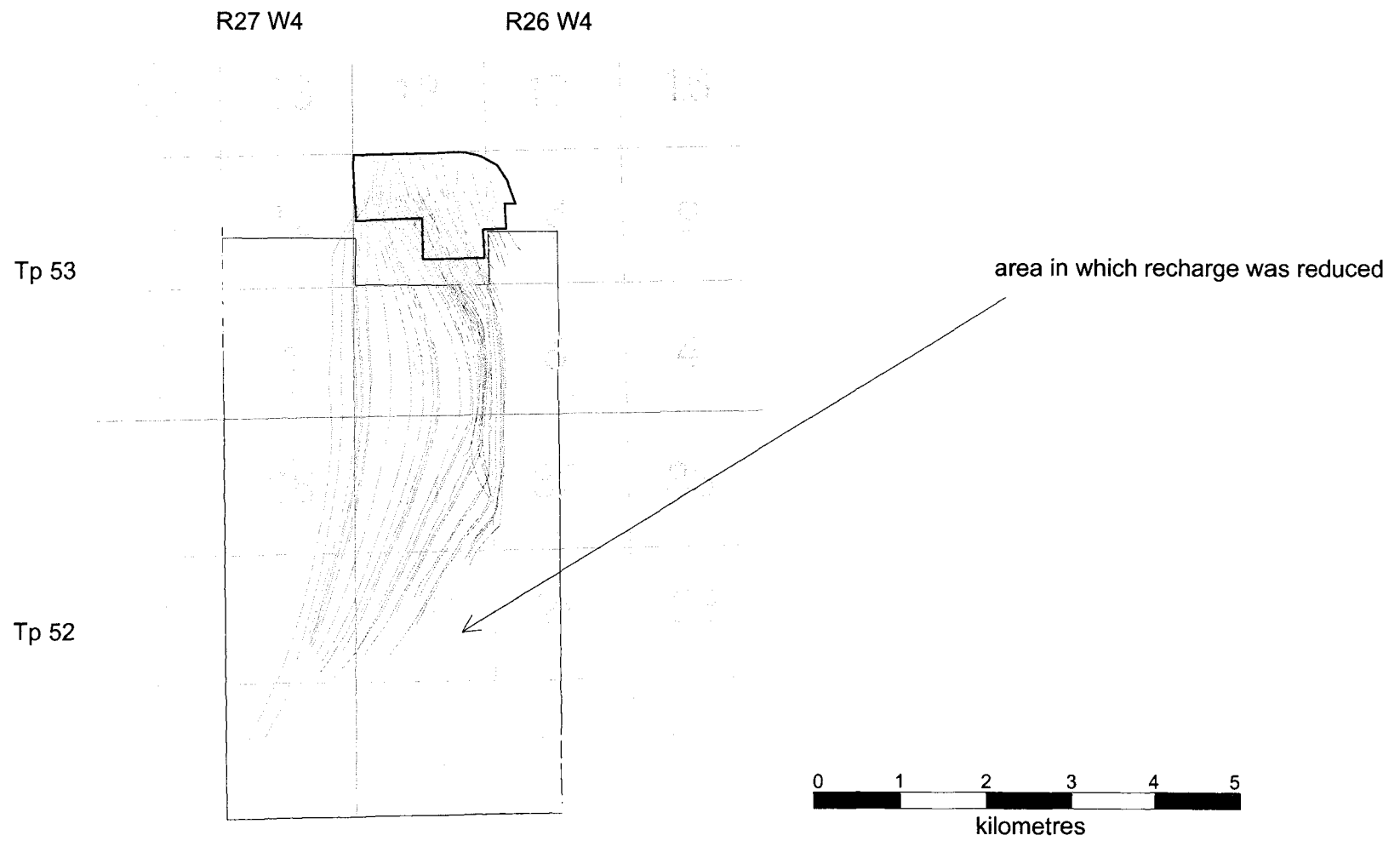


Figure 7.4 Map showing area where recharge was reduced by 25, 50 and 100 percent, blue lines show advective pathlines, numbers denote sections

Since it is difficult to predict how development south of the WNA will occur, the entire area between the WNA and its recharge was included. The perimeter of this area was defined with quarter section boundaries.

Effects were measured by adding 25 observation points in the WNA to Layer 2 of the calibrated model. Points were added to Layer 2 (5 to 10 m below the ground surface) instead of Layer 1, in case the top layer became dry due to the reduced recharge rates. Hydraulic heads calculated at these points for the reduced recharge scenarios were compared to those calculated in the same locations by the calibrated model. Figures 7.5 to 7.7 show the amount hydraulic head decreased at each location when recharge was reduced by 25, 50, and 100 percent, respectively. In the scenario where recharge is reduced by 25 percent (15 mm/year), declines in head range between 0 and 0.6 m in layer 2. When recharge is reduced by 50 percent (10 mm/year), declines in head range between 0 and 1.1 m in layer 2. Finally, when recharge is reduced by 100 percent, declines in head range between 0.1 and 4.2 m layer 2. Declines in head are generally greater in the southeast of the WNA, and decrease toward the northwest.

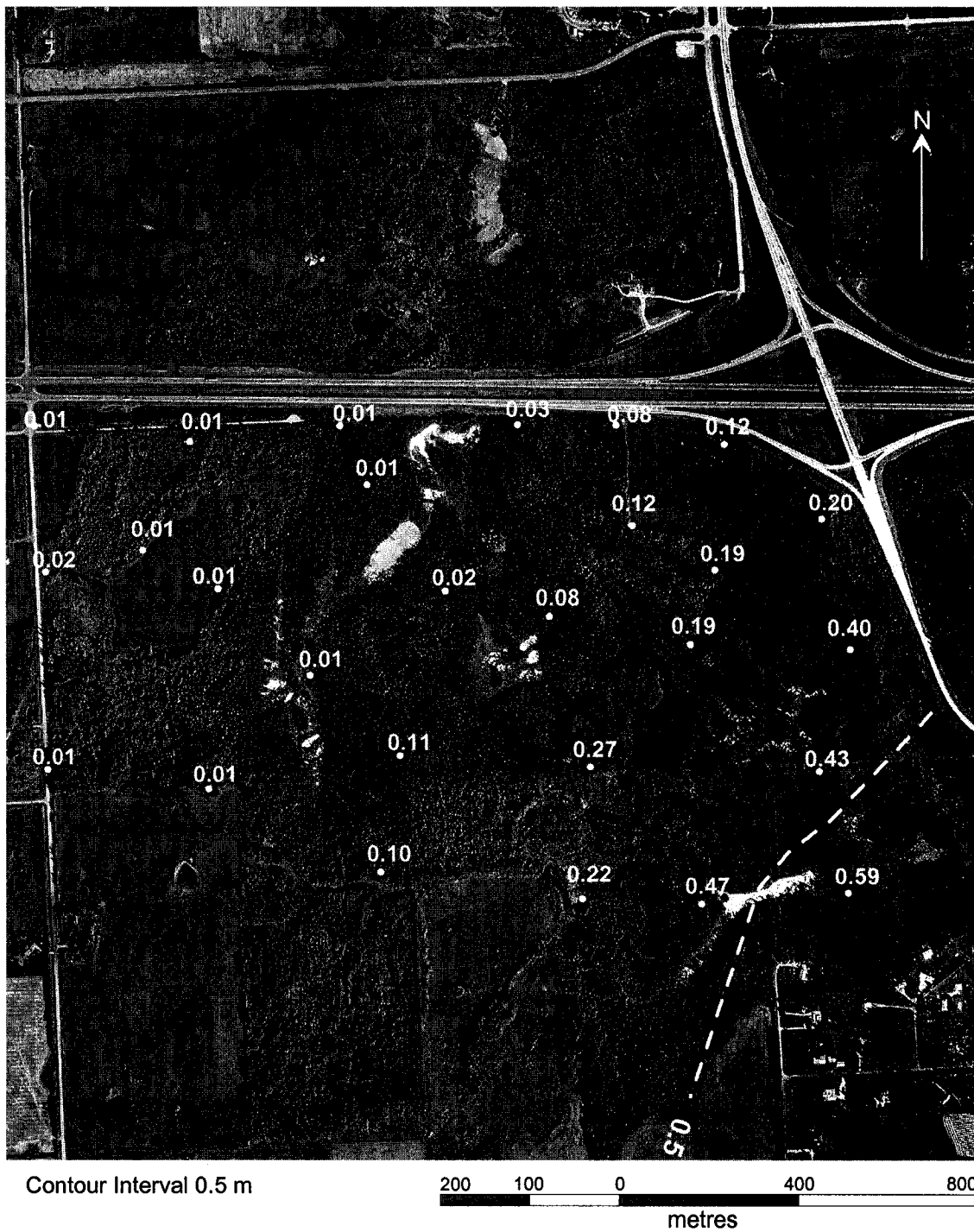


Figure 7.5 Map showing declines in hydraulic head in layer 2 of the WNA resulting from decreasing recharge by 25 percent (airphotograph modified from UMA, 2000)

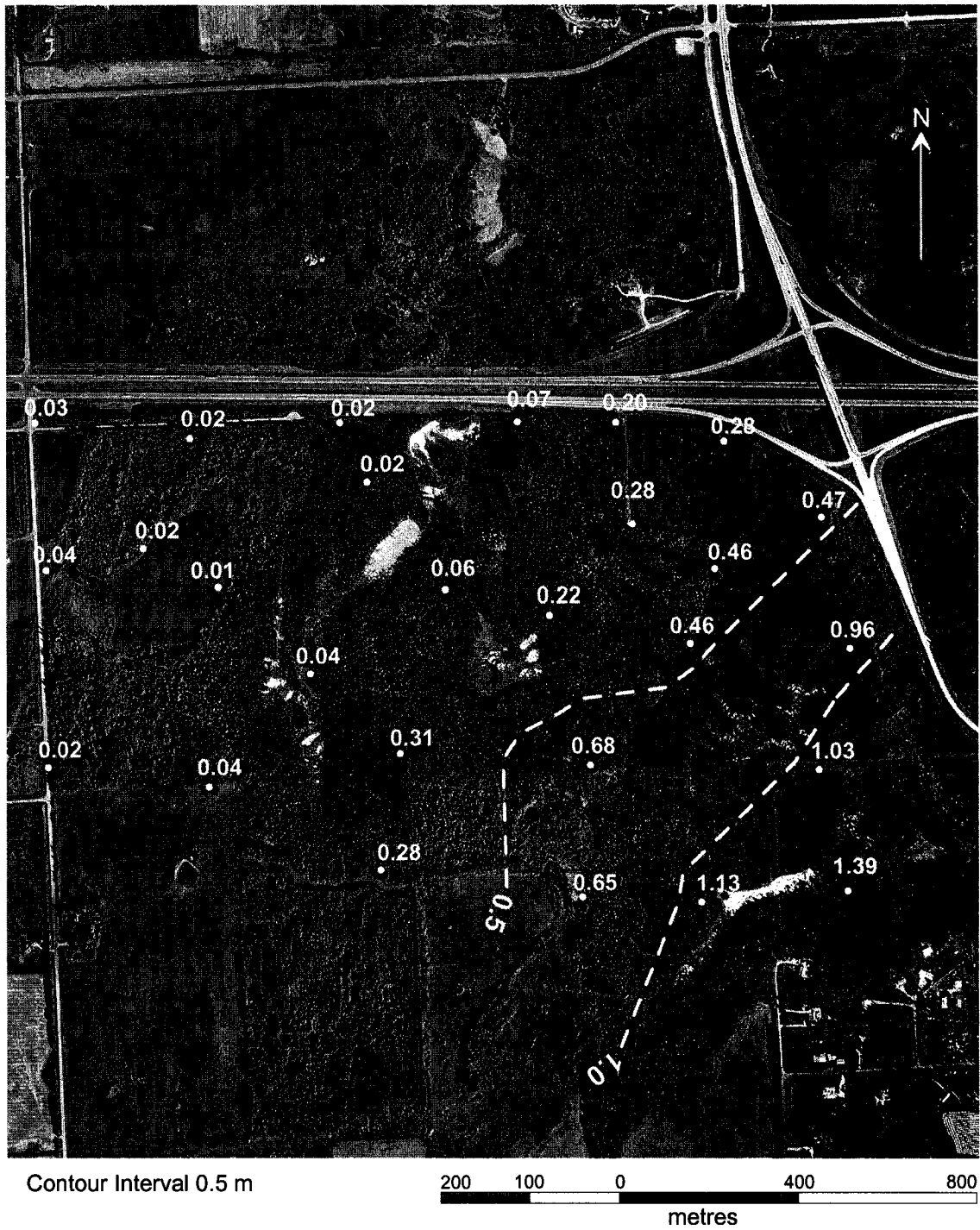


Figure 7.6 Map showing declines in hydraulic head in layer 2 of the WNA resulting from decreasing recharge by 50 percent (airphotograph modified from UMA, 2000)

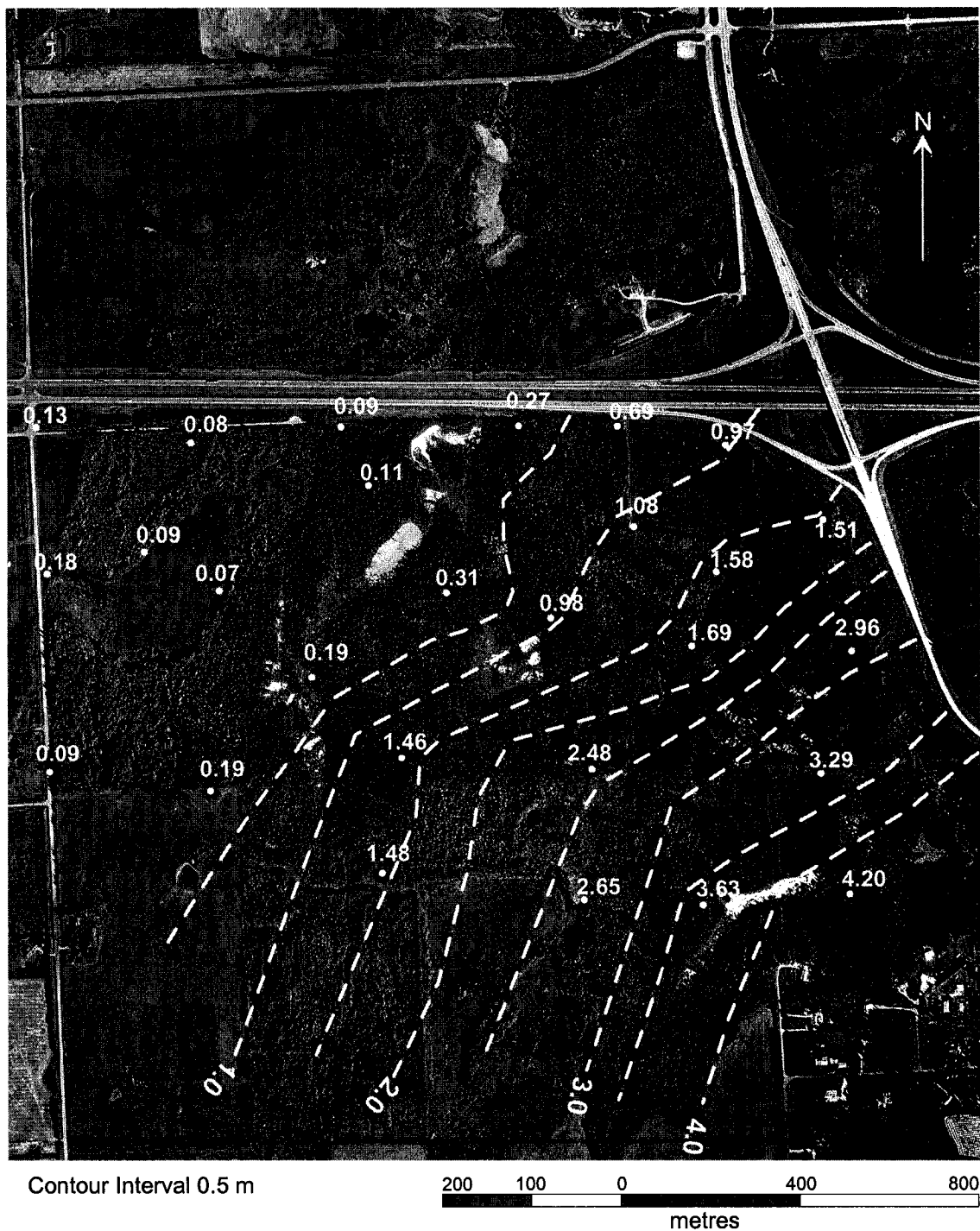


Figure 7.7 Map showing declines in hydraulic head in layer 2 of the WNA resulting from decreasing recharge by 100 percent (airphotograph modified from UMA, 2000)

Chapter 8 Discussion, Conclusions and Recommendations

8.1 Discussion of Results

Discussion of the results presented in this chapter is divided into three sections: (1) regional hydrogeology, (2) location of the WNA recharge area, (3) effects of reduced recharge on the groundwater levels in the WNA.

8.1.1 Regional Hydrogeology

The model predicts groundwater recharge in the uplands located along the north and south perimeters of the domain. Groundwater flow is from the highlands toward the buried Beverly Valley. Regional groundwater flow is controlled primarily by the buried Beverly Valley and is toward the east (Figures 6.1 to 6.3). While this is a function of the boundary conditions, it is likely accurate.

Groundwater discharge occurs along the flanks and bottom of the topographic low that reflects the location of the Beverly Valley. Areas of groundwater discharge in the model coincide with the locations of significant surface water features and mapped groundwater discharge areas (Figures 4.11 and 6.4).

The locations of Big Lake and Atim Creek in the model are characterized by areas of groundwater discharge. Therefore, it can be reasoned that both Big Lake and Atim Creek are groundwater discharge features. In the northwest corner of the domain is a linear discharge area. Figures 4.1 and 4.11 shows this region as being characterized by swampy or marshy land.

The model also predicts groundwater discharge in a linear area trending southwest to northeast through the WNA (Figure 6.4). This area is characterized by high water tables and marshy land (Figures 4.1 and 4.11). It also coincides with the location of a scour channel. Bayrock and Hughes (1962) propose that the large wetland area in which the WNA is located is a result of this channel (Figures 4.1 and 4.3). Model results suggest that this scour channel may be important to the hydrological conditions in the WNA, since groundwater discharge occurs southwest of the WNA (TP53, R27 W4), in the vicinity of this channel. The channel may act to focus groundwater flow from the uplands to the south of the WNA toward the lower lying areas (TP 53, R26 and 27 W4).

When the locations of groundwater discharge areas predicted by the model are compared to mapped surface water features, groundwater discharge areas, and locations of swampy or marshy lands, it appears that the model simulates the regional groundwater flow system very well.

8.1.2 Location of the WNA Recharge Area

Development within the recharge area has the potential to affect the WNA groundwater flow system by introducing contaminants or changing recharge rates. Contaminants have the potential to adversely affect the flora and fauna of the WNA. Reduced recharge rates may lower groundwater levels in the WNA, and thereby affect the springs, which are known to be important to the ecosystem. Thus, in order to preserve the WNA over the long-term, its recharge area needs to be protected, and to do this the recharge area must be delineated.

The results of the particle tracking indicate that the recharge area is located in sections 5, 6, 8 (TP 53, R26, W4), sections 30, 31, 32 (TP 52, R 26, W4), and sections 24, 25, 36 (TP 52, R27, W4). These results confirm Prosser's (1982) hypothesis (Figure 6.9). Additionally, the recharge area occupies the western edge of the Pitted Delta that is located to the southeast of the WNA (Figure 8.1). Alberta Environment (1978) proposed that the artesian conditions around the WNA might be a result of significant and focused recharge occurring at this Pitted Delta; model results support this hypothesis.

The location of the recharge area is sensitive to changes in the hydraulic conductivity of the Lake Edmonton deposits, and the Pitted Deltas (east and west) (Figure 6.11). While the results of the sensitivity analysis show that the location of the recharge area changes with variations in hydraulic conductivity, the results of the sensitivity analysis also show that certain parts of the recharge area are less affected by these changes, or are less sensitive. Portions of the recharge area that are less sensitive to changes in model parameters are likely important, as their location is not influenced significantly by changes in the model. These areas include: sections 24, 25 (TP 52, R27, W4), 31 (TP 52, R26, W4), and section 6 (TP 53, R 26, W4) (Figure 7.2).

8.1.3 Effects of Reduced Recharge

The WNA ecosystem is dependant on a stable supply of good quality groundwater. Decreased recharge rates in the WNA result in lower groundwater levels in the WNA, as shown in Figure 7.5 through 7.7.

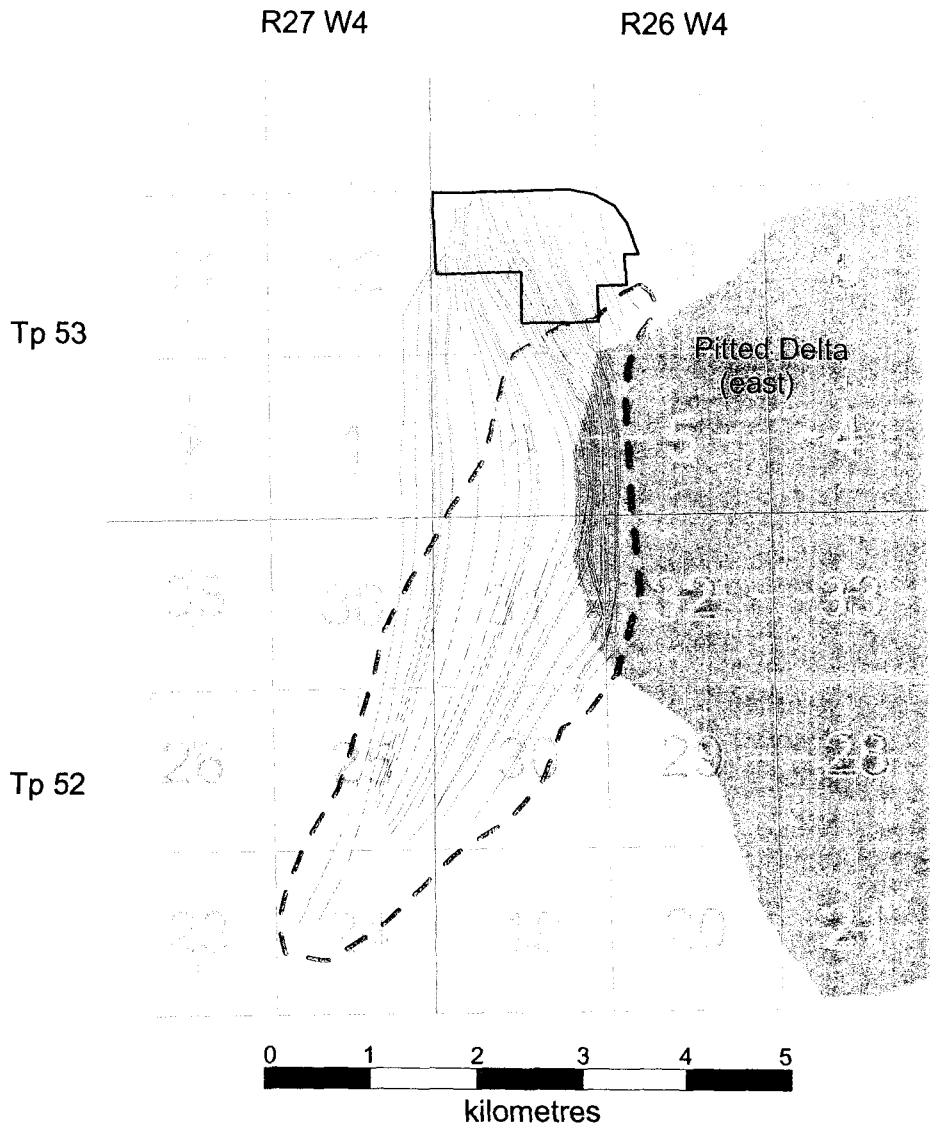


Figure 8.1 WNA recharge area (red dashed lines) overlies the western edge of the Pitted Delta (pink) located southeast of the WNA, blue lines show advective pathlines, section numbers shown

A detailed evaluation of the potential impacts resulting from decreased groundwater levels on the WNA ecosystem and from specific types of development is beyond the scope of this thesis. Figure 8.2 shows the land zoning designated by the County of Parkland in the vicinity of the WNA and its recharge area. Land in this area falls into one of seven categories: *Outdoor Recreation District, Agricultural General District, Agricultural Restricted District, Country Residential Core District, Industrial/Commercial Core District, Industrial Reserve District*, and the *Acheson Commercial Overlay*. Each of these land designations is summarized briefly in Table 8.1; more information can be found in The Parkland County Land Use By-law No. 15-00 (Parkland County, 2000).

Most of the land area occupied by the recharge area is zoned as *Agricultural General District*. This zoning does not allow for intensive development, and for this reason, development in this area, as it is presently zoned, should not have a significant impact on recharge rates. The remainder of the recharge area is zoned as *Agricultural Restricted District, Country Residential Core District, Industrial/Commercial Core District, Industrial Reserve District*, and the *Acheson Commercial Overlay*. *Agricultural Restricted District* land is similar to the *Agricultural General District* land and recharge in this area should not be significantly affected by permitted development in this area. Areas zoned as *Country Residential Core District, Industrial/Commercial Core District, Industrial Reserve District*, and the *Acheson Commercial Overlay* have greater potential to adversely affect recharge to the WNA groundwater flow system because development in these areas tends to be of higher density than in the *Agricultural Districts*. As development density increases, the percentage of the land surface that inhibits recharge also increases, which in turn, decreases recharge.

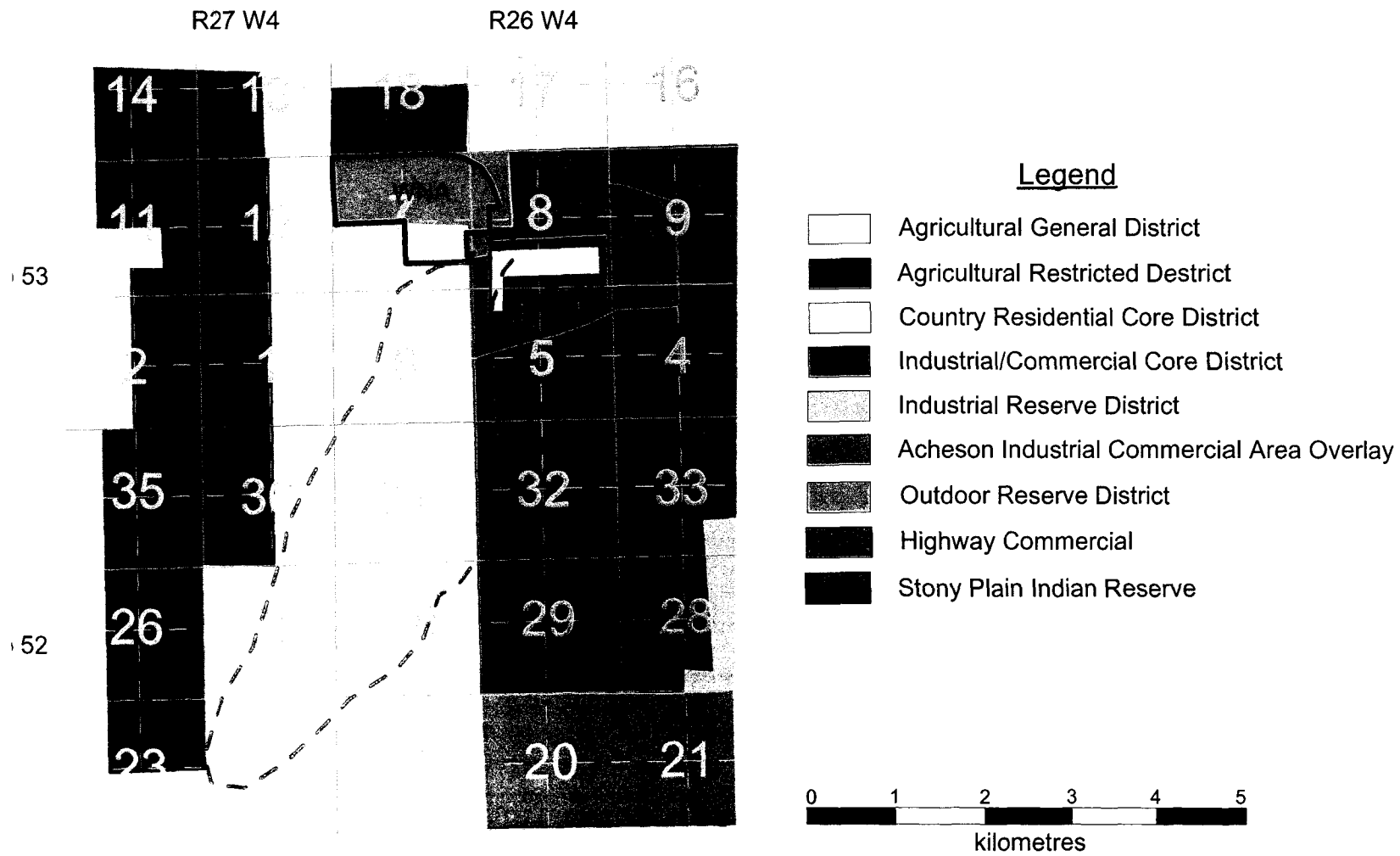


Figure 8.2 Map showing land use zoning in the area occupied by the WNA recharge area, recharge area shown by red dashed lines, section numbers noted (Parkland County, 2000)

Land Use Designation	General Purpose	Permitted Uses	Discretionary Uses
<i>Outdoor Recreation District</i>	Outdoor recreation		
<i>Agricultural General District</i>	Agricultural and farming related activities, limited opportunity on a discretionary basis for compatible non-farming related land uses	Apiary, extensive agricultural, and livestock development.	Agricultural support services, aquaculture, horticulture, small animal breeding/boarding services, recreational vehicle storage, campgrounds, religious assembly, residential, cemetery
<i>Agricultural Restricted District</i>	Agricultural and farming related activities, limited opportunity on a discretionary basis for compatible non-farm related land uses. Scattered subdivision development is discouraged.	Similar to above	Similar to above
<i>Country Residential Core District</i>	Conventional multi-parcel country residential subdivision/development and related uses including minor agricultural pursuits.	Mobile home, single detached dwelling	Agricultural support services, aquaculture, horticulture, small animal breeding/boarding services, recreational vehicle storage, campgrounds, community recreation, religious assembly,
<i>Industrial/ Commercial Core District</i>	Development of a compatible mix of industrial and commercial land uses.	<i>Industrial uses</i> manufacturing, processing, industrial storage, warehousing, natural resource extraction and processing <i>Commercial uses</i> hospitality services, professional services, retail sales, entertainment services, recreational vehicle storage.	
<i>Industrial Reserve District</i>	Accommodate existing development, provide for low intensity development, reserve land for the future expansion of industrial and commercial land uses		Agricultural activities, industrial manufacturing and processing, industrial storage, warehousing landfill development, and natural resource extraction and processing.
<i>Acheson Industrial Commercial Overlay</i>	Ensure the integrity of the Osbourne Acres residential subdivision while meeting the intent and goals of the Acheson Industrial Area Structure Plan (Parkland County, 1997).		

Table 8.1 Land use designation in WNA recharge area (Parkland County, 2000)

8.1.4 Particle Travel Time

Given the long period of time required for groundwater to travel from the recharge area to the WNA, it may take several generations before changes in groundwater quality resulting from human activities are observed. Hydraulic response times would be more

rapid and would depend on the location in the flow system. Because the time required for groundwater to travel from the recharge area to the WNA is dependant, in part, on the distance between the recharge area and the WNA, the accuracy of the location of the recharge area will also affect the accuracy of the predicted travel times. Also, because groundwater velocity varies inversely with porosity, travel time is dependant on porosity. Therefore, because porosity is a material property, improving the geological interpretation of the area occupied by the WNA and recharge area will improve estimates of time required for groundwater to travel from the recharge area to the WNA.

8.2 Conclusions and Recommendations

The WNA ecosystem depends on a stable supply of good quality groundwater from a glacio-surficial aquifer. Currently, the recharge area for the WNA is not formally protected, and is under increasing pressure due to development. Changing land use within the recharge area could have a negative impact on the quantity and quality of the groundwater. The conclusions of this study have significant implications for land use and groundwater resource management, and could be incorporated into land use planning

8.2.1 Conclusions

1. The WNA is located within a large groundwater discharge area that occupies a topographic low in TP 53, extending from R25 W4 to R1 W5. Regional groundwater flow is directed from the uplands to the north and south of this low toward the buried Beverly Valley. Once groundwater reaches the buried Beverly valley it flows eastward out of the study area.

The hydrologic conditions of the WNA are likely influenced by a scour channel, located to the southwest of the natural area. It was proposed by Bayrock and Hughes (1962) that the wetland area in which the WNA is located is an extension of this channel. Results of the model support this hypothesis.

2. The results of the particle tracking indicate that the recharge area is located in sections 5, 6, 8 (TP 53, R26, W4), sections 30, 31, 32 (TP 52, R 26, W4), and sections 24, 25, 36 (TP 52, R27, W4). These results confirm Prosser's (1982) hypothesis.

The recharge area occupies land currently zoned by Parkland County as *Outdoor Recreation District, Agricultural General District, Agricultural Restricted District, Country Residential Core District, Industrial/Commercial Core District, Industrial Reserve District*, and the *Acheson Commercial Overlay* (Parkland County, 2000). The majority of the land area occupied by the recharge area is zoned as *Agricultural General District*.

3. Decreased recharge results in lower groundwater levels in the WNA. In the numerical model, recharge was reduced by 25 percent (to 15 mm per year), 50 percent (to 10 mm per year), and by 100 percent. When recharge was reduced by 25 percent, declines in head of up to 0.6 m were observed in the WNA. When recharge was reduced by 50 percent, and 100 percent declines in head were as much as 1.1 m, and 4.2 m, respectively. The greatest declines in head were observed in the southeast of the WNA, the area characterized by marl ponds. This confirms that lower groundwater levels may impact the springs that support the WNA ecosystem.

4. Particle tracking analysis suggests that changes in the quality of groundwater will take an average of approximately 100 years to be fully realized in the WNA. Thus, it may take several generations before changes in groundwater quality resulting from human activities are observed. Hydraulic response times would likely be more rapid and would depend on the location in the flow system.

8.2.2 Recommendations

1. To improve the delineation of the recharge area it is recommended that the geology and hydrogeology in the vicinity of the WNA be further investigated. The cross-sections presented in Chapter 4 show the complex and interspersed nature of the Lake Edmonton deposits. At the regional scale, individual beds in the Lake Edmonton deposits are discontinuous and difficult to trace over short distances. It is likely that sandy lenses in the Lake Edmonton deposits have a significant effect on the hydrogeology of the WNA. Therefore, further investigation of the surficial geology and more detailed mapping of the sandy deposits within and around the perimeter of the WNA and its recharge area will improve understanding of the groundwater flow system.
2. The location of the recharge area is influenced by the Pitted Delta located southeast of the WNA. Delineation of this large sandy deposit will improve the understanding of the importance of this geological feature.
3. Bayrock and Hughes (1962) proposed that the marshy area, in which the WNA is located, is an extension of a scoured channel to the west of the WNA (Figure

4.1). It appears that this hypothesis is supported by the results of the model. It is recommended that buried channels in the vicinity of the WNA be delineated, as these channels likely have considerable influence on the local hydrogeology.

4. Improved estimates of hydraulic conductivity and recharge would reduce the uncertainty in the model. It is recommended that additional piezometers be installed within the WNA and its recharge area, and that hydraulic conductivity be measured in these wells.

References

- Aguado, E. and Burt, J.E. 2003. *Understanding weather and climate*, 3rd Edition, Prentice Hall, Upper Saddle River, New Jersey, 592 p.
- Alberta Environment. 1978. *Edmonton regional utilities study, v. 4 Groundwater*, Edmonton Metropolitan Regional Planning Commission, Edmonton, Alberta, 53 p.
- Anderson, M.P., and Woessner, W.W. 1992. *Applied groundwater modeling – Simulation of flow and advective transport*, Academic Press, Inc., San Diego, California, 381 p.
- Andriashek, L. 1988. *Quaternary stratigraphy of the Edmonton map area, NTS 83H*, Alberta Research Council Open File Report #198804, Alberta Research Council, Edmonton, Alberta, 29 p.
- Banack, L. 1992. *Hydrogeologic study of the Wagner Natural Area and surrounding region*, B.Sc. Thesis, University of Alberta, Department of Geology, Edmonton, Alberta, 35 p.
- Barr, A.G., van der Kamp, G., Schmidt, R., and Black, T.A. 2000. Monitoring the moisture balance of a boreal aspen forest using a deep groundwater piezometer, *Agriculture and Forest Meteorology*, **102**: 13-24.
- Batelaan, O., De Smedt, F., and Triest, L. 2003. Regional groundwater discharge: phreatophyte mapping, groundwater modeling and impact analysis of land-use change, *Journal of Hydrology*, **275**: 86-108.
- Bayrock, L.A., and Hughes, G.M. 1962. *Surficial geology of the Edmonton district, Alberta*, Research Council of Alberta, Preliminary Report 62-6, Alberta Research Council, Edmonton, Alberta, 40 p.
- Bibby, R. 1974. *Hydrogeology of the Edmonton area (northwest segment), Alberta*, Alberta Research Council, Report 74-10, Alberta Research Council, Edmonton, Alberta, 10 p.
- Bridgeham, S.D., Pastor, J., Janssens, J.A, Chapin, C., and Malterer, T.J. 1996. Multiple limiting gradients in peatlands: a call for a new paradigm, *Wetlands* **16** (1): 45-65.
- Carlson, V.A. 1967. *Bedrock topography and surficial aquifers of the Edmonton District, Alberta*, Research Council of Alberta, Report 66-3, Alberta Research Council, Edmonton, Alberta, 21p.
- Clair, T.R. 1998. Canadian freshwater wetlands and climate change, *Climate Change* **40**: 163-165.

- Cowardin, L.M., Carter, V., Golet, F. C., and LaRoe, E.T. 1979. *Classification of wetlands and deepwater habitats of the United States*, U.S. Fish and Wildlife Service, Department of the Interior, Washington, DC, USA. Report FWS/OBS-79/31, 103 p.
- Covich, A.P., Fritz, S.C., Lamb, P.J., Marzolf, R.D., Matthews, W.J., Poiani, K.A., Prepas, E.E., Richman, M.B., and Winter, T.C. 1997. Potential effects of climate change on aquatic ecosystems of the Great Plains of North America, *Hydrological Processes* **11**: 993-1021.
- Damman, A.W.H. 1986. Hydrology, development, and biogeochemistry of ombrogenous peat bogs with special reference to nutrient relocation in a western Newfoundland bog, *Canadian Journal of Botany* **64**: 384-394.
- Domenico, P.A., and Schwartz, F.W. 1990. *Physical and chemical hydrogeology*, John Wiley & Sons, Toronto, Ontario, 824 p.
- Environment Canada. 2004. URL address: <http://www.climate.weatheroffice.ec.gc.ca>
- Farvolden, R. 1963. Rate of recharge near Devon, Alberta, Alberta Research Council Bulletin **12**: 98-105
- Feng, Y. 2003. *Personal Communication*, Dr. Feng is an Associate Professor in the Department of Renewable Resources at the University of Alberta
- Fetter, C.W. 1994. *Applied Hydrogeology*, 3rd Edition, Prentice Hall, Inc., Upper Saddle River, New Jersey, 691 p.
- Glaser, P.H. and Janssens, J.A. 1986. Raised bogs in eastern North America: transitions in landforms and gross stratigraphy, *Canadian Journal of Botany* **69**: 395-415.
- Golden Software Inc. 1999. *Surfer 7*, Golden Software Inc, Golden, Colorado, 619 p.
- Hillel, D. 1982. *Introduction to soil physics*, Academic Press, Boston, Massachusetts, 364 p.
- Hayashi, M., van der Kamp, G., and Rudolph, D.L. 1998. Water and solute transfer between a prairie wetland and adjacent uplands, 1. Water balance, *Journal of Hydrology* **207**: 42-55.
- Hydrogeological Consultants Ltd. 1998a. *Lac Ste. Anne County, Parts of the North Saskatchewan and Athabasca River Basins, Parts of TP 053 to TP 059, R 01 to R 09, W5M, Regional Groundwater Assessment*, Government of Canada: Prairie Farm Rehabilitation Administration, Edmonton, Alberta, CD.
- Hydrogeological Consultants Ltd. 1998b. *Parkland County, Parts of the North Saskatchewan and Athabasca River Basins, Parts of TP 050 to TP 054, R 25, W4M to R 08, W5M, Regional Groundwater Assessment*, Government of Canada: Prairie Farm Rehabilitation Administration, Edmonton, Alberta, CD.

- Irish, E.J.W. 1970. The Edmonton Group of south-central Alberta, *Bulletin of Canadian Petroleum Geologists* **18** (2): 125-155.
- Kathol, C.P. and McPherson, R.A. 1975. *Urban geology of Edmonton*, Alberta Research Council, Bulletin 32, Alberta Research Council, Edmonton, Alberta, 61 p.
- Klijn, F. and Witte, J-P.M. 1999. Eco-hydrology: groundwater flow and site factors in plant ecology, *Hydrogeology Journal* **7** (1):65-77.
- Maathuis, H. 2000. *Potential Impact of climate change on prairie groundwater supplies: review of current knowledge*, Saskatchewan Research Council Publication No. 11304-2E00, Saskatchewan Research Council, Saskatoon, Saskatchewan, 43 p.
- MacDonald, D.E. 1982. *Marl resources of Alberta*. Alberta Research Council, Earth Sciences Report 82-1, Alberta Research Council, Edmonton, Alberta, 94 p.
- MacDonald, D.E. 1984. Marl in Alberta, *In: Guillet G.R. and Martin W. (eds); The geology of industrial minerals in Canada*, Canadian Institute for Mining and Metallurgy, Montreal, Quebec, p.226-229.
- Harbaugh, A.W., Banta, E.R., Hill, M.C., and McDonald, M.G. 2000. *MODFLOW-2000, the U.S. Geological Survey modular ground-water model -- User guide to modularization concepts and the Ground-Water Flow Process*, U.S. Geological Survey Open-File Report 00-92, 121 p.
- Meinzer, O. E. 1923. *The occurrence of ground water in the United States, with a discussion of principles*: U.S. Geol. Survey, Water-Supply Paper 489, 321 p.
- Meyboom, P. 1966. Unsteady groundwater flow near a willow ring in hummocky Moraine, *Journal of Hydrology* **4**: 38-62.
- Meyboom, P. 1967a. *Groundwater recharge on the prairies*, Water Resources Canada, Royal Society of Canada Symposium: 129-153.
- Meyboom, P. 1967b. *Groundwater studies in the Assinboine River drainage basin, Part II, Hydrogeologic characteristics of phreatophytic vegetation in south-central Saskatchewan*, Geological Survey of Canada Bulletin 139, Part II, 65 p.
- Meyboom, P., Van Everdingen, R.O., and Freeze, R.A. 1966. *Patterns of groundwater flow in seven discharge areas in Saskatchewan and Manitoba*, Geological Survey of Canada Bulletin 147, 57 p.
- Miller, Irl. 2003. Mr. Miller served as President and has been a long-time member of Wagner Natural Area Society.
- Moore, P.D., and Bellamy, D.J. 1974. *Peatlands*, Springer-Verlag, New York, New York, USA, 221 p.
- Mowat, C.M. 1987. *A management plan for the Wagner Natural Area*, M.Sc. Thesis, University of Calgary, Calgary, Alberta, 97 pgs.

- National Wetland Working Group. 1988. *Wetlands of Canada*, Ecological Land Classification Series, no. 24, Sustainable Development Branch, Environment Canada, Ontario, and Polyscience Publications, Montreal, Quebec, Canada, 452 p.
- National Wetland Working Group. 1997. *The Canadian Wetland Classification System*, 2nd Edition, Warner B.G., Rubec C.D.A. (eds) Wetland Research Centre Publication, Waterloo, Ontario, 68 p.
- Parkland County, 2000. Land use bylaw 15-00, Parkland County, Alberta, 163 p.
- Pennman, H.L. 1956. Evaporation an introductory survey, *Netherlands Journal of Agricultural Science* **4**: 9-29.
- Pollock, D.W. 1989. *Documentation of computer programs to compute and display pathlines using results from the U.S. Geological Survey modular three-dimensional finite-difference ground-water flow model*, U.S. Geological Survey Open File Report 89-381, 188 p.
- Price, J.S. and Waddington, J.M. 2000. Advances in Canadian wetland hydrology and Biogeochemistry, *Hydrological Processes* **14**: 1579-1589.
- Prosser, D. 1982. Hydrogeology of Wagner Bog, *The Edmonton Naturalist* **10** (2): 8-13.
- Rosenberry, D.O., Striegl, R.G., and Hudson, D.C. 2000. Plants as indicators of focused ground water discharge to a Northern Minnesota Lake, *Ground Water* **38** (2): 296-303.
- Rutter, N.W., Andriashek, L.D., Stein, R., and Fenton, M.M. 1998. Engineering geology of the Edmonton Area, *In: Karrow, P.F., and White, O.L. (eds) Urban geology of Canadian cities*, Geological Association of Canada, St. John's, Newfoundland, p. 71-92.
- Schwartz, F.W. and Zhang, H. 2003. *Fundamentals of ground water*, Wiley Text Books, New York, New York, USA, 583 p.
- Shjeflo, J.B. 1968. *Evapotranspiration and the water budget of the prairie potholes in North Dakota*, Geological Survey Professional Paper 585 – B, 49 p.
- Siegel, D.I. 1988a. The recharge-discharge functions of wetlands near Juneau, Alaska: Part I, Hydrogeological investigations, *Ground Water* **26** (4): 427-434.
- Siegel, D.I. 1988b. The recharge-discharge functions of wetlands near Juneau, Alaska: Part II, Geochemical investigations, *Ground Water* **26** (5): 580-586.
- Sjörs, H. 1961. Surface patterns in boreal peatlands, *Endeavor* **20**: 217-224.

- Spencer Environmental Management Services Ltd. 1990. Environmental assessment for proposed interchange and connector road for junction of highway 16x and secondary highway 794, Spencer Environmental Management Services, Edmonton, Alberta, 4 vols.
- Stein, R. 1993. The Edmonton region through time: Groundwater, *In*: Godfrey, J.D. (ed.), *Edmonton beneath our feet*, Alberta Research Council, Edmonton, Alberta, p. 33-42.
- Su, M., Stolte, W.J., and van der Kamp, G. 2000. Modelling Canadian prairie wetland hydrology using a semi-distributed streamflow model, *Hydrological Processes* **14**: 2405-2422.
- Thornthwaite, C.W. 1944. Report of the committee on transpiration and evaporation, 1943-44, *Transactions, American Geophysical Union* **25**: 687.
- Tóth, J. 1962. A theory of ground water motion in small drainage basins in central Alberta, Canada, *Journal of Geophysical Research* **67** (11): 4375- 4387.
- Tóth, J. 1963. A theoretical analysis of groundwater flow in small drainage basins, *Journal of Geophysical Research* **68** (16) 4795-4812.
- Tóth, J. 1966. Mapping and interpretation of field phenomena for groundwater reconnaissance in a prairie environment, Alberta, Canada, *Bulletin of the International Association of Scientific Hydrology* **11** (2): 20-68.
- Tóth, J. 1971. Groundwater discharge: a common generator of diverse geologic and morphologic phenomena, *Bulletin of the International Association of Scientific Hydrology* **16** (1-3): 7-24.
- Tóth, J. 1984. The role of regional gravity flow in the chemical and thermal evolution of ground water, *Proceedings of the First Canadian/American Conference on Hydrogeology - Practical Applications of Ground Water Geochemistry*, Banff, Alberta, Canada, National Water Well Association, Dublin, Ohio, 3-39.
- Tóth, J. 1999. Groundwater as a geologic agent: An overview of the causes, processes and manifestations, *Hydrogeology Journal* **7**: 1-14.
- UMA Engineering Ltd. 2000. *Parkland County water management plan for Upper Big Lake Basin*, UMA Engineering, Edmonton, Alberta, 184 p.
- van der Kamp G and Hayashi, M. 1998. The groundwater recharge function of small wetlands in the semi-arid Northern Prairies, *Great Plains Research* **8**: 39-56.
- van der Kamp, G., Hayashi, M., and Gallen, D. 2003. Comparing the hydrology of grassed and cultivated catchments in the semi-arid Canadian prairies, *Hydrological Processes* **17**: 559-575.
- Vitt, D.H, 1982. Peatland formation and vegetation of the Wagner Bog, *The Edmonton Naturalist* **10** (2): 17-23.

- Waterloo Hydrogeologic Software Inc. 1996. *Visual MODFLOW, User's Manual, version 2.60*, Waterloo Hydrogeologic Software Inc., Waterloo, Ontario, 566 p.
- Williams, M.A.J., Dunkerley, D.L., De Deckker, Kershaw, A.P., and Stokes, K. 1993. *Quaternary Environments*, Edward Arnold, New York, New York, 329 p.
- Winter, T.C. 1999. Relation of streams, lakes and wetlands to groundwater flow Systems, *Hydrogeology Journal* 7: 28-45.
- Zoltai, S.C. 1988. Wetland environments and classification in National Wetlands Working Group, *In: Wetlands of Canada*, National Wetlands Working Group, Ecological Land Classification Series, no. 24, Sustainable Development Branch, Environment Canada, Ontario, and Polyscience Publications, Montreal, Quebec, Canada, p. 1-26.
- Zoltai, S.C., Taylor, S., Jeglum, J.K., Mills, G.F., and Johnson, J.D. 1988. Wetlands of Boreal Canada, *In: Wetlands of Canada*, National Wetlands Working Group, Ecological Land Classification Series, no. 24, Sustainable Development Branch, Environment Canada, Ontario, and Polyscience Publications, Montreal, Quebec, Canada, p. 97-151.
- Zoltai, S.C. and Vitt, D.H. 1995. Canadian Wetlands – environmental gradients and Classification, *Vegetatio* 118: 131-137.

Appendix A: Borehole logs

2238 Alberta Environment Observation Well

Date drilled:	November 24, 1983
Driller	Alberta Environment/Earth Sciences Division
Drilling method	Mud rotary
Location	Clearing south of parking lot

Lithologic Description

<i>Depth (m)</i>	<i>Lithology</i>
2.74	Silty brown clay
4.57	Grey clay
8.84	Silty grey clay
11.58	Sandy clay
13.72	Silty clay
14.63	Sand and coal
15.85	Shale

Completion Details

Total depth	15.5 m
Screen interval	14.0 – 15.5 m
Casing	Steel – 177.8 mm (outside diameter)
Screen	Stainless steel (telescoped)
Sand pack	Artificial (12-20) – 100 pounds
Seal	Grout from surface to 5.2 m
Casing protector	Steel – 10.2 mm (outside diameter)

2237 Alberta Environment Observation Well

Date drilled:	November 24, 1983
Driller	Alberta Environment/Earth Sciences Division
Drilling method	Mud rotary
Location	Southwest corner of west meadow

Lithologic Description

<i>Depth (m)</i>	<i>Lithology</i>
0.61	Muskeg
2.44	Silty brown clay
4.57	Silty grey clay
10.06	Silty clay
12.50	Sand
13.72	Shale

Completion Details

Total depth	11.6 m
Screen interval	11.0 – 11.6 m
Casing	Steel – 177.8 mm
Screen	Plastic – 76.2 mm
Sand pack	Artificial (12-20) – 50 pounds
Seal	Grout from surface to 11.0 m
Casing protector	Steel – 10.2 mm

2236 Alberta Environment Observation Well

Date drilled:	November 25, 1983
Driller	Alberta Environment/Earth Sciences Division
Drilling method	Mud rotary
Location	Southwest corner of east meadow

Lithologic Description

<i>Depth (m)</i>	<i>Lithology</i>
0.30	Muskeg
3.66	Silty brown clay
8.23	Silty grey clay
11.58	Sand and gravel
13.11	Clay
13.72	Sand and gravel
17.07	Gravelly clay
19.51	Sand
20.73	Shale and sandstone

Completion Details

Total depth	20.7 m
Screen interval	7.3 – 20.7 m
Casing	Steel – 141.2 mm
Screen	Plastic 76.2 mm
Sand pack	Artificial (12-20) – 100 pounds
Seal	Grout from surface to 7.3 m
Casing protector	Steel – 10.2 mm

02-2001

Date drilled:	April 11, 2001
Driller	Elk Point Drilling
Drilling method	Mud rotary
Location	East side of west meadow

Lithologic Description

<i>Depth (m)</i>	<i>Lithology</i>
0.3	Loam, brown-black
1.5	Silt, brown, <5% clay, iron staining
3.0	Silty brown clay, partially consolidated
4.6	Brown clay, high moisture content
18.3	Dark brown clay, partially unconsolidated

Completion Details

Total depth	18.3 m
Screen interval	12.2 – 15.2 m
Casing	PVC pipe, 51 mm
Screen	PVC slotted pipe (010), 51 mm
Sand pack	20/40 frac sand (15.2 – 11.3 m)
Seal	Bentonite chips from 11.3 m to surface
Casing protector	Steel – 10.2 mm

03-2001

Date drilled:	April 11, 2001
Driller	Elk Point Drilling
Drilling method	Mud rotary
Location	East side of west meadow

Lithologic Description

<i>Depth (m)</i>	<i>Lithology</i>
3.0	Lacustrine clay, brown, partially consolidated, high moisture content
10.7	Lacustrine clay, dark brown, unconsolidated, high moisture content
12.2	Clay, dark brown, unconsolidated, <5% pebbles, high moisture content
13.7	Sand (~90% fine grained sand, ~10% coarse grained), water bearing
15.2	Clay, brown, consolidated, moderate moisture

Completion Details

Total depth	15.2 m
Screen interval	13.7 – 12.2 m
Casing	PVC pipe, 142 mm
Screen	Stainless steel, 15 mm slot
Sand pack	20/40 frac sand (12.2 – 10.6 m)
Seal	Grout from 10.6 m to surface
Casing protector	Steel – 150 mm

A-2001, B-2001

Date drilled:	April 17, 2001
Driller	Researcher
Drilling method	Truck mounted auger rig
Location	East side of west meadow, ~1 m south of 03-2001

Lithologic Description

<i>Depth (m)</i>	<i>Lithology</i>
0.3	Lacustrine clay, brown, partially consolidated, high moisture content
6.1	Lacustrine clay, dark brown, unconsolidated, high moisture content

Completion Details – A-2001

Total depth	6.4 m
Screen interval	6.1 – 6.4 m
Casing	PVC pipe, 25.4 mm
Screen	PVC pipe, slotted (010), 25.4 mm (outside diameter)
Sand pack	20/40 frac sand (6.4 – 5.9 m)
Seal	Bentonite chips from 5.9 m to surface
Casing protector	None

Completion Details – B-2001

Total depth	3.0 m
Screen interval	2.7 – 3.0 m
Casing	PVC pipe, 25.4 mm
Screen	PVC pipe, slotted (010), 25.4 mm (outside diameter)
Sand pack	20/40 frac sand (2.7 – 3.0 m)
Seal	Bentonite chips from 2.7 m to surface
Casing protector	None

01-2002

Date drilled:	April 9, 2002
Driller	Elk Point Drilling
Drilling method	Solid stem auger
Location	Northwest side of west meadow

Lithologic Description

<i>Depth (m)</i>	<i>Lithology</i>
1.5	Yellow-brown, silty mud, soft, plastic
3.0	Yellow-brown, silty mud, wet
4.1	Fine sand lenses in yellow silty mud
4.6	Silty sand interbedded with grey soft mud
5.5	Grey clayey silt with traces of iron staining
7.0	Dark grey silty till with angular clasts (up to 1 cm)
7.6	Blue grey silty clay
11.0	Dark grey poorly consolidated siltstone

Completion Details

Total depth	4.6 m
Screen interval	4.6 – 1.5 m
Casing	PVC pipe, 142 mm
Screen	PVC pipe slotted (010)
Sand pack	20/40 frac sand (4.6 – 1.5 m)
Seal	Bentonite chips from 1.5 m to surface
Casing protector	Steel – 150 mm

02-2002

Date drilled:	April 9, 2002
Driller	Elk Point Drilling
Drilling method	Solid stem auger
Location	West side of west meadow

Lithologic Description

<i>Depth (m)</i>	<i>Lithology</i>
0.9	Topsoil
1.5	Fine sandy silt, grey-brown, stiff
3.0	Sandy, silty clay, brownish-grey, plastic
6.1	Blue-grey clay, traces of silt
10.7	Clayey silt
12.2	Grey clayey silt, very sticky, silt stingers
15.2	Sandstone

Completion Details

Total depth	4.5 m
Screen interval	4.5 – 1.5 m
Casing	PVC pipe, 142 mm
Screen	PVC pipe slotted (010)
Sand pack	20/40 frac sand (4.6 – 1.2 m)
Seal	Bentonite chips from 1.2 m to surface
Casing protector	Steel – 150 mm

01-2003

Date drilled:	April 7, 2003
Driller	Elk Point Drilling
Drilling method	Mud rotary rig
Location	west side of east meadow

Lithologic Description

<i>Depth (m)</i>	<i>Lithology</i>
1.5	Silty clay, trace organics
3.0	Silty clay, lacustrine
4.2	Grey clay
5.7	Silty grey clay
13.4	Shale, soft, pebbles, coal and siltstone
16.8	Shale, medium hard
19.8	Siltstone

Completion Details

Total depth	19.8 m
Screen interval	21.3 - 24.4 m
Casing	PVC pipe, 142 mm
Screen	PVC pipe slotted (020)
Sand pack	20/40 frac sand (21.3 – 24.4 m)
Seal	Bentonite chips from 21.3 m to surface
Casing protector	Steel – 150 mm

02-2003

Date drilled:	April 7, 2003
Driller	Elk Point Drilling
Drilling method	Mud rotary rig
Location	East side of east meadow

Lithologic Description

<i>Depth (m)</i>	<i>Lithology</i>
1.5	Glaciolacustrine clay, with pebbles and coal
3.0	Glaciolacustrine clay, grey, trace organics and pebbles
4.2	Till, sandy, dark grey
5.7	Till, Saskatchewan sands and gravel pebbles
13.4	Shale, soft, pebbles, coal and siltstone
16.8	Shale, medium hard
18.2	Shale

Completion Details

Total depth	18.2 m
Screen interval	5.2 – 8.2
Casing	PVC pipe, 142 mm
Screen	PVC pipe slotted (020)
Sand pack	20/40 frac sand (18.3 – 13.7 m)
Seal	Bentonite chips from 18.3 m to surface
Casing protector	Steel – 150 mm

Appendix B: Locations of wells in cross-sections

Figure 4.6	Figure 4.7	Figure 4.8
SE 01-51-02-W5	SE 06-52-26-W4	NW 07-52-25-W4
NW 12-51-02-W5	NE 07-52-26-W4	SE 18-52-25-W4
SW 13-51-02-W5	NW 18-52-26-W4	NW 30-52-25-W4
NE 24-51-02-W5	SW 30-52-26-W4	NW 31-52-25-W4
NW 25-51-02-W5	NE 30-52-26-W4	NH 06-53-25-W4
NE 36-51-02-W5	SH 31-52-26-W4	SE 07-53-25-W4
NW 01-52-02-W5	NE 31-52-26-W4	SE 18-53-25-W4
SE 12-52-02-W5	NW 06-53-26-W4	SE 19-53-25-W4
NW 13-52-02-W5	NW 07-53-26-W4 (WNA 2237)	NH 31-53-25-W4
SW 24-52-02-W5	NW 07-53-26-W4 (WNA 2236)	SE 01-54-26-W4
SW 25-52-02-W5	NW 07-53-26-W4 (WNA 2238)	NW 07-54-25-W4
SE 36-52-02-W5	SE 18-53-26-W4	
NW 01-53-02-W5	NW 18-53-26-W4	
SW 12-53-02-W5	NE 19-53-26-W4	
NW 13-53-02-W5	SE 30-53-26-W4	
SE 24-53-02-W5	NW 31-53-26-W4	
NE 25-53-02-W5		
SE 36-53-02-W5		
SE 01-54-02-W5		
SE 13-54-02-W5		
NW 24-54-02W5		

Table B.1 Locations of wells used in cross-sections presented in Chapter 4